FINAL EVALUATION OF CORROSION PROTECTION FOR BONDED INTERNAL TENDONS IN PRECAST SEGMENTAL CONSTRUCTION

by

R. M. Salas, A. L. Kotys, J. S. West, J. E. Breen, and M. E. Kreger

Research Report 1405-6

Research Project 0-1405

DURABILITY DESIGN OF POST-TENSIONED BRIDGE SUBSTRUCTURE ELEMENTS

conducted for the
Texas Department of Transportation

in cooperation with the
U.S. Department of Transportation
Federal Highway Administration

by the

CENTER FOR TRANSPORTATION RESEARCH
BUREAU OF ENGINEERING RESEARCH
THE UNIVERSITY OF TEXAS AT AUSTIN

October 2002

Research performed in cooperation with the Texas Department of Transportation and the U.S. Department of Transportation, Federal Highway Administration.

ACKNOWLEDGMENTS

We greatly appreciate the financial support from the Texas Department of Transportation that made this project possible. In particular, we would like to acknowledge the contributions of Rene Vignos who developed the initial concept of the test specimen and fabricated the specimens and the exposure testing devices. We are grateful for the active support of the project director, Bryan Hodges (TYL), and the support of program coordinator, Richard Wilkison, is also very much appreciated. We thank Project Monitoring Committee members, Gerald Lankes (CST), Ronnie VanPelt (BMT), and Tamer Ahmed (FHWA).

DISCLAIMER

J. E. Breen, P.E., TX #18479
M. E. Kreger, P.E., TX #65541

Research Supervisors

TABLE OF CONTENTS

LIST OF FIGURES

LIST OF TABLES

SUMMARY

In 1993, aware of unfortunate experiences in Europe in early non-epoxy segmental joints, Research Project 0-1264 was started with the main purpose of investigating the corrosion protection of internal tendons at segmental joints. This testing program was transferred to Project 0-1405 for long-term testing. Half of the thirty-eight laboratory specimens were autopsied after around four and one-half years of highly aggressive exposure and the preliminary conclusions were reported in 1999. The variables included were joint type (dry or epoxy), duct type (galvanized steel or plastic), grout type (3 grouts with differing additives) and level of joint compression (3 different levels). This report documents the final results, after the second half of the specimens were autopsied with over eight years of very aggressive exposure. The observed conditions after eight years caused a number of changes from the preliminary conclusions. Main among these observations were the presence of some strand corrosion (away from the joint) in epoxy jointed specimens, corrosion at one epoxy joint that was found to be incompletely filled with epoxy, and very extensive corrosion in the galvanized steel ducts. Autopsies confirmed that dry joints should not be used in situations where aggressive exposure may occur, that match-cast epoxy joints provide good corrosion protection, that gaskets in epoxy joints do not appear to be beneficial, that plastic ducts provide excellent corrosion protection and that good grouting procedures and materials are essential. The use of calcium nitrite had little effect on the onset of corrosion but did seem to provide enhanced long-term strand corrosion protection.

CHAPTER 1:
INTRODUCTION

1.1 BACKGROUND AND OBJECTIVES

In recent years, the practice in the use of internal and external post-tensioning for bridge superstructures has been under debate, due to significant tendon corrosion damages, several reported failures of individual tendons as well as a few collapses of non-typical structures[1-5]. While experience in the USA has been very good,[6] some foreign experience has been less than satisfactory. The moratorium in the U.K. established after problems in 1992 still remains in place for precast segmental construction using internal prestressing.[2] The preference in Germany for the use of external prestressing,[7,8] and the preference in Japan for the use of fully external tendons using transparent sheath with grouting[4] are examples of the general concern and show the need for studies regarding the corrosion protection of bonded post-tensioning systems. Recognizing the extent of the problem, in November 2001, engineers from many countries gathered at Ghent University,[9] in Belgium, under the sponsorship of *fib* (federation internationale du béton) and IABSE (International Association for Bridge and Structural Engineering), to review the problems encountered and to discuss the available solutions. Many aspects still remain under discussion.

In the USA, very limited problems with precast segmental bridges[6,10-13] include two tendon failures discovered during the year 2000 at the Mid-Bay Bridge and corroded vertical tendons discovered in the same year in segmental piers of the Sunshine Skyway Bridge. Both bridges are located in the state of Florida. Additionally, grouting deficiencies were found in 2001 in the Sidney Lanier cable-stayed bridge in Georgia and in the Boston Central Artery bridges. A comprehensive inspection of segmental bridges in Texas found no severe problems.

Corrosion protection for bonded internal tendons in precast segmental construction can be very good. Within the segment, internal tendons are well protected by the high quality concrete, duct, and cement grout. The potential weak link in corrosion protection is at the joint between segments. The ducts for internal tendons are not continuous across the joints, and no special coupling of tendon ducts has usually been made with match-cast joints. Thus, the joint represents a preformed crack at the same location where there is a discontinuity in the duct. In dry joints, this crack is not sealed and hence dry joints have been not allowed with internal tendons. In epoxy joints, this crack is sealed if the epoxy is applied correctly. In saltwater exposures or in areas where de-icing salts are used, the joint and duct discontinuity could possibly allow moisture and chlorides to reach the tendon and cause corrosion, as shown in Figure 1.1.

TxDOT Project 0-1264 was started and implemented in 1993 by R.P. Vignos[14] at the University of Texas at Austin, under the supervision of Dr. J. E. Breen and Dr. M. E. Kreger. Its main purpose was to investigate the corrosion protection of internal tendons in segmental construction, with the use of 38 macrocell laboratory specimens. The program was transferred to Project 0-1405 in 1995 for long-term testing. In October 1999, Project 0-1405 reported the conclusions based on four and a half years of exposure of the first 19 macrocell specimens autopsied.[15] These conclusions and the interim and final conclusions based on the additional studies performed under Project 0-1405, including both high performance grouts[6] and long-term corrosion testing using large scale beam and column specimens,[17] are now referenced in recent publications in this field. These include the "Interim Statement on Grouting Practices" published in December 2000 by the American Segmental Bridge Institute (ASBI), the "ASBI-Grouting Certification Training Program" started in August 2001, and the Post-Tensioning Institute's "Specification for Grouting of Post-Tensioned Structures," published in February 2001.[18]

In 2002, after eight years of testing and monitoring of the remaining 19 duplicate macrocell specimens initiated in Project 0-1264, these macrocells have been autopsied and final conclusions drawn. The

objectives of this report are to summarize these autopsy results and to present the final conclusions, recommendations and design guidelines.

The general objectives of the overall macrocell research program were:

1. To evaluate the potential for corrosion of internal tendons at joints in typical precast segmental construction;
2. To examine the effect of typical North American design and construction details on corrosion protection for internal tendons; and
3. To examine methods for improving corrosion protection for internal tendons.

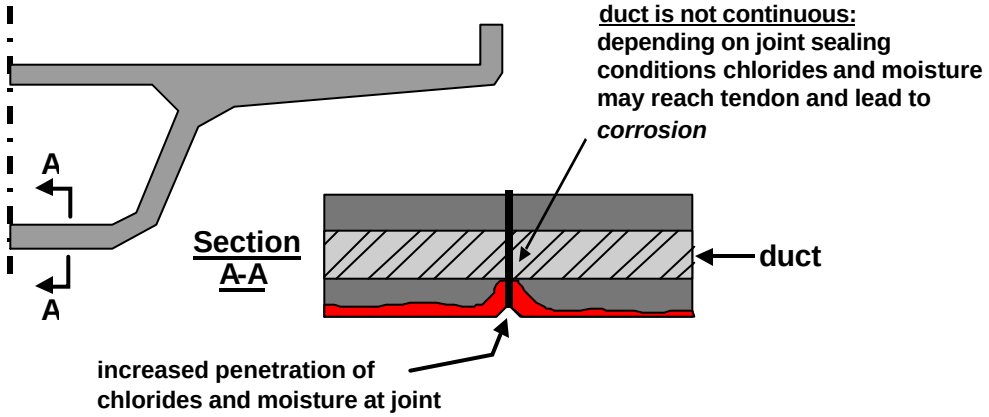

Figure 1.1 Possible Corrosion Mechanism at Precast Segmental Joints.[15]

1.2 RESEARCH PROJECT 0-1405

The research described in this report is now part of the University of Texas at Austin, Center for Transportation Research Project 0-1405: "Durability Design of Post-Tensioned Bridge Substructure Elements." The research is being performed at the Phil M. Ferguson Structural Engineering Laboratory and is sponsored by the Texas Department of Transportation and Federal Highway Administration. The title of Project 0-1405 implies two main components:

1. durability of bridge substructures, and
2. post-tensioned bridge substructures

The durability aspect is in response to the deteriorating condition of bridge substructures in some areas of Texas. Considerable research and design effort has been given to bridge deck design to prevent corrosion damage, while substructures had historically been overlooked. Often details result in substructures having a higher exposure to aggressive agents such as salt water, deicing salts and damaging soils. In some districts of the state, more than ten percent of the substructures are deficient, and the substructure condition is limiting the service life of the bridges.

The second aspect of the research is post-tensioned substructures. Relatively few post-tensioned substructures have been used in the past. As described above, there are many possible applications in bridge substructures where post-tensioning can provide structural and economical benefits, and can possibly improve durability. Post-tensioning is now being used in Texas bridge substructures, and it is reasonable to expect the use of post-tensioning to increase in the future as precasting of substructures components becomes more prevalent and as foundation sizes increase.

Problem:

The problem that bridge engineers are often faced with is that there are few systematic durability design guidelines for post-tensioned concrete structures. Durability design guidelines should provide information on how to identify possible durability problems, how to improve durability using post-tensioning, and how to ensure that the post-tensioning system does not introduce new durability problems.

1.3 RESEARCH OBJECTIVES AND PROJECT SCOPE

1.3.1 Project Objectives

The overall research objectives for Project 0-1405 are as follows:

1. To examine the use of post-tensioning in bridge substructures;
2. To identify durability concerns for bridge substructures in Texas;
3. To identify existing technology to ensure durability or improve durability;
4. To develop experimental testing programs to evaluate protection measures for improving the durability of post-tensioned bridge substructures; and
5. To develop durability design guidelines and recommendations for post-tensioned bridge substructures.

A review of literature early in the project indicated that post-tensioning was being successfully used in past and present bridge substructure designs, and that suitable post-tensioning hardware was readily available. It was decided not to develop possible post-tensioned bridge substructure designs as part of the objectives for two reasons. First, other research[14,19,20] on post-tensioned substructures was already underway, and second, the durability issues warranted the full attention of Project 0-1405. The initial literature review identified a substantial amount of relevant information that could be applied to the durability of post-tensioned bridge substructures. This existing information allowed the scope of the experimental portion of the project to be narrowed. The final objective represents the culmination of the project. All of the research findings are to be compiled into the practical format of durability design guidelines.

1.3.2 Project Scope

The subject of durability is extremely broad, and as a result a broad scope of research was developed for Project 0-1405. Based on the project proposal and an initial review of relevant literature, the project scope and necessary work plan were defined. The main components of Project 0-1405 are:

1. extensive literature review
2. survey of existing bridge substructures
3. long-term corrosion test with large-scale post-tensioned beam and column elements
4. investigation of corrosion protection for internal prestressing tendons in precast segmental bridges
5. development of improved grouts for post-tensioning

Component 4, the investigation of corrosion protection for internal tendons in segmental construction is described in this report. As was stated previously, this testing program was developed and implemented by R.P. Vignos[14] under TxDOT Project 0-1264. This testing program was transferred to Project 0-1405 in 1995 for long-term testing. Although this aspect of the research was developed under Project 0-1264 to address corrosion concerns for precast segmental bridge superstructures, the concepts and variables are equally applicable to precast segmental substructures, and the testing program fits well within the scope of Project 0-1405.

1.4 PROJECT REPORTING

The research tasks in Project 0-1405 were and are performed by graduate research assistants B. D. Koester,[21] A. L. Kotys,[22] C. J. Larosche,[23] R. M. Salas,[24] A. J. Schokker,[25] and J. S. West,[26] under supervision of Dr. J. E. Breen and Dr. M. E. Kreger. Project 0-1405 is not complete, with the long-term beam and column exposure tests currently ongoing. The major tasks to be completed in the future include continued exposure testing and data collection, final autopsy of all beam and column specimens and preparation of the final comprehensive durability design guidelines.

The research presented in this report represents part of a large project funded by the Texas Department of Transportation, entitled, "Durability Design of Post-Tensioned Bridge Substructures" (Project 0-1405). Nine reports are schedule to be developed from this project as listed in Table 1.1. The research performed during the first six years of Project 0-1405 is reported in the first five reports. This report is the sixth of that series.

Table 1.1 Proposed Project 0-1405 Reports.

Number	Title	Estimated Completion
1405-1	State of the Art Durability of Post-Tensioned Bridge Substructures	1999
1405-2	Development of High-Performance Grouts for Bonded Post-Tensioned Structures	1999
1405-3	Long-term Post-Tensioned Beam and Column Exposure Test Specimens: Experimental Program	1999
1405-4	Corrosion Protection for Bonded Internal Tendons in Precast Segmental Construction	1999
1405-5	Interim Conclusions, Recommendations and Design Guidelines for Durability of Post-Tensioned Bridge Substructures	1999
1405-6	Final Evaluation of Corrosion Protection for Bonded Internal Tendons in Precast Segmental Construction	2002
1405-7	Design Guidelines for Corrosion Protection for Bonded Internal Tendons in Precast Segmental Construction	2002
1405-8	Long-term Post-Tensioned Beam and Column Exposure Test Specimens: Final Evaluation	2003
1405-9	Conclusions, Recommendations and Design Guidelines for Durability of Post-Tensioned Bridge Substructures	2003

Report 1405-1 provides a detailed background on the topic of durability design of post-tensioned bridge substructures. The report contains an extensive literature review on various aspects of the durability of post-tensioned bridge substructures and a detailed analysis of bridge substructure condition rating data in the state of Texas.

Report 1405-2 presents a detailed study of improved and high-performance grouts for bonded post-tensioned structures. Three testing phases were employed in the testing program: fresh property tests, accelerated corrosion tests and large-scale pumping tests. The testing process followed a progression of the three phases. A large number of variables were first investigated for fresh properties. Suitable mixtures then proceeded to accelerated corrosion tests. Finally, the most promising mixtures from the first two phases were tested in the large-scale pumping tests. The variables investigated included water-cement ratio, superplasticizer, antibleed admixture, expanding admixture, corrosion inhibitor, silica fume and fly ash. Two optimized grouts were recommended depending on the particular post-tensioning application.

Report 1405-3 describes the development of two long-term, large-scale exposure testing programs, one with beam elements, and one with columns. A detailed discussion of the design of the test specimens and

selection of variables is presented. Preliminary experimental data is presented and analyzed, including cracking behavior, chloride penetration, half-cell potential measurements and corrosion rate measurements. Preliminary conclusions are presented.

Report 1405-4 describes a series of macrocell corrosion specimens developed to examine corrosion protection for internal prestressing tendons in precast segmental bridges. This report briefly describes the test specimens and variables, and presents and discusses four and a half years of exposure test data. One-half (nineteen of thirty-eight) of the macrocell specimens were subjected to a forensic examination after four and a half years of testing. A detailed description of the autopsy process and findings is included. Conclusions based on the exposure testing and forensic examination are presented.

Report 1405-5 contains a summary of the conclusions and recommendations from the first four reports from Project 0-1405. The findings of the literature review and experimental work were used to develop preliminary durability design guidelines for post-tensioned bridge substructures. The durability design process is described, and guidance is provided for assessing the durability risk and for ensuring protection against freeze-thaw damage, sulfate attack and corrosion of steel reinforcement. These guidelines will be refined and expanded in the future under Project 0-1405 as more experimental data becomes available.

Report 1405-6 (this document) describes a series of macrocell corrosion specimens developed to examine corrosion protection for internal prestressing tendons in precast segmental bridges. This report briefly describes the test specimens and variables, and presents and discusses eight years of exposure test data. One-half (nineteen of thirty-eight) of the macrocell specimens were subjected to a forensic examination after four and a half years of testing, and were reported in Report 1405-4. A detailed description of the autopsy process for the remaining macrocell specimens and findings is included. Final conclusions and recommendations based on the exposure testing and forensic examination are presented.

Several dissertations and theses at The University of Texas at Austin were developed from the research from Project 0-1405. These documents may be valuable supplements to specific areas in the research and are listed in Table 1.2 for reference.

Table 1.2 Project 0-1405 Theses and Dissertations, The University of Texas at Austin.

Title	Author	Date
Master's Theses		
Evaluation of Cement Grouts for Strand Protection Using Accelerated Corrosion Tests"	Bradley D. Koester	12/95
"Durability Examination of Bonded Tendons in Concrete Beams under Aggressive Corrosive Environment"	Andrea L. Kotys	In progress
"Test Method for Evaluating Corrosion Mechanisms in Standard Bridge Columns"	Carl J. Larosche	8/99
"Test Method for Evaluating the Corrosion Protection of Internal Tendons Across Segmental Bridge Joints"	Rene P. Vignos	5/94
Ph.D. Dissertations		
"Accelerated Corrosion Testing, Evaluation and Durability Design of Bonded Post-Tensioned Concrete Tendons"	Ruben M. Salas	In progress
"Improving Corrosion Resistance of Post-Tensioned Substructures Emphasizing High-Performance Grouts"	Andrea J. Schokker	5/99
"Durability Design of Post-Tensioned Bridge Substructures"	Jeffrey S. West	5/99

CHAPTER 2:
EXPERIMENTAL PROGRAM

The experimental program followed in this project was previously described in Chapter 2 of Research Report 1405-4.[15] This report gave preliminary results of the first macrocell autopsy program four and one-half years after exposure testing began. It is repeated with minor changes herein.

The test method was originally developed and implemented by Rene Vignos.[14] The basic objectives for development of the testing program were:

- The test method should provide meaningful comparisons in a reasonable amount of time.
- The test method should accommodate the desired variables in a realistic manner.
- The test method should allow measurement of both macrocell and microcell corrosion.
- The test method should be as standardized as possible to allow comparisons with past and future testing and to provide reproducible results.

Vignos patterned the test method after ASTM G109 - "Standard Test Method for Determining the Effects of Chemical Admixtures on the Corrosion of Embedded Steel Reinforcement in Concrete Exposed to Chloride Environments."[27] The standard macrocell corrosion specimens were modified to examine prestressing tendons in grouted ducts and simulate segmental joints. A full description of the development of the testing program and details of the experiment setup are provided in Reference 14. A summary of the general characteristics of the test specimens, variables and measurements is included in the following sections. Exposure testing was initiated by Vignos in August 1993.

2.1 TEST SPECIMEN

The specimens used in this program are patterned after the standard ASTM G109[24] macrocell specimen developed to evaluate the effect of concrete admixtures on the corrosion of mild steel reinforcement. The standard ASTM G109 specimen consisted of a single concrete block with two layers of mild steel reinforcement. During macrocell corrosion, the top layer of steel acts as the anode and the bottom layer acts as the cathode. Several modifications were made to the ASTM G109 specimens to evaluate corrosion protection for internal tendons in segmental bridge construction. These modifications included the introduction of a transverse joint in the concrete block to allow the effect of the segmental joint type to be evaluated, the use of a grouted prestressing strand in the top layer (anode) in place of one of the mild steel reinforcement layers, and the addition of longitudinal compressive stress on the specimen to simulate prestress in the structure. The revised specimen configuration is shown in Figure 2.1.

Each specimen consists of two match-cast segments. Continuity between the segments is provided by a 0.5-inch diameter, seven-wire prestressing strand inside a grouted duct, representing a typical bonded internal tendon in segmental bridge construction. The duct is cast into each of the match-cast segments and is not continuous across the joint. Due to the small specimen size, the strand cannot be post-tensioned effectively. To simulate precompression across the joint due to post-tensioning, the pairs of match-cast segments were stressed together using external loading frames.

Similar to ASTM G109, two 0.5 in. (#4) mild steel bars were used as the cathode. These bars would represent non-prestressed reinforcement within the segment. The use of two bars increases the ratio of cathode area to anode area, accelerating macrocell corrosion. The cathode bars were discontinuous across the transverse joint, consistent with precast segmental construction. The end cover for the cathode bars at the segmental joint was 0.25 in. Following ASTM G109, the exposed length of the anode and cathode were limited to 5 in. by painting the strand and the mild steel bars with epoxy paint as shown in Figure 2.2.

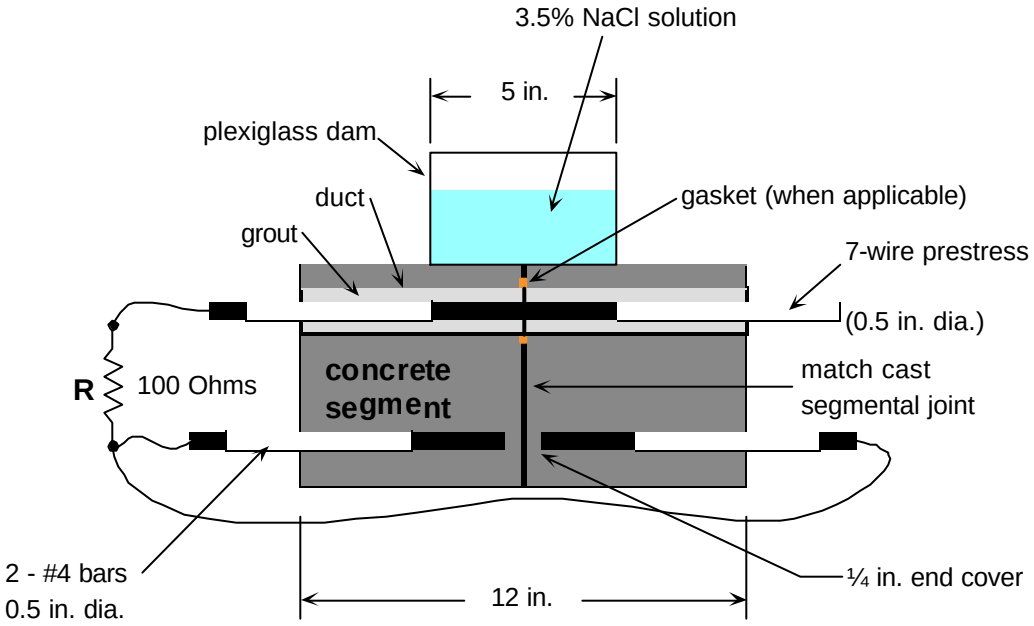

Longitudinal Section

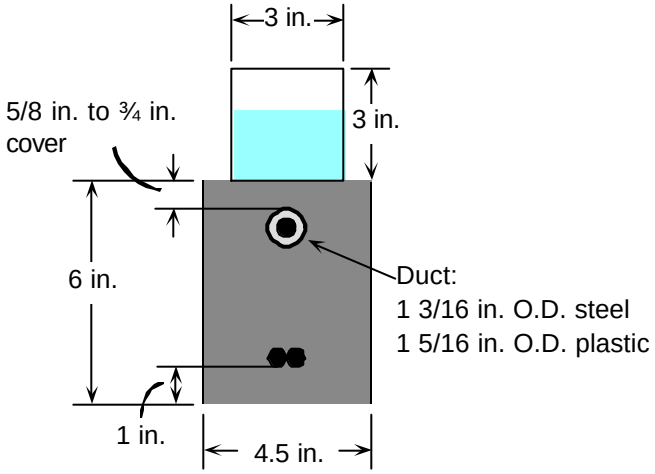

End View

Figure 2.1 Macrocell Specimen Details.

Electrical contact must exist between the anode and cathode for macrocell corrosion to develop. This contact is achieved in the test specimen by wiring the protruding ends of the anode and cathode steel together, as shown in Figure 2.1. Zinc ground clamps are used to connect the wire to the steel. A 100-Ohm resistor is placed in the wire connection between the anode and cathode, as shown in Figure 2.1, to allow assessment of the corrosion current by measuring the voltage drop across the resistor ($I_{corr} = V_{meas}/R$).

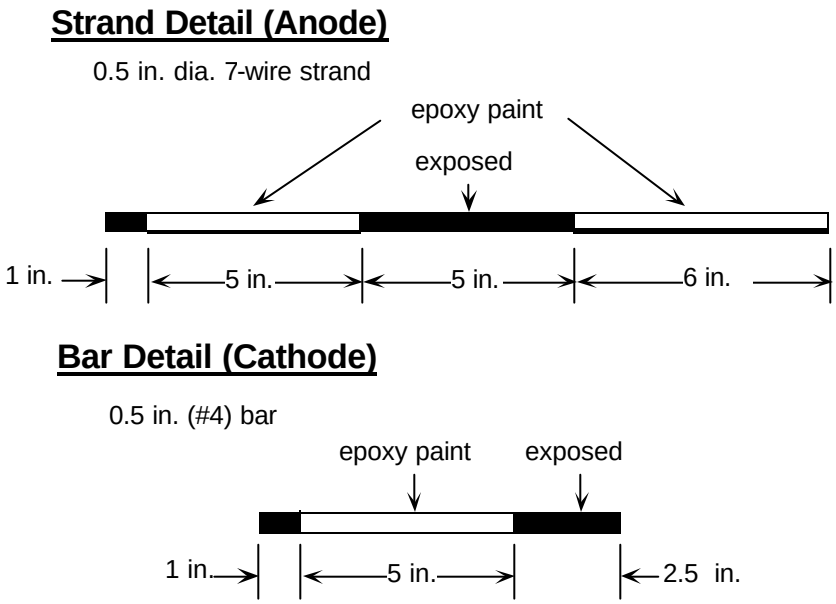

Figure 2.2 Anode and Cathode Bar Details.

Exposure conditions for the specimens consist of a 4-week cycle of 2 weeks dry and 2 weeks wet. During the wet period of the cycle, a portion of the top surface of the specimen is ponded with 3.5% NaCl solution, as shown in Figure 2.1. At the end of the wet period, the NaCl solution is removed from the Plexiglas dam using a wet/dry vacuum.

The specimen was chosen as an extreme aggressive environment to indicate relative effects of variables and is not representative of actual exposure and cover conditions.

2.2 VARIABLES

A broad scope of protection variables was selected for investigation in this program. These variables cover four components of the precast concrete segmental bridge related to corrosion of internal tendons. Included are; joint type, duct type, joint precompression and grout type.

2.2.1 Joint Type

Precast segmental joints are either dry or wet. Wet joints include mortar joints, concrete joints but most frequently epoxy joints. Dry joints and epoxy joints require match casting, and are the most common segmental joints used in North America. When match-cast epoxy joints are used, the entire face of the segment is coated with a thin layer of epoxy immediately before each segment is placed in the bridge. The segments are held in firm contact with temporary post-tensioning while the epoxy cures and the prestressing tendons are placed and stressed. In some situations, a small gasket is used around each duct opening to prevent epoxy from entering the duct when the segment is placed and initially stressed. If a gasket is not used, the duct is swabbed out immediately after initial stressing to prevent epoxy from blocking the duct.

To address typical North American practice, dry joints and epoxy joints, with and without gaskets, were selected for investigation in this testing program. All joint types were match-cast. The AASHTO Guide Specifications[6] for Segmental Bridges[28] do not permit the use of dry joints with internal tendons. However, dry joints were included as a worst case scenario for comparison purposes. The epoxy-jointed specimens were assembled according to the standard practice. Both match-cast faces were coated with epoxy and the segments were pushed together. The joint was precompressed at 50 psi for 48 hours after

which the specimens were unloaded and reloaded to the desired level of precompression (Section 2.2.3). In the epoxy/gasket joint, a foam gasket was glued to the face of one segment around the duct opening prior to application of the epoxy. Details of the foam gasket are shown in Figure 2.3. In the epoxy joint without a gasket, the duct was swabbed out immediately after stressing to prevent the epoxy from blocking the duct.

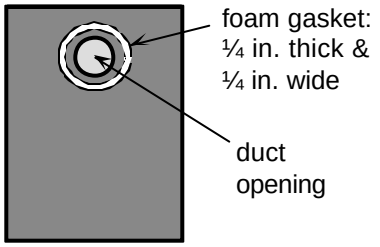

Figure 2.3 Gasket Details.

2.2.2 Duct Type

Two duct types were investigated; standard galvanized steel duct and plastic duct. Due to size limitations, PVC pipe was used for the plastic duct.

2.2.3 Joint Precompression

The joint precompression refers to the level of prestress provided by the internal and/or external tendons in the bridge. Three levels of precompression were selected; 5 psi, 50 psi and $3\sqrt{f'_c}$ psi. The lowest level of 5 psi could represent the level of precompression encountered in a precast segmental column under self-weight. The precompression of 50 psi is based on the *AASHTO Guide Specifications*.[28] The highest precompression value of $3\sqrt{f'_c}$ psi corresponds to 190 psi for this testing program.

2.2.4 Grout Type

Three cement grout types were selected for evaluation; normal grout (plain cement grout, no admixtures, w/c = 0.40), grout with silica fume (13% cement replacement by weight, w/c = 0.32, superplasticizer added) and grout with a commercial calcium nitrite corrosion inhibitor (w/c = 0.40). Grout mix proportions are provided in Section 2.3.

2.2.5 Specimen Types

A total of nineteen specimen types were selected to address all of the variables. Each specimen type was duplicated for a total of thirty-eight specimens. The notation used in the specimen designations is described in Table 2.1. Details of the specimen types and corresponding designations are listed in Table 2.2.

Table 2.1 Specimen Notation.

<table>
<tr><th>Joint Type</th><th>Duct Type</th><th>Joint Precompression</th><th>Grout type</th></tr>
<tr><td>DJ: Dry Joint</td><td rowspan="2">S: Galvanized Steel</td><td>L: Low, 5 psi</td><td>NG: Normal Grout</td></tr>
<tr><td>SE: Standard Epoxy</td><td rowspan="2">M: Medium, 50 psi</td><td rowspan="2">SF: Silica Fume Added</td></tr>
<tr><td>EG: Epoxy with Gasket</td><td>P: Plastic</td></tr>
<tr><td colspan="3">Example: DJ – S – L – NG</td><td>H: High, 190 psi (3vf’c)</td><td>CI: Corrosion Inhibitor</td></tr>
</table>

Table 2.2 Specimen Types and Variables.

Specimen No.	Name	Duct Type	Joint Precompression	Grout Type
Dry Joints:				
1,2	DJ-S-L-NG	Steel	5 psi	Normal
7,8	DJ-S-M-NG	Steel	50 psi	Normal
11,12	DJ-S-H-NG	Steel	190 psi	Normal
31,32	DJ-P-L-NG	Plastic	5 psi	Normal
33,34	DJ-P-M-NG	Plastic	50 psi	Normal
3,4	DJ-S-L-CI	Steel	5 psi	Corrosion Inhibitor
9,10	DJ-S-M-CI	Steel	50 psi	Corrosion Inhibitor
Standard Epoxy Joints:				
15,16	SE-S-L-NG	Steel	5 psi	Normal
21,22	SE-S-M-NG	Steel	50 psi	Normal
27,28	SE-S-H-NG	Steel	190 psi	Normal
35,36	SE-P-L-NG	Plastic	5 psi	Normal
37,38	SE-P-M-NG	Plastic	50 psi	Normal
17,18	SE-S-L-CI	Steel	5 psi	Corrosion Inhibitor
23,24	SE-S-M-CI	Steel	50 psi	Corrosion Inhibitor
29,30	SE-S-H-CI	Steel	190 psi	Corrosion Inhibitor
19,20	SE-S-L-SF	Steel	5 psi	Silica Fume
Epoxy/Gasket Joints:				
5,6	EG-S-L-NG	Steel	5 psi	Normal
25,26	EG-S-M-NG	Steel	50 psi	Normal
13,14	EG-S-H-NG	Steel	190 psi	Normal

2.3 MATERIALS

Details of the materials used in this testing program are summarized in Table 2.3. All materials and proportions were selected to match segmental bridge usage as closely as possible. Concrete was batched using a six cubic foot mixer in the laboratory. Grouts were batched in five gallon buckets using a paddle mixer mounted to a drill press. Complete details of specimen construction are provided in Reference 14.

2.4 MEASUREMENTS DURING EXPOSURE TESTING

Two forms of regular measurements were taken to evaluate macrocell and microcell corrosion in the test specimens. Macrocell corrosion current can be measured directly as described in Section 2.1. In addition, the probability of macrocell corrosion can be estimated using half-cell potential measurements. Microcell corrosion cannot be measured directly. However, significant half-cell potential readings in the absence of measured macrocell corrosion current would indicate a high probability for microcell corrosion.

2.4.1 Macrocell Corrosion Current Measurements

The nature of the macrocell specimen allows direct measurement of the macrocell corrosion current. Macrocell corrosion currents provide three forms of information:

- The time at which corrosion began can be determined from regular measurements during testing.
- Corrosion rate or severity can be calculated from corrosion current measurements.
- The polarity of the corrosion current indicates which steel is corroding (prestressing strand or mild steel reinforcing bars).

The corrosion current is determined by measuring the voltage drop across a resistor placed between the anode and cathode steel, as shown in Figure 2.4. The corrosion current, I_{corr}, is calculated dividing the measured voltage drop by the known resistance (Ohm's Law). Each specimen is connected to a data acquisition system, allowing voltages (currents) for all specimens to be measured simultaneously. Corrosion currents are measured at one-week intervals.

Table 2.3 Material Details.

Item	Description		
Segment Concrete	• w/c = 0.44, f'c =5000 psi		
	• batch proportions:	Coarse Aggregate	383 lb (3/4 in. max.)
		Fine Aggregate	300 lb
		Type I/II Cement	150 lb
		Water	66 lb
	• cylinder strengths:	7-day	4493 psi
		28-day	5145 psi
Normal Grout	• w/c = 0.40		
	• batch proportions:	Type I/II Cement	28.8 lb
		Water	11.6 lb
Corrosion Inhibitor Grout	• w/c = 0.40		
	• corrosion inhibitor:	calcium nitrite	
	• batch proportions:	Type I/II Cement	28.8 lb
		Water	11.6 lb
		Corrosion Inhibitor	187 ml
Silica Fume Grout	• w/c = 0.32		
	• silica fume:	Sikacrete 950DP	
	• superplasticizer:	WRDA-19	
	• batch proportions:	Type I/II Cement	21.7 lb
		Water	8.0 lb
		Silica Fume	3.26 lb
		Superplasticizer	88.5 ml
Prestressing Strand	• 0.5 in. diameter seven wire strand		
	• Grade 270 (270 ksi), low relaxation		
Mild Steel Reinforcement	• 0.5 in. diameter bars (#4)		
	• ASTM A615, Grade 60 (60 ksi)		
Steel Duct	• Corrugated, semi-rigid, galvanized steel duct for post-tensioning		
	• 1-3/16 in. outside diameter		
Plastic Duct	• ASTM D1785 PVC pipe		
	• 1-5/16 in. outside diameter, 1 in. inside diameter		
Segment Epoxy	• B-73 Mid-Range two-part span epoxy		

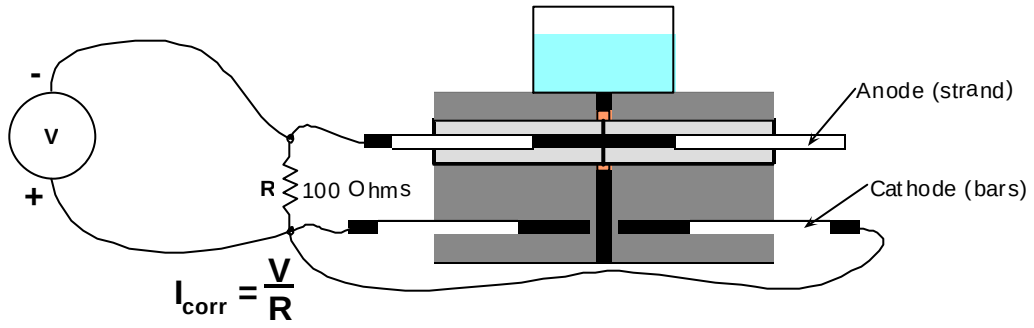

Figure 2.4 Macrocell Corrosion Current Measurement.

During corrosion, the electrons liberated at the anode travel through the electrical connection provided by the wire and resistor to the cathode. Since current moves in the direction opposite to electron flow, the current in the macrocell flows from the cathode to the anode. With the leads of the voltage measuring device attached as indicated in Figure 2.4, the measured voltage across the resistor will have a positive polarity if the anodic reaction is occurring on the prestressing strand. Thus, the polarity of the measured voltage allows the direction of the electron flow to be determined, indicating whether or not the expected corrosion cell has developed.

2.4.2 Half-Cell Potential Readings

Half-cell potential readings also provide three forms of information regarding the condition of the specimen:

- The magnitude of half-cell potential readings indicate the probability of corrosion at a given location.
- The time at which corrosion initiation occurred can be determined from regular potential readings taken during testing.
- Significant half-cell potentials in the absence of macrocell corrosion currents suggest the occurrence of microcell corrosion.

Half-cell potential readings were taken every two weeks at the start of the wet period and the start of the dry period. All measurements are performed according to ASTM C876[29] using a saturated calomel electrode (SCE). Three half-cell potential measurements are made manually on each specimen, as shown in Figure 2.5. One measurement is taken with the Plexiglas dam filled with NaCl solution and the electrode immersed in the solution. Two measurements are taken directly on the surface of each segment with the dam empty. The surface of the concrete is damp for these readings. In all cases, electrical contact between the anode and cathode is interrupted to ensure that the half-cell potential reading is for the strand only.

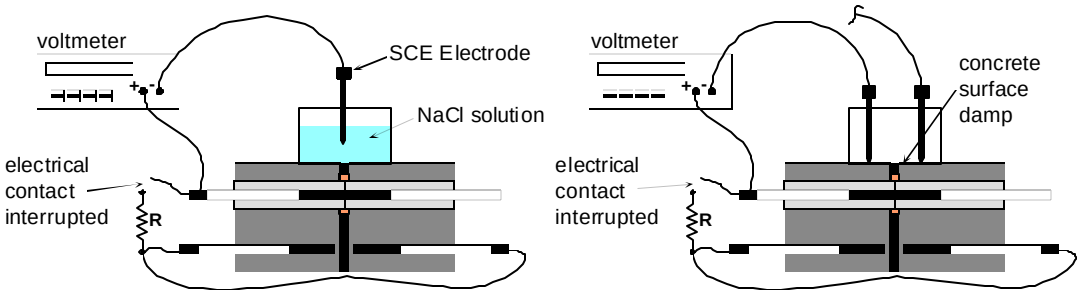

Figure 2.5 Half-Cell Potential Readings.

The numerical significance of the half-cell potential readings is shown in Table 2.4, as defined by ASTM C876. This standard was developed for half-cell potential readings of uncoated reinforcing steel in concrete, and therefore the values reported in Table 2.4 may not necessarily be appropriate for grouted prestressing strand in concrete. In general, half-cell potential readings are not an effective method for monitoring corrosion activity in bonded post-tensioned structures. In structures with galvanized steel ducts, the prestressing tendon will be in contact with the duct in most cases, and half-cell potentials taken on the prestressing tendon may in fact reflect the potential of the zinc on the galvanized steel duct. Because the potential of the zinc will be more negative than that of the tendon, this contact could lead to erroneous results and conclusions. In situations where the tendon is completely encapsulated in an impervious plastic duct system, half-cell potentials are not possible since the duct will act as a barrier to the ion flow necessary for half-cell potential readings.

In spite of these issues, half-cell potential readings were used effectively in the macrocell corrosion specimens in this testing program for two reasons. First, in all cases the prestressing tendon is not in contact with the galvanized duct. Second, for both galvanized ducts and plastic ducts the discontinuity in the duct at the segmental joint should allow ion movement and measurement of half-cell potentials. However, it is still possible that the presence of the duct, whether galvanized steel duct or plastic, may affect the magnitude of the half-cell potentials. Thus, it is important to consider both the magnitude and variation of the measured potentials over time.

Table 2.4 Interpretation of Half-Cell Potentials for Uncoated Reinforcing Steel.[29]

Measured Potential (vs SCE)	Probability of Corrosion
More positive than –130 mV	less than 10% probability of corrosion
Between -130 mV and –280 mV	corrosion activity uncertain
More negative than –280 mV	greater than 90% probability of corrosion

CHAPTER 3:
EXPOSURE TEST RESULTS

Exposure testing was initiated on August 23, 1993. Exposure testing continued without interruption until January 13, 1998, a period of four years and five months, (1603 days). At that time, one specimen from each pair of duplicates was removed for forensic examination and was reported in Reference 15. The exposure program and half-cell readings continued for the remaining nineteen specimens, and they were interrupted only during the months of January 1998 to January 1999 (Days 1603 to 1977), and July to December 2000 (Days 2523 to 2725) when the specimens remained in a dry condition. Corrosion current readings were interrupted from January 8,1998 to January 13, 2000 (Days 1598 to 2333 days after exposure testing was initiated) and from May 17, 2000 to January 2001 (Days 2458 to 2717). Exposure testing ended on August 22, 2001, when the remaining specimens were removed for forensic examination, after a period of eight years (2920 days). The exposure testing data indicated that at least ten specimens of the nineteen specimens had experienced corrosion with measurable corrosion activity, while the other nine specimens showed low probability of corrosion or uncertain corrosion activity.

3.1 MACROCELL CORROSION CURRENT RESULTS

Macrocell corrosion currents over time were plotted for all remaining specimens, after eight years of very aggressive exposure, grouped according to test variables, and are included in Appendix A. Figures 3.1 to 3.4 show examples of corrosion current plots comparing joint type, duct type, joint precompression and grout type, respectively. When examining these plots, the "polarity" of the current is important. As described in Section 2.4.1, the measured voltages and thus the corrosion currents are positive if the assumed macrocell corrosion mechanism (prestressing strand actively corroding) has developed. Negative corrosion currents indicate that a reversed corrosion cell has developed. That is, the prestressing strand is acting as the cathode, while the mild steel reinforcement bars are actively corroding.

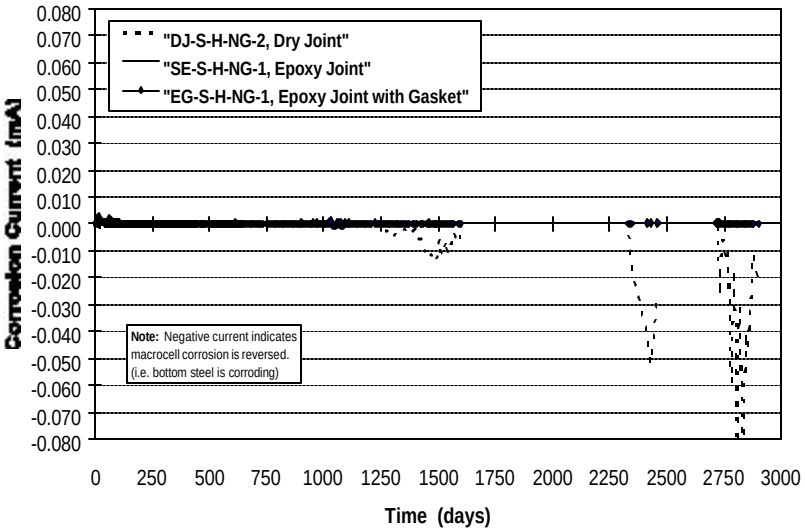

Figure 3.1 Macrocell Corrosion Current: Dry, Epoxy and Epoxy with Gasket Joint, Steel Duct, High Precompresion and Normal Grout.

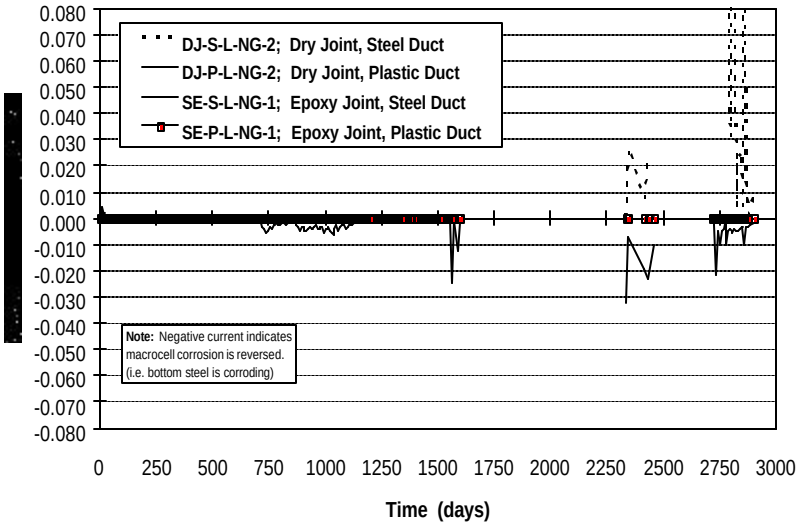

Figure 3.2 Macrocell Corrosion Current: Dry and Epoxy Joint, Steel and Plastic Duct, Low Precompresion and Normal Grout.

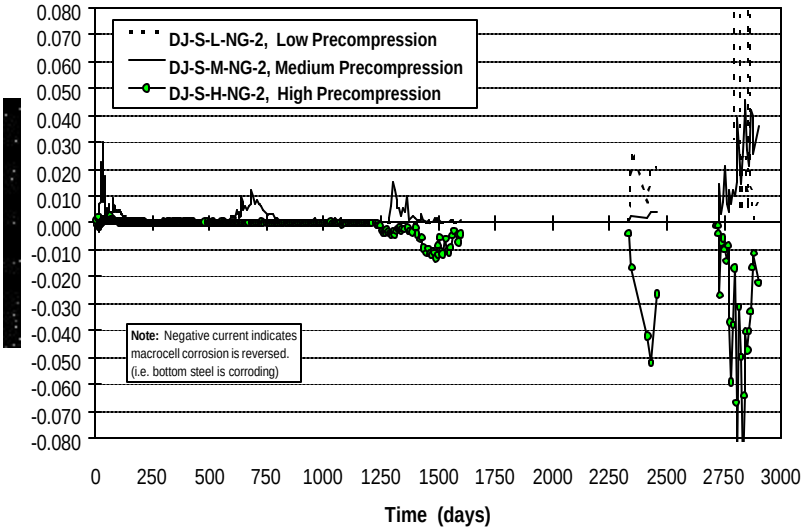

Figure 3.3 Macrocell Corrosion Current: Dry Joint, Steel Duct, Low, Medium and High Precompression and Normal Grout.

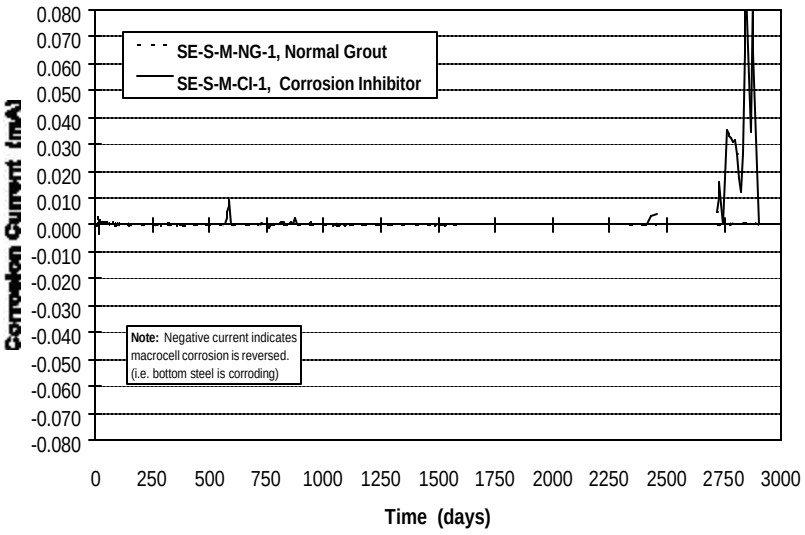

Figure 3.4 Macrocell Corrosion Current: Epoxy Joint, Steel Duct, Medium Precompresion and Different Grouts (Normal and Corrosion Inhibitor added).

Macrocell corrosion current plots for all dry joint specimens show active corrosion. Specimens DJ-S-L-NG-2, DJ-S-L-CI-2 and DJ-S-M-NG-2 show strand corrosion, while the remaining four specimens show reversed macrocell corrosion.

Seven out of nine epoxy joint specimens show stable corrosion currents close to zero, which suggests that the steel in these specimens had low or no corrosion. Only two epoxy joint specimens show a clear initiation of corrosion: specimen SE-S-M-CI-1 with strand corrosion, and specimen SE-S-H-CI-1 with reversed macrocell corrosion.

Epoxy joint specimens with gaskets show a random behavior, with no corrosion, reversed macrocell corrosion and strand corrosion, in specimens EG-S-M-NG-1, EG-S-L-NG-1 and EG-S-H-NG-1, respectively. Table 3.1 shows the general results according to corrosion current activity and polarity.

Out of the 484 corrosion current data points for each specimen over 2902 days of exposure testing, a very few were considered outliers. These values clearly separated from the trend in an unpredictable and/or out of scale manner. They were clearly isolated from the rest of the data set. These data points would disproportionately affect the later calculations with regard to the time to initiation of corrosion, weighted average corrosion current, corrosion current density, and metal loss. A thorough examination of the data was made, finding outliers in the following specimens (number of outlier data in brackets): DJ-S-L-NG-2 (3), DJ-S-H-NG-2 (2),SE-S-L-NG-1 (5), SE-P-L-NG-1 (1), SE-S-M-CI-1 (27), SE-S-M-NG-1 (4), and EG-S-H-NG-1 (14). These values were probably the product of lost or bad connection between the strand and the cable system. The very few outlier values have been excluded from Figures 3.1 to 3.4 and Figures A.1 to A.13.

In addition to the above, corrosion current data for specimen DJ-P-M-NG-2 was collected up to January 8, 1998, (1598 days after exposure testing was initiated). After this date, data values for this specimen were not consistent or coherent, and therefore, are not considered reliable.

Table 3.1 Corrosion Current results based on Corrosion Activity and Polarity.

Zero currents (no corrosion)	Strand corrosion activity	Reversed macrocell corrosion
SE-P-L-NG-1	DJ-S-L-CI-2	DJ-S-M-CI-2
SE-S-L-CI-1	DJ-S-L-NG-2	DJ-P-M-NG-2
SE-S-L-SF-1	DJ-S-M-NG-2	DJ-P-L-NG-2
SE-S-L-NG-1	SE-S-M-CI-1	DJ-S-H-NG-2
SE-S-M-NG-1	----------	SE-S-H-CI-1
SE-P-M-NG-1	----------	EG-S-L-NG-1
SE-S-H-NG-1	----------	----------
EG-S-M-NG-1	----------	----------
EG-S-H-NG-1	----------	----------

3.2 HALF-CELL POTENTIAL READINGS

Three half-cell potential readings were made on each specimen at the start of each of the dry and wet periods of the cycles, as explained in Section 2.4.2. When this data was examined for each specimen, little or no difference was observed between the three readings and thus only the half-cell potential readings immersed in the salt solution were plotted. The ASTM C876[29] guidelines of 130 mV and -280 mV (Table 2.4) are shown on each figure.

The half-cell potential measurements suggest a medium to high probability of corrosion for twelve specimens, including all dry joint specimens, three epoxy joint specimens (SE-S-M-NG-1, SE-S-M-CI-1, SE-S-H-CI-1), and two epoxy joint specimens with gasket (EG-S-L-NG-1, EG-S-H-NG-1).

As with the corrosion current plots, half-cell potential readings over time were plotted for all nineteen specimens after eight years of very aggressive exposure, grouped according to test variables, and included in Appendix A. Figures 3.5 to 3.8 show examples of corrosion current plots comparing joint type, duct type, joint precompression and grout type, respectively. Figures A.14 to A.26 complement those presented herein. The specimens plotted in each figure correspond to the same specimens in Figure 3.1 through Figure 3.4, and Figure A.1 through A.13, respectively. Table 3.2 summarizes the general results based on half-cell readings, according to ASTM C876.

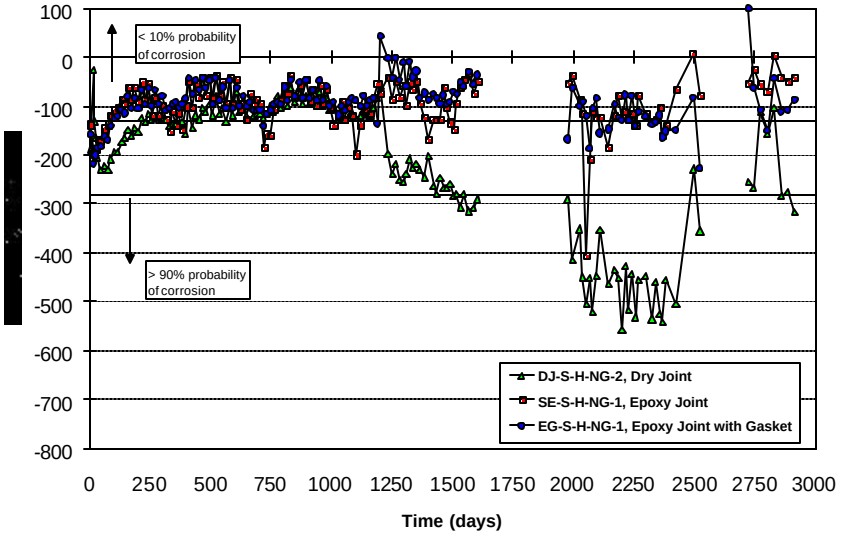

Figure 3.5 Half-Cell Potentials: Dry, Epoxy and Epoxy with Gasket Joints, Steel Duct, High Precompresion and Normal Grout.

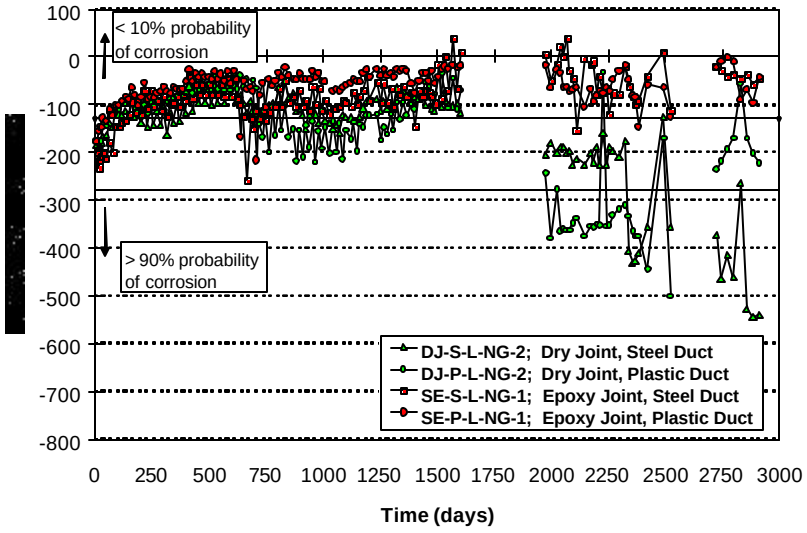

Figure 3.6 Half-Cell Potentials: Dry and Epoxy Joint, Plastic and Steel Duct, Low Precompression, and Normal Grout.

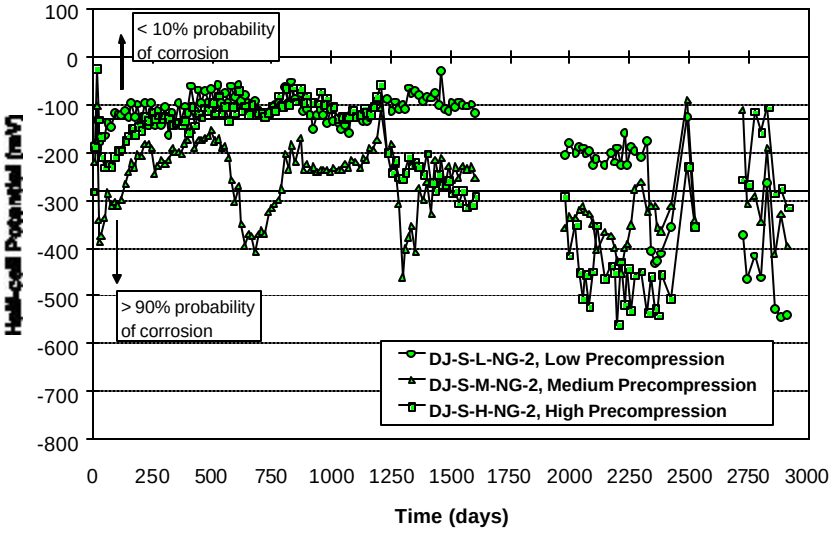

Figure 3.7 Half-Cell Potentials: Dry Joint, Steel Duct, Low, Medium and High Precompression, and Normal Grout.

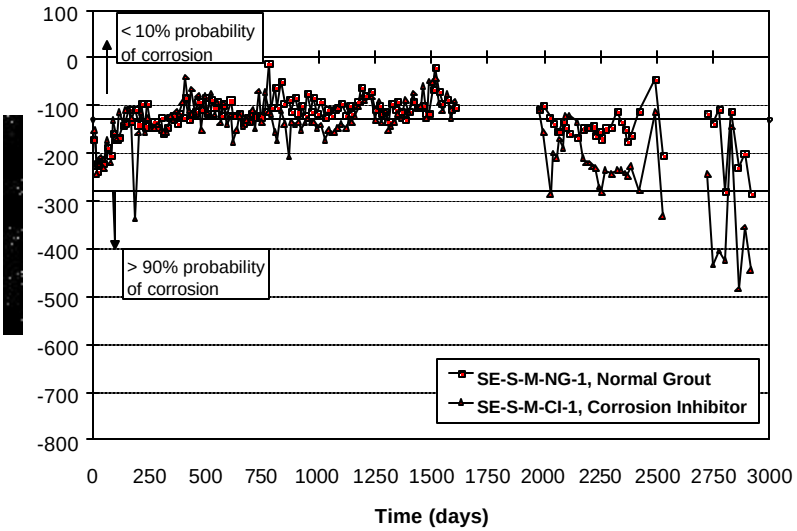

Figure 3.8 Half-Cell Potentials: Epoxy Joint, Steel Duct, Medium Precompression, and Different Grouts (Normal, and Corrosion Inhibitor Added).

Table 3.2 Half-cell Potential results (Based on ASTM C876[29], See Table 2.4).

Less than 10% probability of corrosion	Between 10% to 90% probability of corrosion	More than 90% probability of corrosion
SE-P-L-NG-1	DJ-S-M-CI-2	DJ-S-L-NG-2
SE-S-L-CI-1	SE-S-M-NG-1	DJ-S-M-NG-2
SE-S-L-SF-1	EG-S-L-NG-1	DJ-S-H-NG-2
SE-S-L-NG-1	EG-S-H-NG-1	DJ-S-L-CI-2
SE-P-M-NG-1	----------	DJ-P-L-NG-2
SE-S-H-NG-1	----------	DJ-P-M-NG-2
EG-S-M-NG-1	----------	SE-S-M-CI-1
----------	----------	SE-S-H-CI-1

3.3 ANALYSIS AND DISCUSSION OF EXPOSURE TEST RESULTS

3.3.1 Time to Initiation of Corrosion

The relative length of exposure before corrosion initiation is detected may be used to compare the effectiveness of corrosion protection variables. For the purposes of this research program, the initiation of corrosion is defined as:

a) a sudden and significant increase (in the order of 0.003 mA and above) in measured corrosion current, and/or

b) half-cell potential measurements more negative than -280 mV, and/or

c) a sudden and significant change (in the order of -100 mV) more negative in half-cell potential

Criterion (a) is evaluated by examining the plots of macrocell corrosion current over time for a significant increase in corrosion current. Criteria (b) is based on the guidelines of ASTM C876,[29] as described in Section 2.4.2. However, the non-typical details of the macrocell specimens in this program may affect the reliability of the ASTM C876 guidelines, and corrosion may occur at potentials less negative than -280 mV. For this reason, Criterion (c) is included, where plots of half-cell potential over time are examined for a significant change more negative.

Based on corrosion current readings, ten specimens displayed some amount of increased corrosion activity or an initiation of corrosion, as described in Section 3.1, and shown in Figures 3.1 through Figure 3.4, and Figures A.1 through Figure A.13. Half-cell potential readings include two additional specimens, for a total of twelve specimens showing increased corrosion activity, as described in Section 3.2, and shown in Figures 3.5 through 3.6, and Figures A.14 through A. 26. Using these plots and the above definitions for corrosion initiation, the approximate time to the initiation of corrosion for these specimens are listed in Table 3.3. The initiation of corrosion based on macrocell corrosion current was very clear for all specimens. The times to corrosion based on half-cell potentials was estimated using Criterion (b) for most specimens. In some cases, it was apparent that Criterion (c) better indicated the onset of corrosion. Examples include specimens DJ-S-M-CI-2, DJ-S-H-NG-2, DJ-P-M-NG-2, EG-S-L-NG-1, and EG-S-H-NG-1.

From Table 3.3, it is observed that most specimens show a good correlation between times to corrosion initiation based on macrocell current and half-cell potential. However, four specimens show different corrosion initiation times, these are: DJ-S-M-CI-2, SE-S-M-CI-1, SE-S-H-CI-1, EG-S-L-NG-1. For these specimens, half-cell corrosion initiation dates correspond to the period when corrosion current readings

were interrupted (period defined between 1598 days to 2333 days after exposure testing was initiated), as was indicated previously in this chapter. However, as it is observed in the plots that have been referred to above and in Table 3.3, corrosion current readings at 2333 days were not able to show any corrosion activity in those specimens. This suggests that analysis based on corrosion current readings did not fail to detect the corrosion initiation time based on the available data.

Table 3.3. Time to Initiation of Corrosion for Specimens Autopsied at Eight Years of Exposure.

Specimen Name	Time to Corrosion		Comments
	Macrocell Current	Half-Cell Potentials	
DJ-S-L-NG-2	2347 days	2340 days	- strand is corroding - very high corrosion currents after corrosion initiation.
DJ-S-M-NG-2	580 days	588 days	- strand is corroding - three distinct periods of corrosion activity
DJ-S-H-NG-2	1250 days	1225 days	- mild steel bars are corroding
DJ-P-L-NG-2	710 days	714 days	- mild steel bars corroding - two distinct periods of corrosion activity
DJ-P-M-NG-2	640 days	644 days	- data up to 1598 days
DJ-S-L-CI-2	2782 days	2788 days	- strand is corroding - corrosion current is very small
DJ-S-M-CI-2	2717 days	2187 days	- mild steel bars are corroding - corrosion current is very small - two distinct periods of corrosion activity based on HC potentials (after 2187 days and 2725 days)
SE-S-M-NG-1	NS	2802 days	- NS: No signs of corrosion initiation.
SE-S-M-CI-1	2431 days	2026 days	- strand is corroding
SE-S-H-CI-1	2347 days	2061 days	- mild steel bars are corroding - corrosion current is very small
EG-S-L-NG-1	2431 days	2096 days	- mild steel bars are corroding - corrosion current is very small
EG-S-H-NG-1	NS	1977 days	- NS: No signs of corrosion initiation.

As a reference, Table 3.4 contains those macrocell specimens that were autopsied at four and one and half years of exposure testing, which had showed sings of corrosion activity based on macrocell corrosion currents and half-cell Potentials. The complete details for these series are included in Reference 26.

Table 3.4. Time to Initiation of Corrosion for Specimens Autopsied at Four and One Half Years of Exposure.[15,26]

Specimen Name	Time to Corrosion		Comments
	Macrocell Current	Half-Cell Potentials	
DJ-S-L-NG-1	128 days	129 days	- strand is corroding - corrosion current reduced to zero after 400 days
DJ-S-M-NG-1	1110 days	1110 days	- strand is corroding - corrosion current reduced to zero near 1600 days
DJ-S-H-NG-1	615 days	616 days	- mild steel bars are corroding
DJ-S-L-CI-1	580 days	714 days	- strand is corroding
DJ-S-M-CI-1	833 days	842 days	- mild steel bars are corroding - two distinct periods of corrosion activity
DJ-P-L-NG-1	1250 days	1225 days	- mild steel bars are corroding
DJ-P-M-NG-1	565 days	560 days	- mild steel bars are corroding - corrosion current decreased to zero after 950 days
SE-S-M-NG-2	1330 days	1337 days	- mild steel bars are corroding - corrosion current is very small

The length of time to corrosion for each of the twelve specimens showing activity does not suggest any trend between time to corrosion and levels of precompression, although conceptually, higher precompression may be expected to limit moisture and chloride ion penetration at the joint.

Corrosion inhibitor in grout appear to positively affect the time to corrosion, when comparing Specimens DJ-S-L-NG-2 and DJ-S-M-NG-2 with Specimens DJ-S-L-CI-2 and DJ-S-M-CI-2, respectively. However, this trend is contradicted when comparing Specimen SE-S-M-NG-1 with Specimen SE-S-M-CI-1.

Epoxy joint Specimen SE-S-M-NG-1, shows a longer time for corrosion initiation when compared to dry joint Specimen DJ-S-M-NG-2; however, this trend is contradicted when comparing Specimens SE-S-M-CI-1 and DJ-S-M-CI-2.

After carefully analyzing the reasons for the above contradictions with respect to the expected trends and results, it is deducted that this is due to the poor performance shown for Specimen SE-S-M-CI-1. This conclusion suggests that an additional variable may be affecting this specimen, which is not fully understood based on nondestructive evaluations (macrocell currents and half-cell potentials). Total autopsy of this specimen is expected to reveal the cause.

3.3.2 General Behavior over Exposure Time

3.3.2.1 Macrocell Currents

Table 3.5 summarizes the general test results from macrocell current plots, when main test variables are compared after eight years of aggressive exposure.

Table 3.5. General Macrocell Current Results.

Main Variable	Reference Plots	General Results
Joint Type	Figure 3.1 and Figures A.1, A.2, A.3, A.4	SE specimens show less corrosion currents than EG specimens. EG specimens show less corrosion currents than DJ specimens. Exception: SE-S-M-CI-1.
Duct Type	Figure 3.2 and Figure A.5	DJ specimens with plastic duct clearly show less corrosion currents (with reversed macrocell behavior) than DJ specimens with steel duct (active strand corrosion).
Joint Precompression	Figure 3.3 and Figures A.6, A.7, A.8, A.9	No clear trend is shown with respect to joint precompression.
Grout Type	Figure 3.4 and Figures A.10, A.11, A.12, A.13	Specimens with CI show in general less corrosion currents than NG specimens, with reversed macrocell behavior in most cases. Exception: SE-S-M-CI-1.

DJ: Dry Joint; SE: Epoxy Joint; EG: Epoxy Joint with Gasket; CI: Corrosion Inhibitor; NG: Normal Grout

3.3.2.2 Half-Cell Potentials

Table 3.6 summarizes the general test results from Half-Cell Potential Plots, when main test variables are compared after eight years of aggressive exposure.

Table 3.6. General Half-Cell Potential Results.

Main Variable	Reference Plots	General Results
Joint Type	Figure 3.5 and Figures A.14, A.15, A.16, A.17	SE and EG specimens show less probability of strand corrosion than DJ specimens. Exception: SE-S-M-CI-1.
Duct Type	Figure 3.6 and Figure A.18	DJ and SE specimens with plastic duct (discontinuous at the joint) show less probability of strand corrosion than similar specimens with steel duct.
Joint Precompression	Figure 3.7 and Figures A.19, A.20, A.21, A.22	DJ specimen data indicate less probability of strand corrosion with increasing levels of precompression. This trend is not observed in SE specimens due to behavior of specimen SE-S-M-CI-1. No clear trend is shown in EG specimens with respect to joint precompression.
Grout Type	Figure 3.8 and Figures A.23, A.24, A.25, A.26	DJ specimens with CI show less probability of strand corrosion with respect to specimens with NG. The contrary is found in SE specimens where more probability of strand corrosion is shown in specimens with CI than those with NG, these include specimen SE-S-M-CI-1 and specimen SE-S-H-CI-1.

DJ: Dry Joint; SE: Epoxy Joint; EG: Epoxy Joint with Gasket; CI: Corrosion Inhibitor; NG: Normal Grout

3.3.3 Corrosion Rate or Severity

Corrosion severity is commonly evaluated in three ways using measured macrocell corrosion currents: weighted average corrosion current, corrosion current density and metal loss.

3.3.3.1 Weighted Average Corrosion Current

The weighted average corrosion current over the duration of testing, I_{wa}, was computed using the following expression:

$$I_{wa} = \frac{\sum I_{ai} T_i}{\sum T_i} \qquad i = 1, n \qquad \textit{Eq. 3.1}$$

where,

I_{ai} = average current in time interval i

T_i = duration of time interval i

n = number of measurements

The effect of different time intervals between readings requires a weighted average. Table 3.8 gives weighted averages for the active specimens. ASTM G109[27] defines failure as an average corrosion current of 10 μA (0.010 mA). All specimens except specimen DJ-S-L-NG-2 are below this value.

3.3.3.2 Corrosion Current Density

The corrosion current density is the amount of corrosion current per unit surface area of the anode, calculated as the weighted average corrosion current divided by the total anode surface area.

$$\text{Corrosion Current Density} = \frac{I_{wa}}{A_{surf}} \ (\mu A / cm^2) \qquad \textit{Eq. 3.2}$$

The anode surface area (A_{surf}) is taken as the total (nominal) surface area of the anode bar, assuming that corrosion is occurring over the entire exposed length of the anode. For this testing program, the non-typical macrocell specimens make estimation of the anode surface area very difficult. If the strand is the anodic site, the total surface area is computed as the sum of the surface areas of each of the 7 wires of the strand. The presence of the duct and segmental joint raise further questions as to whether corrosion will occur over the exposed length of strand. For specimens in which the corrosion macrocell is reversed the anode cross-sectional area is the area of the two reinforcing bars. However, chlorides may not have reached the entire bar length.

The uncertainty surrounding the computation of A_{surf} significantly affects the usefulness of calculated values of corrosion current density. For analysis purposes, the following values of A_{surf} were used:

For normal macrocell corrosion: (positive I_{wa})	use A_{surf} based on total surface area of 7 wires (5 in. exposed length)
For reversed macrocell corrosion: (negative I_{wa})	use A_{surf} based on surface area of two 0.5 in. (#4) bars (5 in. exposed length)

Guidelines have been proposed[30,31,32] to assess the rate of corrosion based on corrosion current densities, as shown in Table 3.7. Calculated values of corrosion current density are shown in Table 3.8. The computed corrosion current densities for all specimens are within the range of negligible corrosion, except for specimen DJ-S-L-NG-2 that falls in the range of moderate corrosion. However, because the corroded surface area is uncertain, overestimation of A_{surf} could produce unconservative results.

Table 3.7 Corrosion Severity Based on Current Density.[30,31,32]

Corrosion Current Density	Corrosion Severity
Less than 0.1 μA/cm^2	Negligible
Between 0.1 and 0.2 μA/cm^2	Low (threshold for active deterioration mechanism)
Between 0.2 and 0.5 μA/cm^2	Moderate

3.3.3.3 Metal Loss

The amount of steel "consumed" by macrocell corrosion is directly related to the total amount of electrical charge, or number of electrons, exchanged between the anode and cathode. One amp of corrosion current consumes 1.04 grams of steel (iron) per hour.[33] The total amount of current passed, or charge flux, is computed by numerically integrating the macrocell corrosion current data over the duration of exposure. Although an absolute measurement of corrosion severity is difficult to obtain using metal loss (charge flux), a relative comparison of corrosion severity between specimens is possible. Calculated values of metal loss are listed in Table 3.8.

Table 3.8 Calculated Weighted Average Current, Current Density and Metal Loss for Active Specimens after Eight Years of Exposure.

Specimen No.	Specimen Name	Weighted Average Corrosion Current (mAmps)	Corrosion Current Density (mA/cm^2)	Metal Loss (mg)
	DJ-S-L-NG-2	29.417	0.253	2135
	DJ-S-M-NG-2	2.572	0.022	187
	DJ-S-H-NG-2	-6.392	0.064	464
	DJ-S-L-CI-2	0.068	0.001	5
	DJ-S-M-CI-2	-0.422	0.004	31
	DJ-P-L-NG-2	-6.475	0.065	470
	SE-S-M-CI-1	2.664	0.023	193
	SE-S-H-CI-1	-0.266	0.003	19
	EG-S-L-NG-1	-0.211	0.002	15

Note: Negative average corrosion current indicates mild steel bars are corroding.
Specimen DJ-P-M-NG-2 due has been excluded. See discussion in Section 3.1.

As mentioned in Section 3.3.3.1, ASTM G109[27] defines failure as an average macrocell corrosion current over the duration of testing of more than 10 μA. For an average corrosion current of 10 μA and the exposure duration of eight years, a metal loss of 729 milligrams (10^-5 Amp. x 1.04 g/hour x 70080 h x 1000mg/g) would be expected. Only specimen DJ-S-L-NG-2 is above this value. Slightly below are specimens DJ-P-L-NG-2 and DJ-S-H-NG-2 with mild steel metal loss close to 465 mg corresponding to a weighted average corrosion current of approximately 6.4 μA; and, below are specimens DJ-S-M-NG-2 and SE-S-M-CI-1 with strand metal loss close to 190 mg corresponding to a weighted average corrosion current of approximately 2.6 μA. The other macrocell specimens are below 1 μA, with only very minor corrosion activity.

3.3.3.4 Discussion: Corrosion Rate Calculations

The corrosion rate calculations for weighted average corrosion current, corrosion current density, and metal loss indicate that the corrosion activity is important for Specimen DJ-S-L-NG-2, and moderately important for Specimens DJ-S-M-NG-2, DJ-S-H-NG-2, DJ-P-L-NG and SE-S-M-CI-1. For all other specimens, corrosion activity is considerably lower than what would be defined as failure.

The calculated corrosion rates using the three different methods are plotted in Figure 3.9 through Figure 3.11 where the relative performance of the nine specimens included in Table 3.8 is the same for all three cases. All three corrosion rate calculations are related to the charge flux or the number of electrons exchanged between the anode and cathode. The charge flux is calculated by integrating the corrosion current over time:

$$\text{Charge Flux} = \int I_{corr}\,dt \equiv \sum I_{ai} T_i \quad (i = 1, n) \quad \text{(Coulombs)} \qquad \textit{Eq. 3.3}$$

where,
- I_{corr} = instantaneous corrosion current
- I_{ai} = average current in time interval i
- T_i = duration of time interval i
- n = number of measurements

The calculation of charge flux appears in the computation of weighted average corrosion current, current density and metal loss:

$$\text{Weighted Avg. Current, } I_{wa} = \frac{\int I_{corr}\,dt}{t_d} \equiv \frac{\sum I_{ai} T_i}{\sum T_i} \quad \text{(amps)}$$

$$\text{Current Density} = \frac{I_{wa}}{A_{surf}} \equiv \frac{\int I_{corr}\,dt}{t_d} \times \frac{1}{A_{surf}} \quad (\text{amps}/\text{cm}^2)$$

$$\text{Metal Loss} = \int I_{corr}\,dt \times \left(\frac{1\ \text{hr}}{3600\ \text{sec}} \times \frac{1.04\text{g}}{\text{amp} - \text{hr}} \times \frac{1000\text{mg}}{\text{g}} \right) (\text{mg})$$

where,
- t_d = duration of testing
- A_{surf} = corroded surface area

In general, any one of the three forms of corrosion rate calculations would be appropriate for comparing the performance of the protection variables. Calculated metal loss will be used for discussion purposes in the remainder of this document.

The corrosion rate calculations provide a means for relative comparison of corrosion activity in the different specimens. However, it is difficult to use the calculated corrosion rates to obtain an absolute measure of corrosion severity. Corrosion current density can be used for this purpose if the area over which corrosion is occurring is known. The non-typical details of the segmental macrocells make estimation of the corroded surface area uncertain at best, and thus the use of corrosion current density to assign a corrosion severity using Table 3.7 is questionable for this testing program.

The effect of the different variables (other than joint type) is not clear based on the calculated corrosion rates (Figures 3.9 through Figure 3.11). However, data suggests that a higher level of precompression or protection to the strand (in the case of plastic ducts or corrosion inhibitor in grout), somewhat produces a higher tendency of reversed macrocell behavior, which may relate to lower strand corrosion.

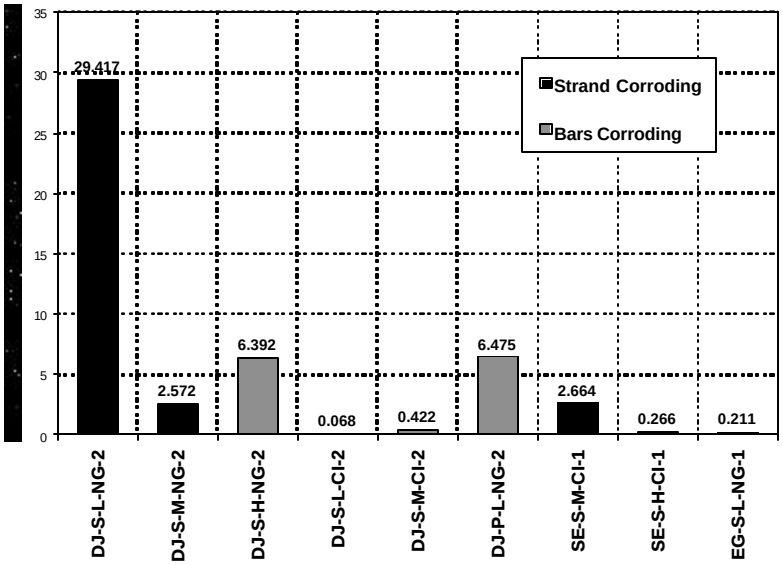

Figure 3.9 Calculated Weighted Average Corrosion Current for Active Specimens after Eight Years of Exposure.

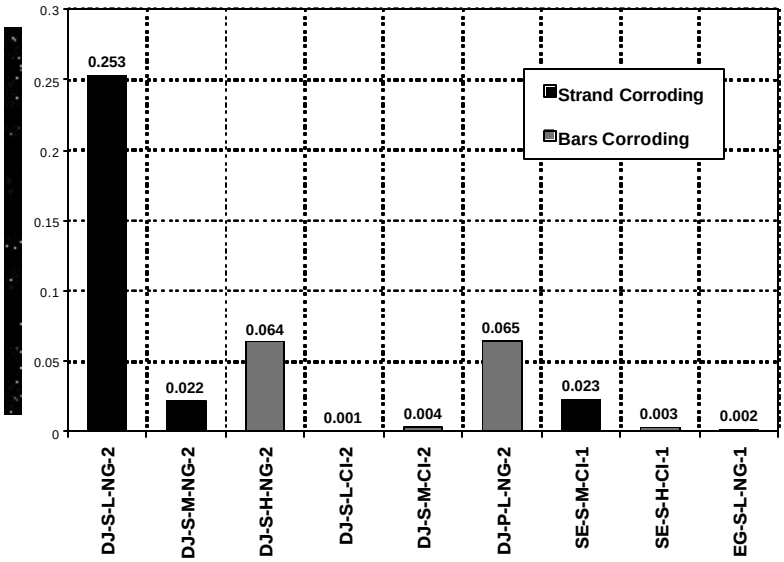

Figure 3.10 Calculated Corrosion Current Densities for Active Specimens after Eight Years of Exposure.

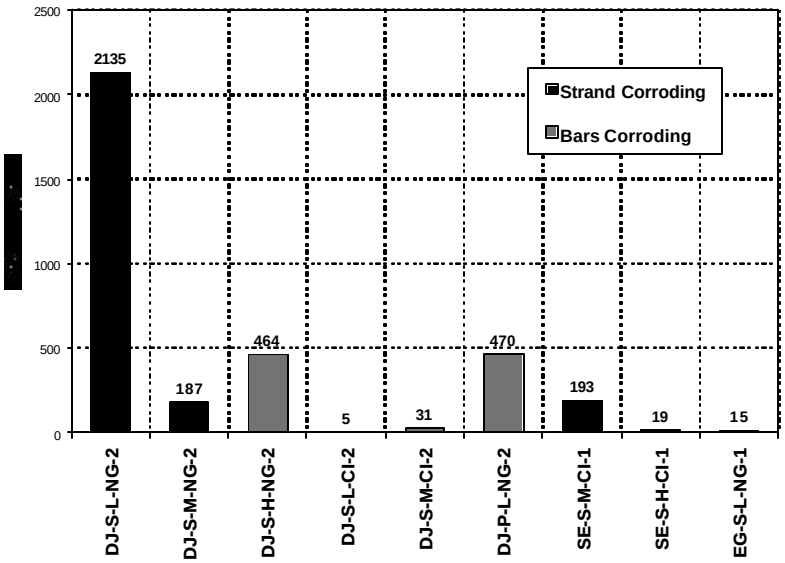

Figure 3.11 Calculated Metal loss for Active Specimens after Eight Years of Exposure.

CHAPTER 4:
FORENSIC EXAMINATION

After 2920 days of exposure (taking place over eight years), the remaining 19 specimens out of the initial 38 were removed from testing for forensic examination or autopsy. The previous 19 specimens had been autopsied three and a half years before, at 1603 days of exposure. The objectives of the forensic examinations are as follows:

1. Obtain visual evaluation of corrosion damage on duct, strand and mild steel reinforcement.
2. Obtain visual evaluation of joint condition.
3. Determine chloride ion penetration at locations adjacent to and away from the segmental joint.
4. Examine mechanisms of corrosion in segmental macrocell corrosion specimens.

The notation scheme shown in Figure 4.1 was assigned for record keeping purposes. "Clamp end" refers to the end of the specimen where ground clamps were attached to complete the macrocell circuit. Segment B was cast first. Segment A was match –cast against Segment B. All specimens were numbered on Side C at the clamp end. This marking ensured that the orientation of all specimens was known throughout the forensic examination process. The notation scheme will be referred to throughout this chapter.

The following Sections 4.1 through 4.3 have been repeated from Reference 15, with only minor changes, as they refer to the same procedure followed in the first autopsy, at four years and five months of aggressive exposure.

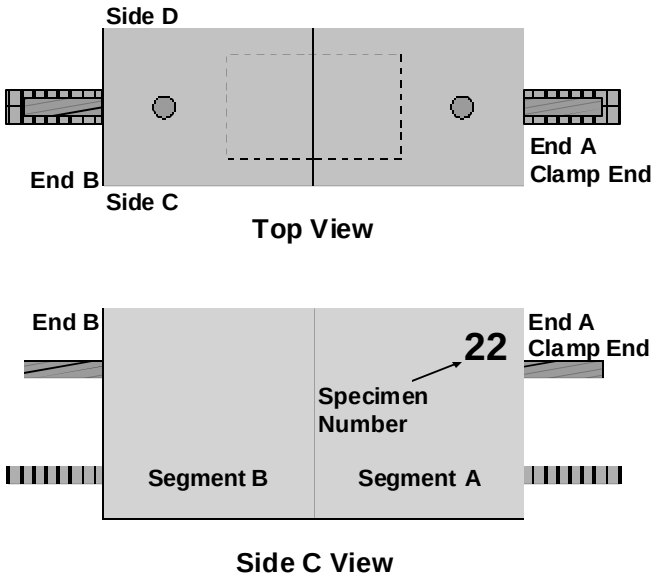

Figure 4.1 Specimen Labeling Scheme.

4.1 PROCEDURE

4.1.1 Specimen Condition at End of Testing

The exterior surfaces of each specimen were examined for cracking and rust staining upon removal from testing. Duct ends were examined for grout voids and rust stains. The joint perimeter was examined for visible salt stains, joint epoxy and grout.

4.1.2 Concrete Powder Samples for Chloride Analysis

One of the objectives of the forensic examination was to determine the influence of the three joint types on the penetration of moisture and chlorides. It was expected that chloride contents could be higher in the vicinity of the joint, particularly for dry joint specimens. To examine the influence of joint type on chloride penetration, concrete powder samples were collected at multiple depths and locations to determine chloride ion profiles adjacent to the joint and away from the joint. Sample locations are shown in Figure 4.2. Concrete powder samples were collected using a rotary hammer and following a procedure based on AASHTO T 260-94.[34] Two 1.5 g samples were collected at each depth. Samples were analyzed for acid soluble chlorides using a specific ion probe (CL Test System by James Instruments).

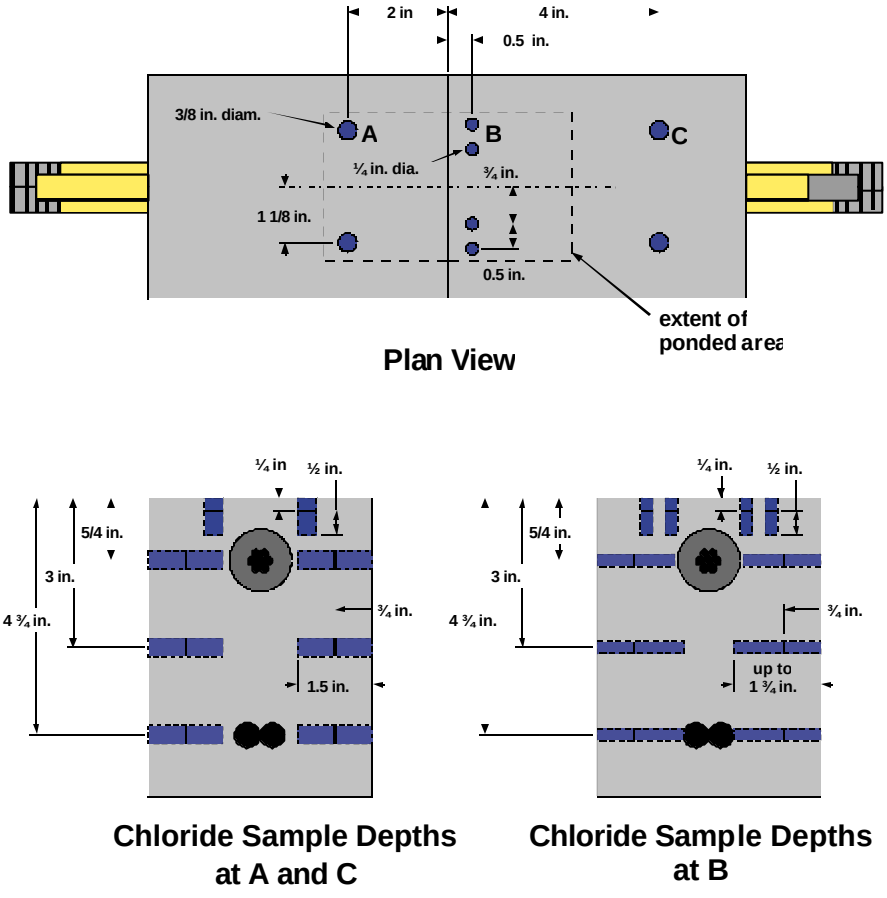

Figure 4.2 Chloride Sample Locations.

4.1.2.1 Location A

Samples at A were taken at a distance of 2 in. from the segmental joint using a 3/8 in. diameter drill bit. Two holes were drilled at each depth to later averaged the chloride content results. The first sample was taken on the top surface of the specimen. Initially, the holes were drilled to a depth of 0.25 in. The holes and bit were then cleaned, and the holes were drilled an additional depth of 0.5 in. An average depth of 0.5 in. was assumed for this sample. The remaining three samples at location A were obtained by drilling into the sides of the specimen. One hole was drilled into each side of the specimen at the desired depths. The holes were drilled to an initial depth of 0.75 in. so that the collected sample will be from concrete directly below the ponded area. Following cleaning, the holes were drilled an additional 0.5 to 0.75 in. to obtain the sample amount (total depth up to 1.5 in.).

4.1.2.2 Location B

Samples at B were collected at a distance of 0.5 in. from the segmental joint. Due to the close proximity of the joint, a smaller bit size of 0.25 in. was used for these samples. The procedure for obtaining the powder samples at location B was similar to that at location A with some minor modifications due to the smaller drill bit size. Four holes were required for the two samples on the top surface of the specimen, and the holes for the other samples were drilled slightly deeper (up to 1.75 in.) to obtain the necessary sample amount.

4.1.2.3 Location C

Samples at C were taken at a distance of 4.25 in. from the segmental joint. The procedure for collecting samples at C is identical to that for samples at A.

4.1.3 Longitudinal Saw Cuts

Four longitudinal saw cuts were made on each specimen to facilitate removal of the duct/strand unit and mild steel bars. Saw cuts were made to a depth of 1.5 in. at the level of the tendon and bars, as shown in Figure 4.3. These cuts are referred to as the strand cut line and bar cut line respectively. The specimen remained intact after cutting, but was easily opened using a hammer and chisel. Saw cuts were performed using a high torque circular saw fitted with a diamond dry-cut concrete blade as shown in Figure 4.4. Some cracked samples needed to be wrapped with duct tape to permit cutting of the specimen.

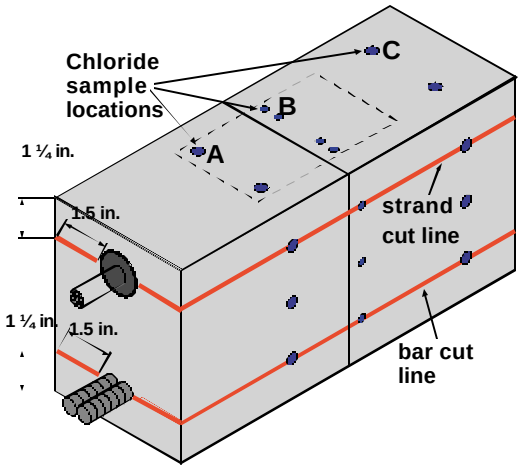

Figure 4.3 Longitudinal Saw Cuts.

4.1.4 Expose and Remove Duct and Strand

The duct was exposed by opening the specimen at the strand cut line, as shown in Figure 4.4. The duct and strand were then removed from the concrete as one unit. The concrete surrounding the duct was examined for voids, cracks, rust staining, salt collection and damage. After thorough examination, the duct was cut open by making two longitudinal cuts along the sides of the duct/strand unit using a small air-driven grinder. The grout was examined for voids and cracks and indications of moisture and chloride ingress. If desired, grout samples were taken from the grout for chloride analysis at this time (see Section 4.1.5). The grout was then carefully removed, exposing the strand for examination. The extent and severity of corrosion on both the strand and duct was rated according to the corrosion rating scheme described in Section 4.3.

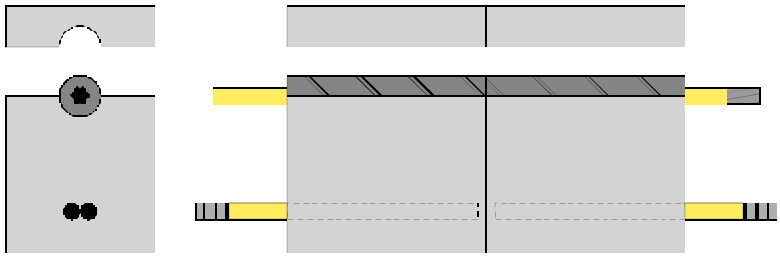

Figure 4.4 Specimen Opened to Expose Duct/Strand.

4.1.5 Grout Samples for Chloride Analysis

Grout samples were collected from selected specimens for chloride analysis. Samples were carefully removed from the strand at the location of the joint and at a distance of 2 in. from the joint. The grout pieces were crushed between two steel plates and ground into powder using a mortar and pestle. Grout powder samples were analyzed for acid soluble chlorides using a specific ion probe (CL Test System by James Instruments).

4.1.6 Expose and Remove Mild Steel

The mild steel bars were exposed by opening the specimen at the bar cut line, as shown in Figure 4.5. The bars were then removed from the concrete for examination. The extent and severity of corrosion on the bars was rated according to the corrosion rating scheme described in Section 4.3.2. The concrete surrounding the bars was examined for voids, rust staining, salt collection and any damage.

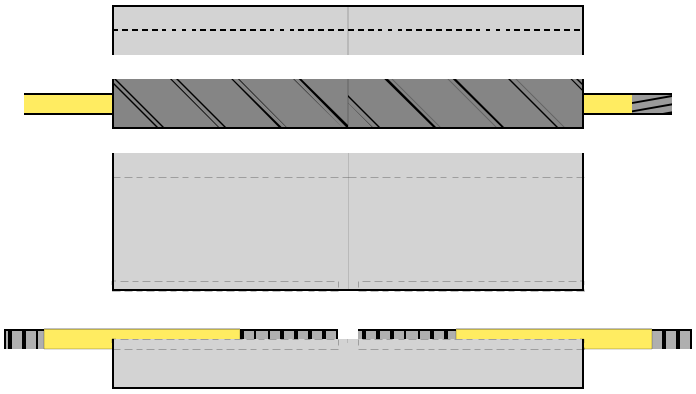

Figure 4.5 Specimen Opened to Expose Mild Steel Bars.

4.1.7 Examine Joint Condition

In the dry joint specimens, the specimen readily separated into its two segments after the duct/strand unit was removed (Section 4.1.4). This separation allowed the condition of the joint face to be examined directly for cracking, rust staining, evidence of moisture and chloride penetration and general soundness of the joint.

The intention of the epoxy joint is to bond the two segments together. As a result, it was not possible to examine the joint in the same manner as the dry joint specimens. An indication of the epoxy joint condition was obtained by examining several sections through the joint, as shown in Figure 4.6. The saw cuts at the strand line and bar line (Section 4.1.3) revealed the epoxy joint condition at sections 1 and 3 in Figure 4.6. An addition longitudinal saw cut was made at the mid-height of the specimen to obtain a third section through the joint (Joint Section 2 in the figure). The joint was also examined around the perimeter of the specimen. The joint sections were examined for indications of voids in the epoxy or the presence of moisture, salt or corrosion products.

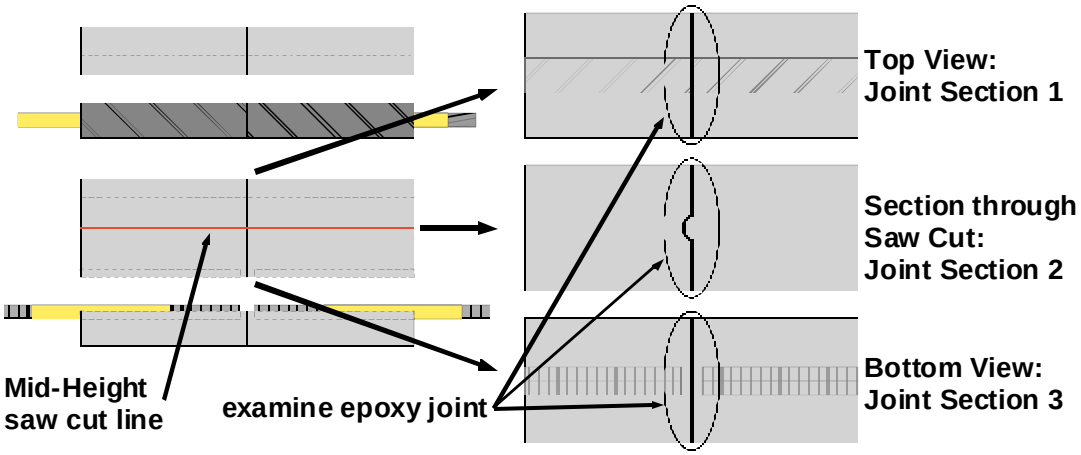

Figure 4.6 Examining Epoxy Joint Condition.

4.2 AUTOPSY PROGRAM

The remaining specimen from each duplicate pair of specimen types was finally prepared for forensic examination.

Chloride samples were collected from ten of the nineteen specimens autopsied, in order to coincide with the specimen pair that was analyzed previously. The ten specimens were selected out of the nineteen to provide a representative sample and address the major variables expected to influence chloride penetration. The mid-height cut for epoxy-jointed specimens was performed on six of the twelve specimens with epoxy joints. Specimens selected were standard epoxy joints and epoxy/gasket joints at each of the three levels of joint precompression. Details of the nineteen specimens selected for autopsy are listed in Table 4.1.

Table 4.1 Specimens Selected for Forensic Examination.

Specimen	Time to Corrosion	Corrosion Location	Chloride Samples	Mid-Height Cut
DJ-S-L-NG-2	2347 days	Strand	A, B, C	n/a
DJ-S-M-NG-2	580 days	Strand	A, B	n/a
DJ-S-H-NG-2	1250 days	Bars	A, B	n/a
DJ-P-L-NG-2	710 days	Bars	A, B	n/a
DJ-P-M-NG-2	640 days	Bars	None	n/a
DJ-S-L-CI-2	2782 days	Strand	A, B	n/a
DJ-S-M-CI-2	2717 days	Bars	A, B	n/a
SE-S-L-NG-1	n/a	n/a	A, B, C	Yes
SE-S-M-NG-1	n/a	n/a	A, B	Yes
SE-S-H-NG-1	n/a	n/a	A, B	Yes
SE-P-L-NG-1	n/a	n/a	None	No
SE-P-M-NG-1	n/a	n/a	None	No
SE-S-L-CI-1	n/a	n/a	None	No
SE-S-M-CI-1	2431 days	Strand	None	No
SE-S-H-CI-1	2347 days	Bars	None	No
SE-S-L-SF-1	n/a	n/a	None	No
EG-S-L-NG-1	2347 days	Bars	A, B	Yes
EG-S-M-NG-1	n/a	n/a	None	Yes
EG-S-H-NG-1	n/a	n/a	none	Yes

4.3 EVALUATION AND RATING OF CORROSION FOUND DURING FORENSIC EXAMINATION

A generalized evaluation and rating system was developed to quantify the severity and extent of corrosion damage in the test specimens. The procedure is presented in a universal form with the intention of applying the same rating system to other situations. The length of strand, mild steel reinforcement or galvanized steel duct was subdivided into eight increments. At each increment, the steel was examined and a rating was assigned to describe the corrosion severity within that increment. The ratings for the eight increments were summed to give a total corrosion rating for the element that could be compared for different specimens. By assigning a corrosion severity at eight locations, both the extent and severity of corrosion is considered.

The corrosion severity ratings are described below. The rating system is essentially the same for prestressing strand, mild steel reinforcement and galvanized duct, with some modifications to reflect unique corrosion aspects of each type of steel. In general, the evaluation system doubles the severity rating for each category of increasing corrosion damage.

4.3.1 Prestressing Strand

The strand was examined at eight intervals, as indicated in Figure 4.7. The interval sizes have been adjusted to provide four intervals in the unpainted region of the strand, and two intervals in each of the painted regions at both ends. Corrosion ratings were assigned to indicate the severity of corrosion on the outer six wires of the strand and on the center wire (after de-stranding) at each interval to address the possibility of different corrosion activity on the strand exterior and interstices between wires. The

corrosion rating system for prestressing strand is described in Table 4.2. The total strand corrosion rating was calculated as follows:

$$\text{Strand Corrosion Rating} = \sum_{i=1}^{8} R_{outer,i} \times n_i + R_{center,i} \qquad \textit{Eq. 4.1}$$

where,
$R_{outer,i}$ = outer wires corrosion rating, interval i
n_i = number of corroded outer wires, interval i
$R_{center,i}$ = center wire corrosion rating, interval i
i = interval, 1 to 8

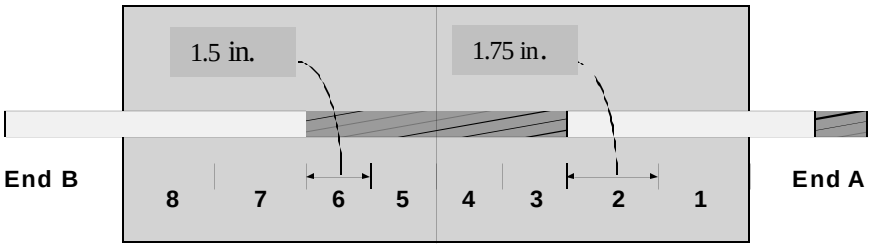

Figure 4.7 Intervals for Corrosion Ratings on Prestressing Strand.

The corrosion rating system for prestressing strand was adapted from Poston[35] and Hamilton.[36] The use of a cleaning pad to assess corrosion severity was proposed by Sason[37] for classifying the degree of rusting on prestressing strand for new construction. The recommended cleaning pad is a 3M Scotch Brite cleaning pad. The pad is held by hand and rubbed longitudinally along the strand axis with a pressure similar to that used when cleaning pots and pans. The classification of pitting severity was based on tensile tests performed on corroded prestressing strand.[38] The tests were used to assign a reduced tensile capacity of 97% GUTS to pitting damage at the level of P1. Moderate pitting (P2) was assigned a capacity of 90% GUTS, and severe pitting (P3) 77% GUTS. In general, the presence of any pitting visible to the unaided eye is deemed cause for rejection in new construction.[37]

Table 4.2 Evaluation and Rating System for Corrosion Found on Prestressing Strand.

Code	Meaning	Description	Rating
NC	No Corrosion	No evidence of corrosion.	0
D	Discoloration	No evidence of corrosion, but some discoloration from original color.	1
L	Light	Surface corrosion on less than one half of the interval, no pitting. Surface corrosion can be removed using cleaning pad.	2
M	Moderate	Surface corrosion on more than one half of the interval, no pitting. **and/or** Corrosion can not be completely removed using cleaning pad.	4
P1	Mild Pitting	Broad shallow pits with a maximum pit depth not greater than 0.02 in.	8
P2	Moderate Pitting	Pitting where the maximum pit depth ranged between 0.02 and 0.04 in.	16
P3	Severe Pitting	Pitting where the maximum pit depth is greater than 0.04 in.	32

4.3.2 Mild Steel Reinforcement

The mild steel reinforcing bars were examined at eight intervals, as indicated in Figure 4.8. The interval sizes have been adjusted to provide four intervals in the unpainted region of the bars, and two intervals in the painted regions at both ends. Corrosion ratings were assigned to indicate the severity of corrosion on the top and bottom surfaces of each bar to reflect the possibility of different corrosion severity and extent. The corrosion rating system is described in Table 4.3. The total bar corrosion rating was calculated as follows:

$$\text{Bar Corrosion Rating} = \sum_{i=1}^{8} R_{Bar1Top,i} + R_{Bar1Bot,i} + R_{Bar2Top,i} + R_{Bar2Bot,i} \qquad \textit{Eq. 4.2}$$

where,

$R_{Bar1Top,i}$ = Bar 1, top surface corrosion rating, interval i
$R_{Bar1Bot,i}$ = Bar 1, bottom surface corrosion rating, interval i
$R_{Bar2Top,i}$ = Bar 2, top surface corrosion rating, interval i
$R_{Bar2Bot,i}$ = Bar 2, bottom surface corrosion rating, interval i
i = interval, 1 to 8

Table 4.3 Evaluation and Rating System for Corrosion Found on Mild Steel Bars.

Code	Meaning	Description	Rating
NC	No Corrosion	No evidence of corrosion	0
D	Discoloration	No evidence of corrosion, but some discoloration from original color	1
L	Light	Surface corrosion on less than one half of the interval, no pitting. Surface corrosion can be removed using cleaning pad.	2
M	Moderate	Surface corrosion on more than one half of the interval, no pitting. **and/or** Corrosion can not be completely removed using cleaning pad.	4
P	Pitting	Pits visible to unaided eye.	8
AR	Area Reduction	Measurable reduction in bar cross-sectional area due to corrosion	R^2

R = Estimated cross-sectional area reduction in percent

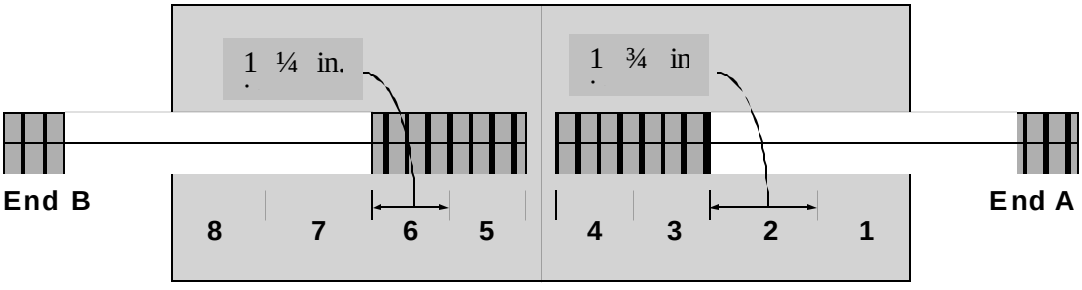

Figure 4.8 Intervals for Corrosion Ratings on Mild Steel Bars.

4.3.3 Galvanized Steel Duct

The galvanized steel duct was examined for eight equal intervals of 1.5 in., as indicated in Figure 4.9. At each location, corrosion ratings are assigned to indicate the severity of corrosion on the top and bottom surfaces of the inside and outside of each duct to reflect the possibility of different corrosion severity and extent. The corrosion rating system is described in Table 4.4. The total duct corrosion rating was calculated as follows:

$$\text{Duct Corrosion Rating} = \sum_{i=1}^{8} R_{\text{TopOuter},i} + R_{\text{BotOuter},i} + R_{\text{TopInner},i} + R_{\text{BotInner},i} \qquad \textit{Eq. 4.3}$$

where,

$R_{\text{TopOuter,i}}$ = top outer surface corrosion rating, interval i
$R_{\text{BotOuter,i}}$ = bottom outer surface corrosion rating, interval i
$R_{\text{TopInner,i}}$ = top inner surface corrosion rating, interval i
$R_{\text{BotInner,i}}$ = bottom inner surface corrosion rating, interval i
i = interval, 1 to 8

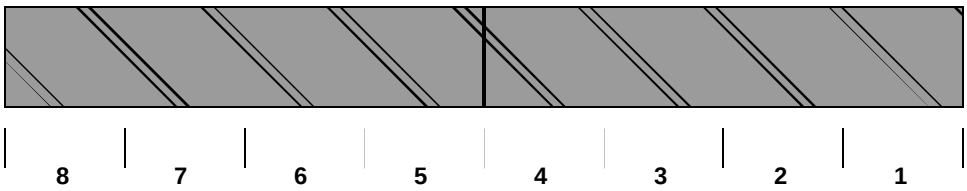

Figure 4.9 Intervals for Corrosion Ratings on Galvanized Duct

Table 4.4 Evaluation and Rating System for Corrosion Found on Post-Tensioning Duct.

Code	Meaning	Description	Rating
NC	No Corrosion	No evidence of corrosion	0
D	Discoloration	No evidence of corrosion, but some discoloration from original color	1
L	Light	Surface corrosion on less than one half of the interval, no pitting.	2
M	Moderate	Surface corrosion on more than one half of the interval, no pitting.	4
S	Severe	Corrosion completely covers the interval. **and/or** Presence of pitting.	8
H	Hole Through Duct	Hole corroded through duct. Used in conjunction with ratings D, L, M and S.	$32 + A_h$

A_h = Area of hole(s) in mm^2

4.4 FORENSIC EXAMINATION RESULTS

4.4.1 Detailed Visual inspection

A brief summary of the forensic examination results after eight years exposure is provided for each specimen in the following sections. The previous rating results from the autopsy performed at four years and five months are included in the individual tables, for comparison. The detailed description for the previous autopsy results is included in Reference 15.

4.4.1.1 Specimen DJ-S-L-NG-2 (Dry Joint, Steel Duct, Low Precompression, Normal Grout)

Duct corrosion produced a crack in the top of the concrete specimen extending its whole length, as shown in Figure 4.10. The crack had a maximum top width of 0.12 in., and extended the full depth of cover to the duct, and was clearly visible when the specimen was opened at the strand cut line. Rust staining was visible around the crack.

Corrosion Rating:

Specimen	(1)	(2)
	4.4 yrs	8 yrs
Strand	26	612
Bars	12	54
Duct	528	15779

A 0.020 in. maximum width crack was also evident in the side, at the level of the strand. Also, at one end of the specimen, three cracks were found extending from the duct perimeter to the outer limits of the specimen, corresponding to the cracks described above, in the top, and side directions. No cracks were found in the bottom of the specimen, below the location of the mild steel bars.

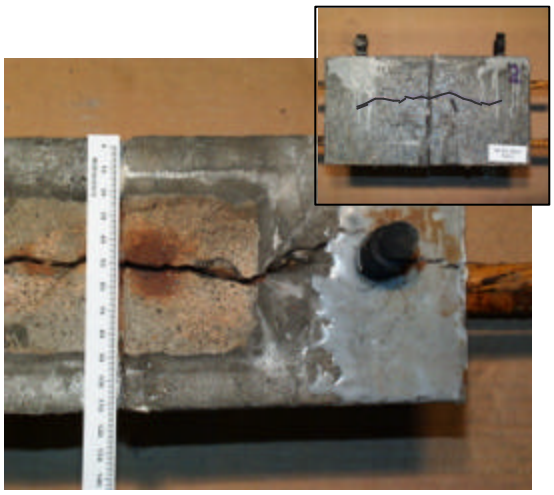

Specimen condition prior to autopsy (Top view) [Side view in detail]

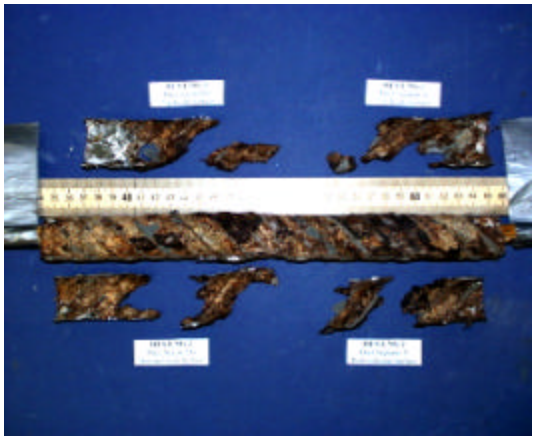

Duct

Strand

Mild Steel bars

Figure 4.10 Concrete, Duct, Strand and Bar Condition for Specimen DJ-S-L-NG-2.

More than 50% of the duct had been consumed by corrosion, leaving a build up of corrosion products around the surface of the grout. Corrosion products were mixed with a white powder (that was analyzed with X-Ray Diffraction and was found to be Zinc Oxide and Zinc Hydroxide). At the remaining areas of the duct metal, severe uniform corrosion and pitting was found, as shown in Figure 4.10. The duct corrosion rating for this specimen was the maximum of all specimens examined.

Three shallow voids of around 0.016 $in.^2$ each, were found in the grout surface, when extracting the remaining duct material. The voids appear to have resulted from insufficient grout fluidity rather than due to trapped air or bleed water collection. The grout was also cracked in the top, corresponding with the crack observed in the concrete cover.

The strand showed one of the highest corrosion rates when compared to the other 18 specimens. Uniform corrosion and pitting extended the complete length of the strand, including those sections where the epoxy paint had peeled off, which represented more than 50% of the painted area

The mild steel showed moderate corrosion away from the joint, in the vicinity of the epoxy paint area, as shown in Figure 4.10. Additionally, light to moderate corrosion was found under the epoxy paint and in all those areas where the epoxy had peeled off, which represented around 15% to 20% of the epoxy area in the bars.

The match-cast dry joint was intact with no voids or cracks. Some grout infiltrated the joint during grouting. The entire face of the joint was covered with a white residue that may be salt or leaching.

4.4.1.2 Specimen DJ-S-M-NG-2 (Dry Joint, Steel Duct, Medium Precomp., Normal Grout)

Corrosion Rating:

Specimen	(1)	(2)
	4.4 yrs	8 yrs
Strand	43	780
Bars	12	44
Duct	325	3054

Duct corrosion produced a 0.040 in. max. width crack at the top of the specimen, extending the whole length. No cracks were found in the sides or bottom of the specimen.

The crack extended the complete concrete cover depth, having a max width at the strand cut line of 0.080 in.

The duct was severely corroded at the top, with maximum corrosion occurring around the joint section and also at approximately 60 mm, on both sides, from the joint location. Corrosion products accumulated in thin layers. White powder was found in the duct, mixed with steel corrosion products, and was observed specially in the half duct below. Underneath the duct, a black stain of about 0.039 $in.^2$ against the concrete surface was found, with moisture. Within a few minutes, this black stain rapidly changed color to a lighter dark rust color, after the duct was removed from the concrete and moisture was lost.

The most severe corrosion found in the duct corresponded to a large void in the grout of about 0.40 $in.^2$ The grout was covered with corrosion products from the duct metal.

The strand had moderate to severe corrosion in the top areas, where the epoxy paint had peeled off; and light corrosion in the exposed steel areas. On the bottom of the strand, moderate to severe corrosion was found at the epoxy paint areas, and very severe corrosion and pitting in the exposed steel area. The strand corrosion rating was the highest when compared to the other specimens.

Discoloration and light to moderate corrosion was found in the reinforcing bars, mainly underneath the epoxy paint, as shown in Figure 4.11. The epoxy paint seemed to have retained moisture, forcing the paint to peel off and triggering corrosion. Few small voids were found in the concrete surface underneath the reinforcing bars.

The entire face of the dry joint was covered with a white residue that may be salt or leaching.

Specimen condition prior to autopsy (Top view)

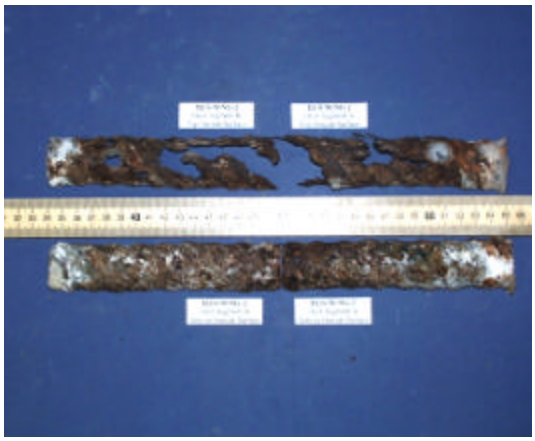

Duct

Strand

Mild Steel bars

Figure 4.11 Concrete, Duct, Strand and Bar Condition for Specimen DJ-S-M-NG-2.

4.4.1.3 Specimen DJ-S-H-NG-2 (Dry Joint, Steel Duct, High Precompression, Normal Grout)

A 0.040 in. maximum width crack was evident at the top of the specimen, with a length of about 7 in., centered with respect to the joint location. At the bottom of the specimen, there was another crack, extending one half of the specimen, with a maximum crack width in the order of 0.080 in. No cracks were visible in the sides of the specimen.

Corrosion Rating:

Specimen	(1)	(2)
	4.4 yrs	8 yrs
Strand	38	137
Bars	60	606
Duct	64	361

Severe uniform corrosion and pitting was found on the top and bottom of the galvanized steel duct, around the joint. Additionally, a black stain with moisture was found at approximately 2.35 in. from the joint in the top of the duct in Segment B. One hole of around 0.17 in.^{2} was located in the duct at the joint and a 0.09 in.^{2} hole was at approximately 1.2 in. from the joint, at the top of the duct in Segment A, corresponding to the location of a void in the grout. White stains (powder) and discoloration of the duct was evident in the bottom of the duct in Segments A and B.

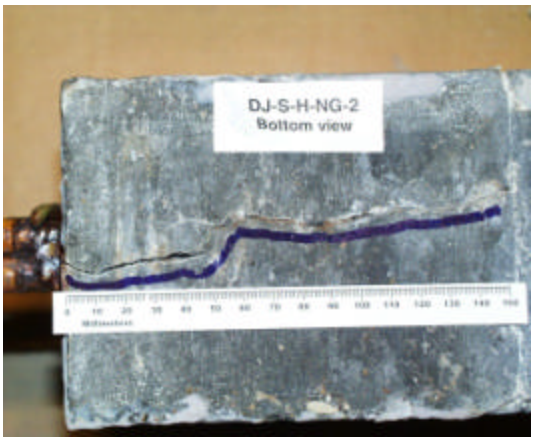

Specimen condition prior to autopsy (bottom view)

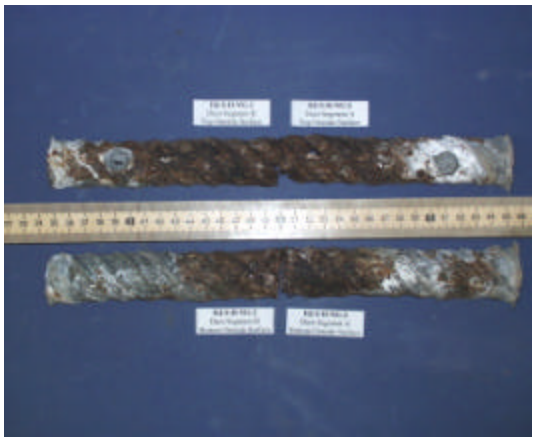

Duct

Strand

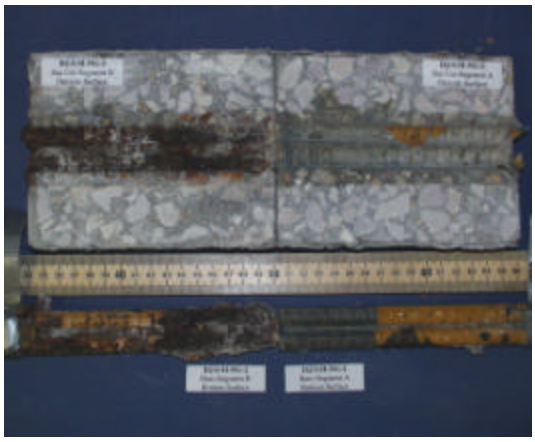

Mild Steel bars

Figure 4.12 Concrete, Duct, Strand and Bar Condition for Specimen DJ-S-H-NG-2.

Moderate to severe corrosion was found on the strand in Segment A, in the areas where the epoxy had peeled off. Light to moderate corrosion was found on the unpainted areas.

Mild steel was severely corroded, with extensive pitting and severe volume decrease due to corrosion products, in Segment B. The bar corrosion produced a crack in the concrete cover in the bottom of the specimen. Mild steel in Segment A was only lightly corroded and discolored, especially in the areas where the epoxy paint had peeled off. See Figure 4.12. The mild steel corrosion rating was the highest when compared to the other specimens. White dust covered the dry joint.

4.4.1.4 Specimen DJ-P-L-NG-2 (Dry Joint, Plastic Duct, Low Precompression, Normal Grout)

Corrosion in the reinforcing bars produced a 0.040 in. maximum width crack in Segment B, in the bottom of the specimen. No cracks were found in the top or sides of the specimen.

White dust, corresponding to leaching or salt, was found in the inside surface of the concrete, at the duct/strand cut line, around the silicone holding the grouting ducts to the plastic duct. Also white dust was found at the joint section at the level of the plastic duct, where silicone was used to seal the duct joint.

Corrosion Rating:

Specimen	(1)	(2)
	4.4 yrs	8 yrs
Strand	6	116
Bars	17	201
Duct	0	0

A very deep void centered at 2 in. from the joint, in Segment A, was found in the top of the grout. Also shallow voids were found in the top of the grout at approximately 3 in. from the joint, in Segment B.

Light corrosion was found on the strand.

The mild steel had very severe corrosion and pitting in the exposed areas in Segment B, at the top and bottom of the bars. Severe corrosion and pitting was also observed in the same segment, in the areas where the epoxy paint had peeled off. The build-up of corrosion products was severe, causing the concrete cover to crack. At the adjoining segment, moderate corrosion was found at the bars, close to the joint section. The dry joint was intact, with a white residue in the entire joint.

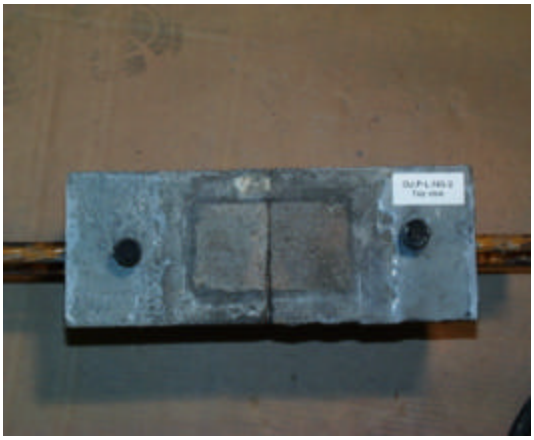

Specimen condition prior to autopsy (Top view)

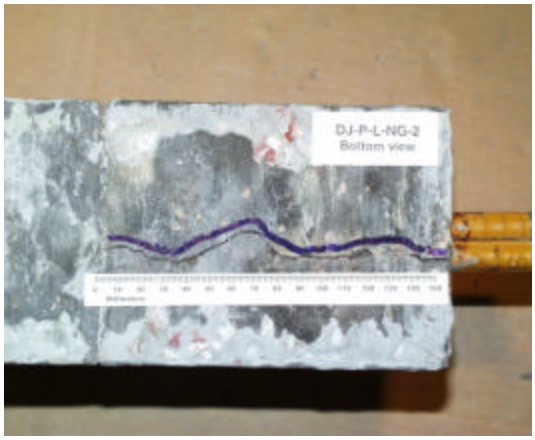

Specimen condition prior to autopsy (Bottom view of Segment B)

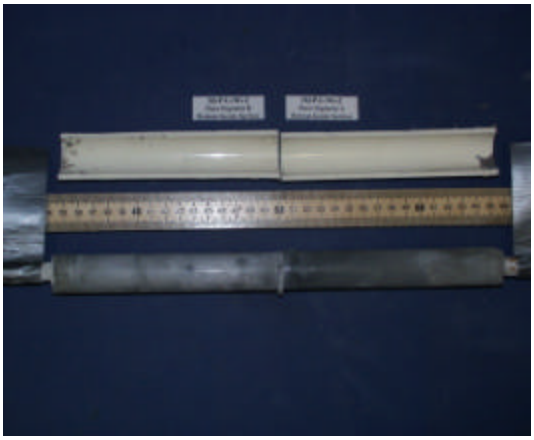

Duct and grout condition

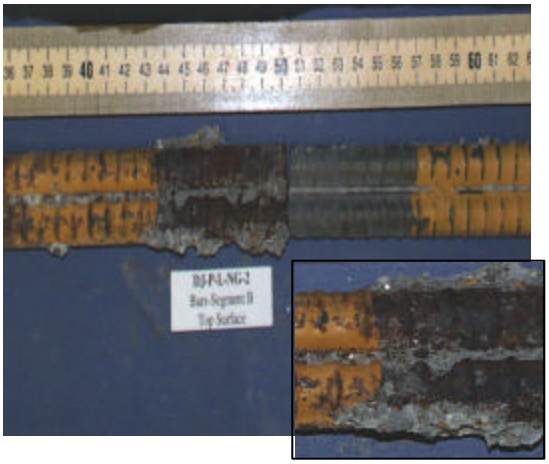

Mild Steel bars

Figure 4.13 Concrete, Duct, Strand and Bar Condition for Specimen DJ-P-L-NG-2.

4.4.1.5 Specimen DJ-P-M-NG-2 (Dry Joint, Plastic Duct, Medium Precompression, Normal Grout)

Mild steel corrosion was responsible for a 0.020 in. maximum width crack at the bottom of the specimen in Segment A. No cracks were visible at the top and sides of the specimen.

White residue was found in the inside concrete surface, at the duct/strand cut line, between the silicone used at the joint section and sides of the plastic duct and in the connection of the grouting duct and the plastic duct.

Corrosion Rating:

Specimen	(1)	(2)
	4.4 yrs	8 yrs
Strand	9	80
Bars	24	77
Duct	0	0

The dry joint was clean, with no signs of crystals or corrosion stains; however, little concrete discoloration was observed in the joint concrete surface in the top of the duct/strand level.

The plastic duct was intact, with no signs of damage.

Minor discoloration was observed at the outer wires of the strand, in the exposed surface area close to the joint section. The areas where the epoxy paint had peeled off, at both sides of the strand in Segments A and B, had light corrosion.

Moderate to severe corrosion was observed in the mild steel bars of Segment A, in the exposed areas close to the joint section. Additionally, light to moderate corrosion was found where the epoxy paint had peeled off. In Segment B, light corrosion was found where the epoxy paint had peeled off, and no corrosion was observed in the exposed steel areas, closer to the joint.

A few small voids (approx. 0.012 in.^{2}) were found in the grout surface, close to the joint section. Salt crystals were found inside the voids, in the interior concrete surface.

Specimen condition prior to autopsy (Bottom view, Segment A)

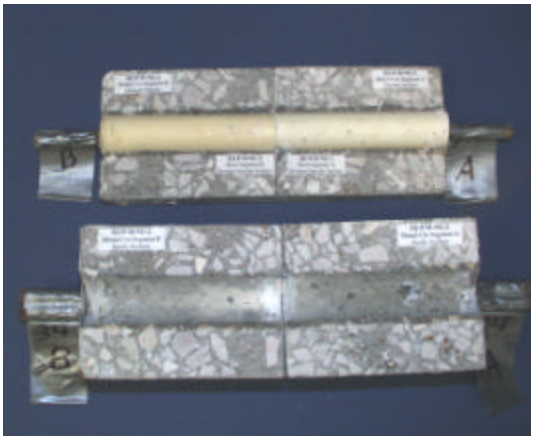

Duct

Strand

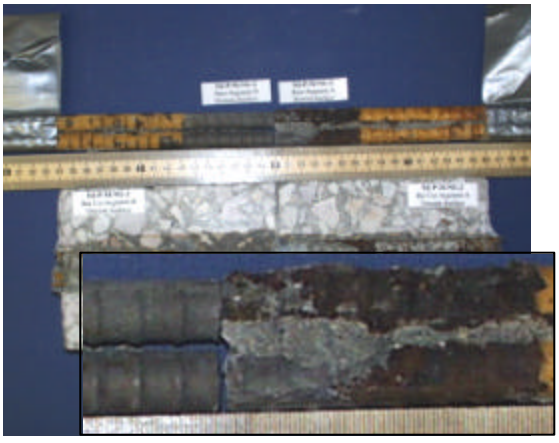

Mild Steel bars

Figure 4.14 Concrete, Duct, Strand and Bar Condition for Specimen DJ-P-M-NG-2.

4.4.1.6 Specimen DJ-S-L-CI-2 (Dry Joint, Steel Duct, Low Precompression, Corrosion Inhibitor in Grout)

The top of the specimen had a 0.010 in. maximum width crack, extending a length of 4.75 in., centered in the specimen. No cracks or signs of corrosion were observed in the sides or bottom of the specimen.

Corrosion Rating:

Specimen	(1)	(2)
	4.4 yrs	8 yrs
Strand	114	86
Bars	4	22
Duct	42	674

The galvanized steel duct had severe corrosion on the top surface, close to the joint section. The duct was consumed in approximately 0.72 in.^{2} at the joint section and had another hole in the top on Segment A, within 0.75 in. to 2 in. from the dry joint. The duct also showed areas with white stains or products in the bottom sections against the concrete and in the top sections against the concrete around the grouting duct locations. Duct corrosion produced a 0.010 in. crack in the concrete cover.

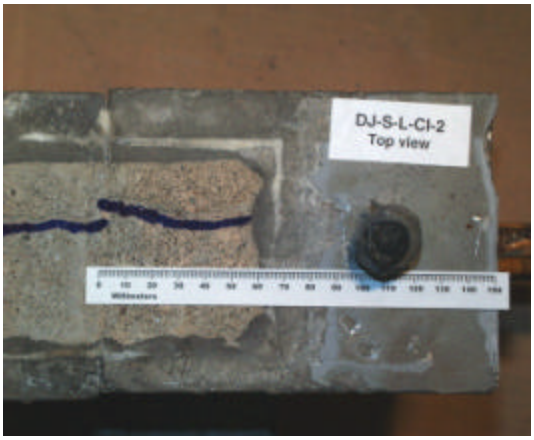

Specimen condition prior to autopsy (Top view)

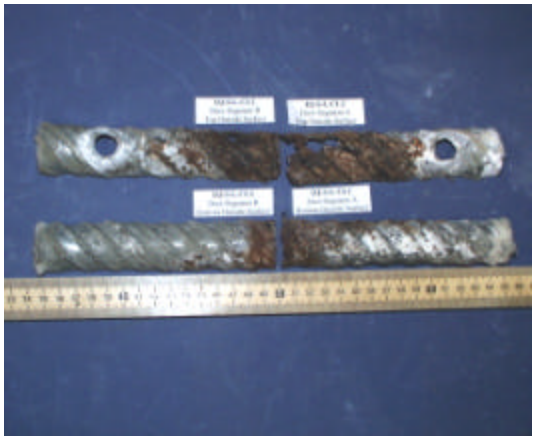

Duct

Strand

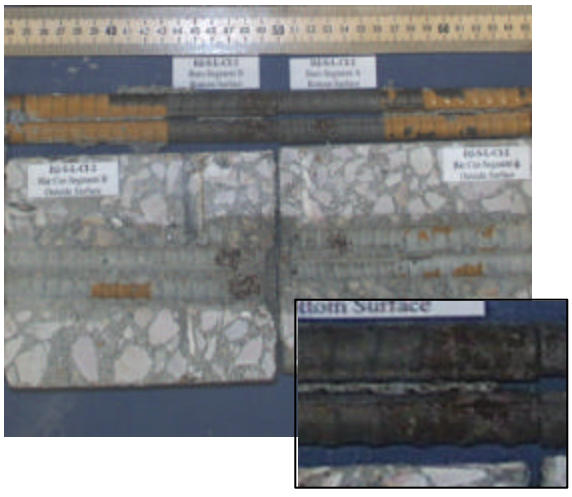

Mild Steel bars

Figure 4.15 Concrete, Duct, Strand and Bar Condition for Specimen DJ-S-L-CI-2.

Some small 0.015-0.030 in.^{2} voids were observed in the top of the grout, underneath the galvanized steel duct. Salt crystals were found inside of the voids.

Minor discoloration and light corrosion was observed at the prestressing strand. Light corrosion was found on the exposed areas of the mild steel bars, next to the joint section in Segment B and at 20 mm from the joint section on Segment A. Light to moderate surface corrosion was observed were the epoxy paint had peeled off. The dry joint was clean, except for white stains – salt crystals or leaching – around the duct area.

4.4.1.7 Specimen DJ-S-M-CI-2 (Dry Joint, Steel Duct, Medium Precompression, Corrosion Inhibitor in grout)

A fine crack, 0.020 in. maximum width and 6 in. length, was visible in the top of the specimen, centered with respect to the dry joint section, as shown in Figure 4.16. No cracks or signs of corrosion were found at the sides or the bottom of the specimen.

At the duct/strand cut line, the concrete had several bubble holes under the duct, but there were no corrosion products inside the holes.

Corrosion Rating:

Specimen	(1)	(2)
	4.4 yrs	8 yrs
Strand	24	54
Bars	20	27
Duct	151	346

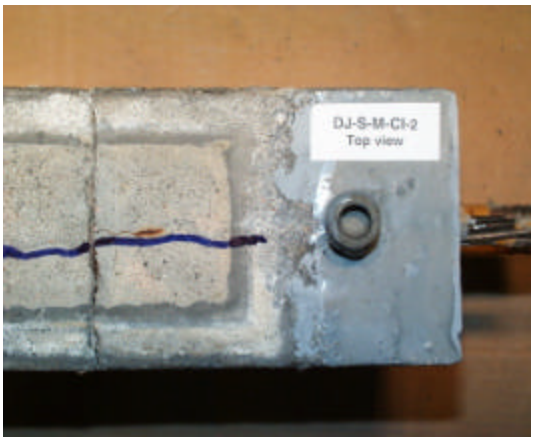

Condition prior to autopsy (Top view)

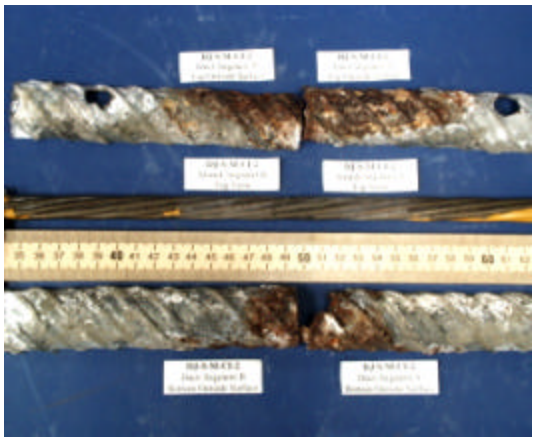

Duct

Strand

Mild Steel bars

Figure 4.16 Concrete, Duct, Strand and Bar Condition for Specimen DJ-S-M-CI-2.

Moderate to severe corrosion was found in the galvanized steel duct, mixed with white deposits, corresponding to zinc oxide and zinc hydroxide, as examined by X-Ray diffraction. The duct in Segment B had a small hole of approximately 0.030 $in.^2$, corresponding to a void in grout. Corrosion action was also responsible for a hole of an approximate area of 0.40 $in.^2$ next to the joint section. The white residue was present in the top of the duct around the areas where the grouting vents were attached. At 0.6 in. from the joint in the bottom of the duct in Segment B, there was a black spot of corrosion products with moisture.

The grout had large voids across the top and bottom, with salt crystals deposited inside.

Discoloration was observed on the strand and corrosion was negligible.

The mild steel bars had moderate corrosion in the unpainted area of Segment B. Discoloration was observed under the epoxy paint. In Segment A, light to moderate corrosion was found in the unpainted area of the bars close to the dry joint.

4.4.1.8 Specimens SE-S-L-NG-1 (Epoxy Joint, Steel Duct, Low Precompression, Normal Grout)

A hairline crack of about 3.5 in. in length was located in the top of the specimen, inside the ponded region, extending mainly in Segment B. No cracks or corrosion stains were found in the sides or bottom of the specimen.

The duct halves did not meet at the joint, leaving a gap of approximately 0.12 in.

Corrosion Rating:

Specimen	(2)	(1)
	4.4 yrs	8 yrs
Strand	22	64
Bars	6	26
Duct	13	167

Severe corrosion covered most of the top of the duct in Segment B, as seen in Figure 4.17, and half the top of the duct in Segment A, extending from the joint face. Corrosion in Segment B produced a horizontal crack in the duct of approximately 1.5 in. that lead to another vertical crack of about 0.75 in. in length with a hole of 0.015 in^2. The bottom of the duct was covered mostly with a white residue (white powder) with only a few areas of light to moderate corrosion near the joint section.

A large void of an approximate length of 4 in. and width of 0.75 in. was found in the top of the duct, extending 2.5 in. into Segment B and 1.5 in. into Segment A. Another void of approximately 0.039 $in.^2$ was found in the top of the grout in Segment B, with duct corrosion products inside.

Light to moderate corrosion was found on the strand in one of the outer wires, where the epoxy paint had peeled off, at 3 in. from the joint. The other outer wires had discoloration in the unpainted areas and light surface corrosion in the areas where the epoxy paint had peeled off. The inner wire had light corrosion in its entire length.

The mild steel bars showed discoloration in the unpainted areas and light corrosion in the few areas where the epoxy paint had peeled off, as shown in Figure 4.17.

4.4.1.9 Specimen SE-S-M-NG-1 (Epoxy Joint, Steel Duct, Medium Precompression, Normal Grout)

The top of the specimen had a crack with an approximate maximum width of 0.016 in., extending a length of 6.3 in., centered with the joint. No cracks were found on the sides or bottom of the specimen.

The epoxy at the joint did not cover the entire face. There were small holes in the epoxy in the top surface of the specimen. Epoxy bond on the lower part of the bar cut line broke along the joint.

Corrosion Rating:

Specimen	(2)	(1)
	4.4 yrs	8 yrs
Strand	2	119
Bars	16	41
Duct	61	732

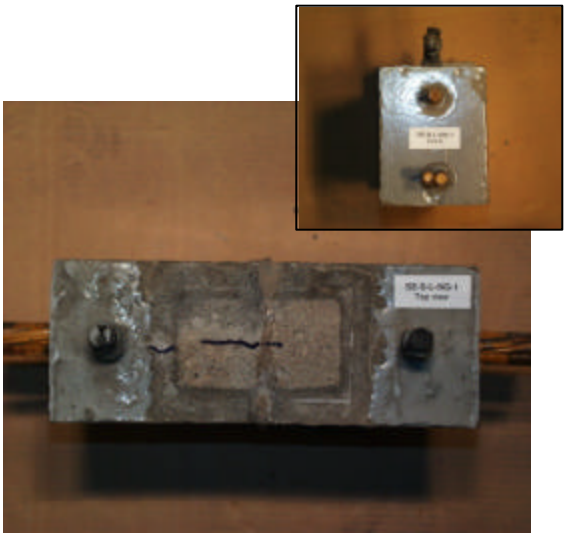

Specimen condition prior to autopsy (Top view) [Side view in detail]

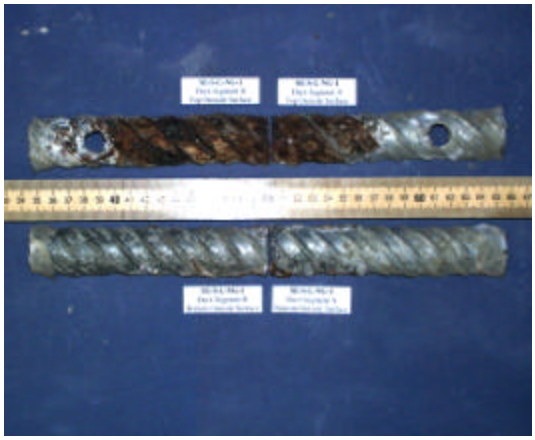

Duct

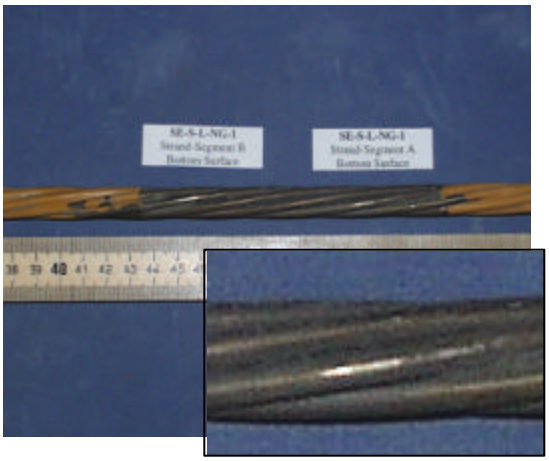

Strand

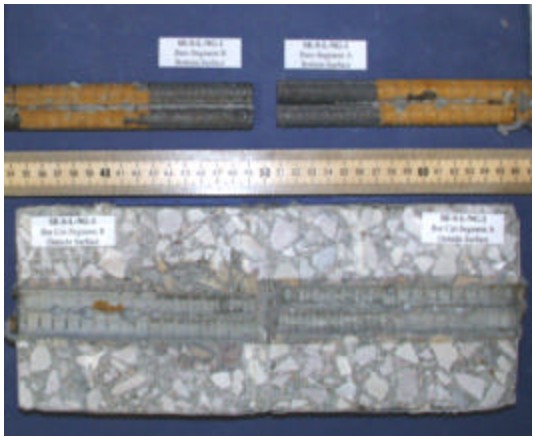

Mild Steel bars

Figure 4.17 Concrete, Duct, Strand and Bar Condition for Specimen SE-S-L-NG-1.

At the duct/strand cut line, severe corrosion was found on the top of the galvanized steel duct, as shown on Figure 4.18. Corrosion produced several small holes through the duct in Segment B. In Segment A, one large longitudinal hole of about 0.55 $in.^2$ was centered at approximately 23.6 in. from the joint. White powder was impregnated to the duct metal in various locations, especially in the bottom of the duct in Segment A and in the top of duct in Segments A and B, around the grout vent locations, as shown in Figure 4.18.

Moderate to severe corrosion was found on one of the outer wires of the strand of the unpainted section, in Segment B. The center wire has also moderately corroded at the same place. Light to moderate corrosion was found on the rest of the wires in that segment. Light corrosion and discoloration was found under the epoxy paint.

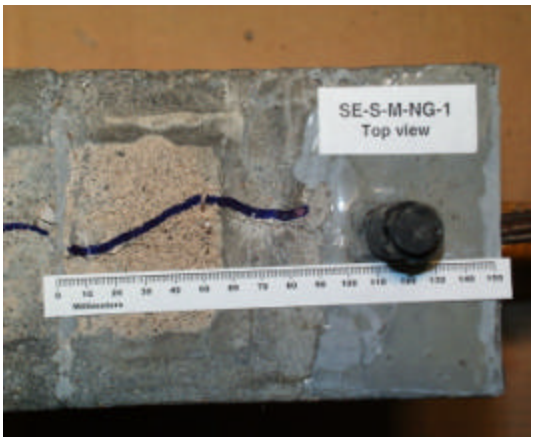

Specimen condition prior to autopsy (Top view)

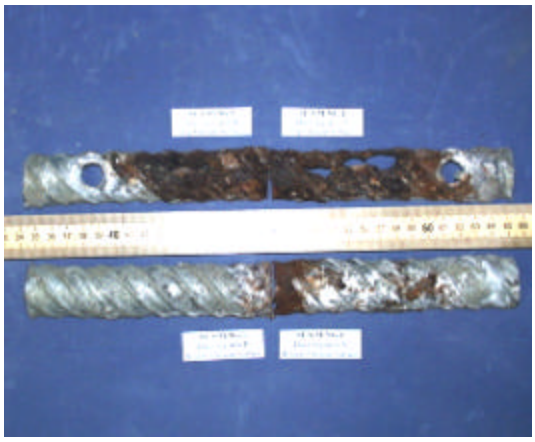

Duct

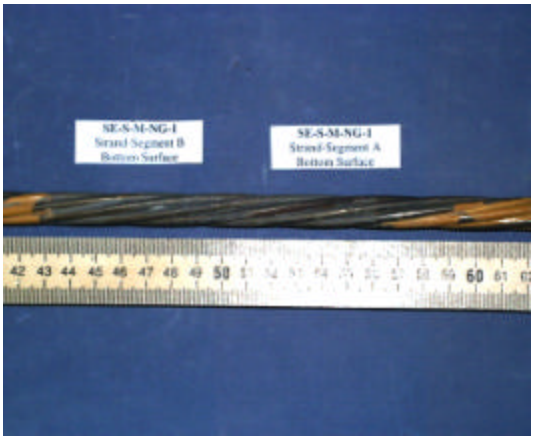

Strand

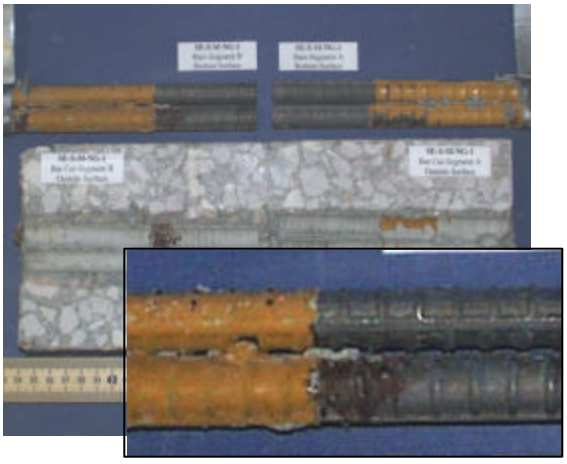

Mild Steel bars

Figure 4.18 Concrete, Duct, Strand and Bar Condition for Specimen SE-S-M-NG-1.

Large amounts of corrosion were found on one of the bars in Segment B, under the epoxy paint, close to Face B. Severe corrosion was found on all areas were the epoxy paint had peeled off, being more severe and concentrated than seen on other specimens. Severe corrosion was found on the same bar, on Segment B, starting where the epoxy coating ends, and extending approximately 0.6 in.

4.4.1.10 Specimen SE-S-H-NG-1 (Epoxy Joint, Steel Duct, High Precompression, Normal Grout)

The specimen had a hairline crack in the top, with a length of 4.3 in., as seen in Figure 4.19. No cracks were found in the sides or bottom of the specimen.

The top of the galvanized metal duct had severe corrosion in two thirds of the total length of Segment B and one third of the length in Segment A, extending from the joint section. The most severe corrosion on both sides was found at approximately 2 in. from the joint.

Corrosion Rating:

Specimen	(2)	(1)
	4.4 yrs	8 yrs
Strand	3	88
Bars	0	29
Duct	8	268

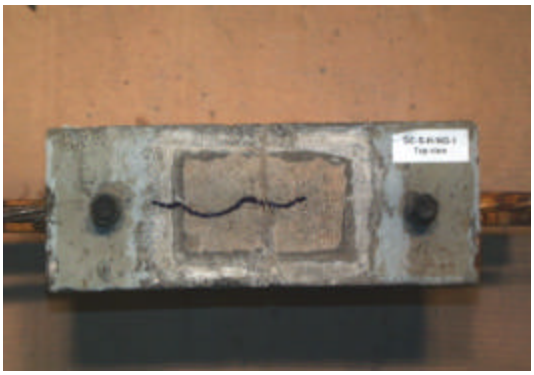

Specimen condition prior to autopsy (Top view)

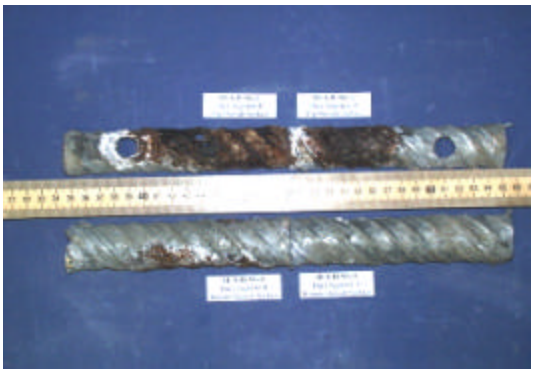

Duct

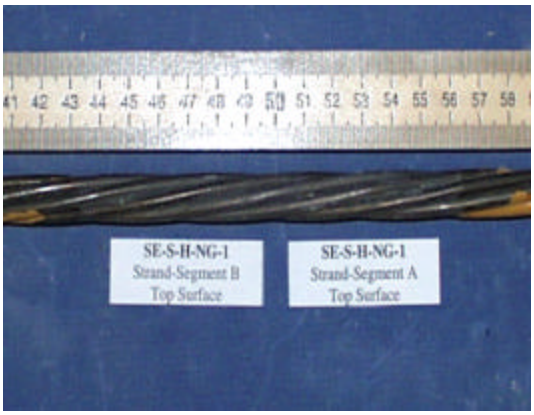

Strand

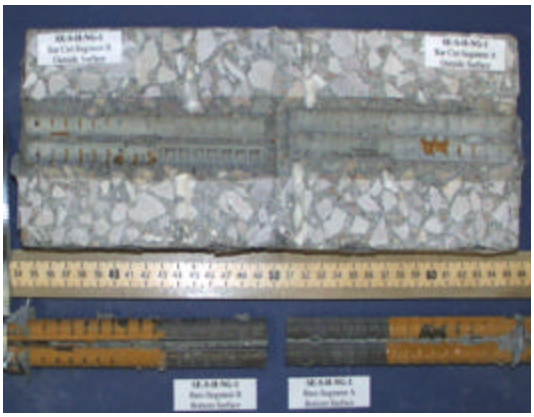

Mild Steel bars

Figure 4.19 Concrete, Duct, Strand and Bar Condition for Specimen SE-S-H-NG-1.

Corrosion products in the duct were dark (black). Two holes, one of 0.18 in.^{2} and another of 0.016 in.^{2} were found centered at 2 in. from the joint in Segment B. The voids did not correspond to a large deep void in the grout located by the joint in the top of the grout in Segment A. White powder was found in the metal duct around the grout vent locations and by the joint section in the top of the duct in Segment A.

The strand had light corrosion in the areas were the epoxy paint had peeled off. In the unpainted areas, the outer wires were only discolored. The inner wire had light corrosion in its entire length.

Mild steel bars had discoloration in the unpainted areas and light corrosion where the epoxy paint had peeled off.

4.4.1.11 Specimen SE-P-L-NG-1 (Epoxy Joint, Plastic Duct, Low Precompression, Normal Grout)

No cracks were found in the top, sides or bottom of the specimen.

The plastic duct was intact, with no signs of damage.

The top of the hardened grout had a large void in Segment A beginning 1 in. from the joint section and extending 1.4 in. The void was clean without salt deposits. In the Segment B side, the grout had a smaller void 0.8 in. from the joint extending 0.8 in. vertically with an approximate width of 0.080 in. At the joint location there was a small circular void of 0.20 in. in diameter. The grout was smooth in the bottom surface.

Corrosion Rating:

Specimen	(2)	(1)
	4.4 yrs	8 yrs
Strand	5	80
Bars	0	0
Duct	0	0

Specimen condition prior to autopsy (Top view)

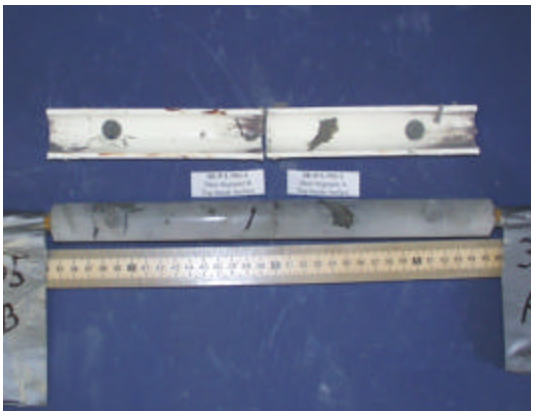

Duct

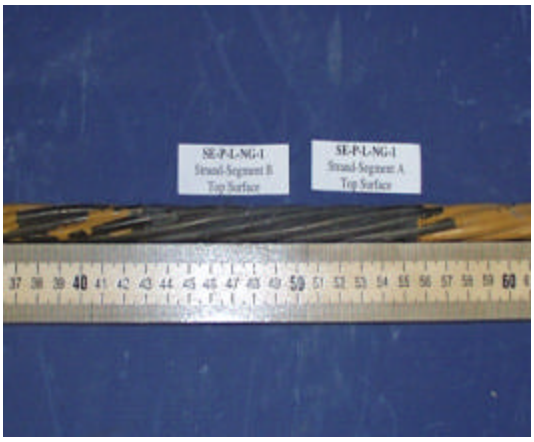

Strand

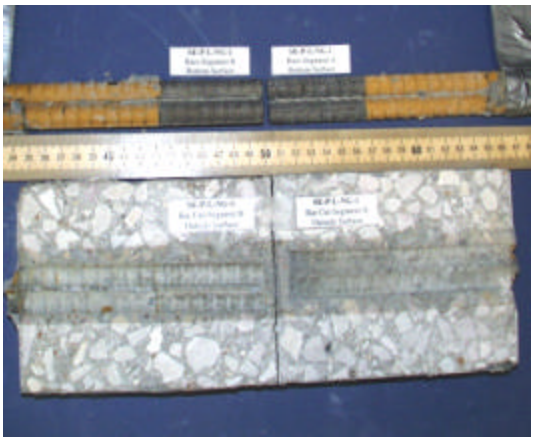

Mild Steel bars

Figure 4.20 Concrete, Duct, Strand and Bar Condition for Specimen SE-P-L-NG-1.

Light corrosion was found at the sides of the strand, closer to Faces A and B, suggesting that some water may have seeped from the ends. Around the joint and under the ponded region the outer wires of the strand were in excellent condition. The inner wire had light corrosion. Minor discoloration was found on the areas where the epoxy had peeled off. No corrosion was found on the mild steel bars.

The epoxy segmental joint was intact around its perimeter, with no signs of moisture, salt or rust penetration at the strand and bar cut lines.

4.4.1.12 Specimen SE-P-M-NG-1 (Epoxy Joint, Plastic Duct, Medium Precompression, Normal Grout)

No cracks were found on the top, sides or bottom of the specimen. The plastic duct was intact, without any signs of deterioration. Several large voids were found on the top surface of the grout. In most cases, the voids were less than 0.16 in. deep. The voids appear to have resulted from insufficient grout fluidity.

Corrosion Rating:

Specimen	(2)	(1)
	4.4 yrs	8 yrs
Strand	5	88
Bars	0	18
Duct	0	0

Discoloration and very light corrosion was found on the outer wires of the prestressing strand in the unpainted area. The inner wire showed light corrosion. In the areas with epoxy coating, the strand showed light corrosion, where the paint had peeled off.

Light corrosion occurred in the mild steel bars under the epoxy coating. No corrosion was found in the unpainted areas.

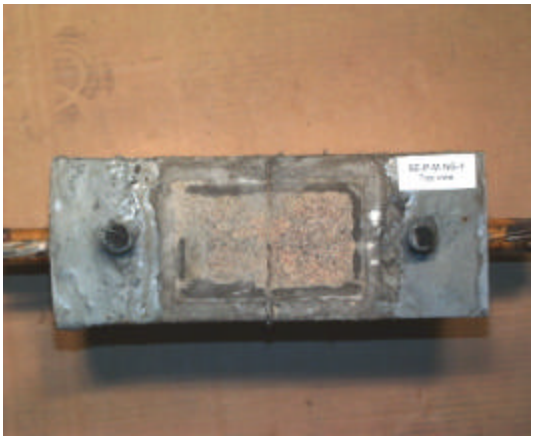

Specimen condition prior to autopsy (Top view)

Duct

Strand

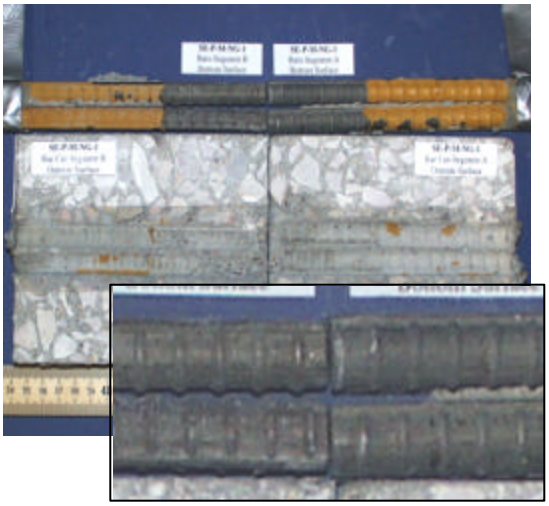

Mild Steel bars

Figure 4.21 Concrete, Duct, Strand and Bar Condition for Specimen SE-P-M-NG-1.

4.4.1.13 Specimen SE-S-L-CI-1 (Epoxy Joint, Steel Duct, Low Precompression, Corrosion Inhibitor in grout)

No cracks were found on the top, sides or bottom of the specimen

Severe corrosion was found on the top of the galvanized metal duct in Segment B, extending half of the segment from the joint section, and with the most severe corrosion at 1.75 in. from the joint. Also, moderate to severe corrosion was found on the top of the metal duct in Segment A, centered at 1.75 in. from the joint, as shown in Figure 4.22. White residue (powder) was found mixed with the dark corrosion products. The bottom of the duct showed no signs of corrosion products either in the form of dark or white residues.

Corrosion Rating:

Specimen	(2)	(1)
	4.4 yrs	8 yrs
Strand	24	95
Bars	0	28
Duct	85	126

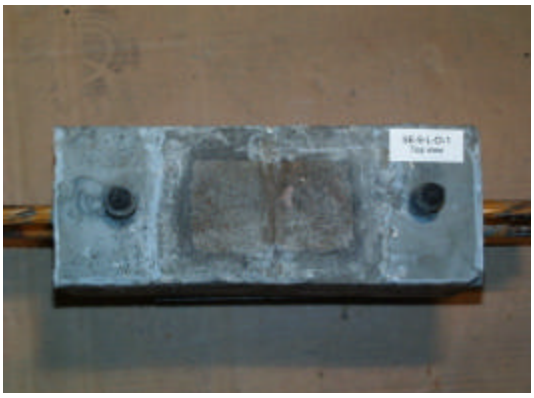

Specimen condition prior to autopsy (Top view)

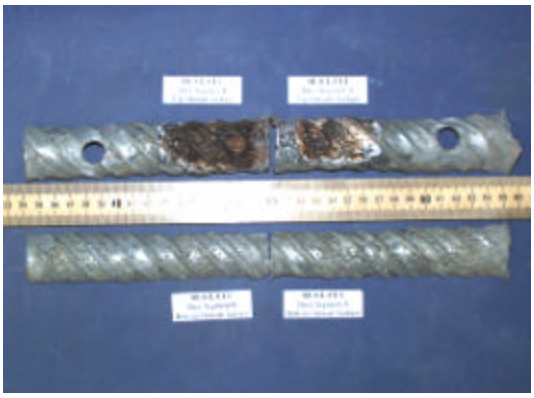

Duct

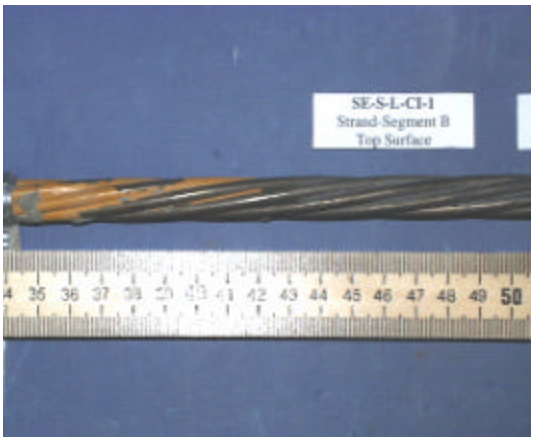

Strand

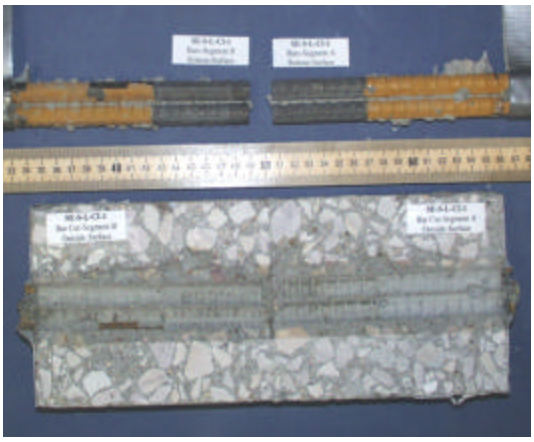

Mild Steel bars

Figure 4.22 Concrete, Duct, Strand and Bar Condition for Specimen SE-S-L-CI-1.

Eleven small voids were found on the top of the grout surface, one of approximately 0.05 in.^{2} was deep enough to expose the strand. The voids appear to have resulted from insufficient grout fluidity.

Corrosion in the strand was very light in the unpainted areas and light in the areas where the epoxy paint had peeled off. The inner wire was more corroded than the outer wires, having light to moderate corrosion in its entire length.

4.4.1.14 Specimen SE-S-M-CI-1 (Epoxy Joint, Steel Duct, Medium Precompression, Corrosion Inhibitor in grout)

The specimen had cracks in the top with a maximum width of 0.040 in. and extending a length of 7 in., centered in the ponded region as shown in Figure 4.23. No cracks were found in the sides and bottom of the specimen.

The galvanized metal duct was severely corroded in its entirety. Holes accounted for 2.85 in.^{2} The duct was practically consumed in the center section, under the ponded region. The sides had severe corrosion.

Corrosion Rating:

Specimen	(2)	(1)
	4.4 yrs	8 yrs
Strand	2	308
Bars	0	29
Duct	114	2445

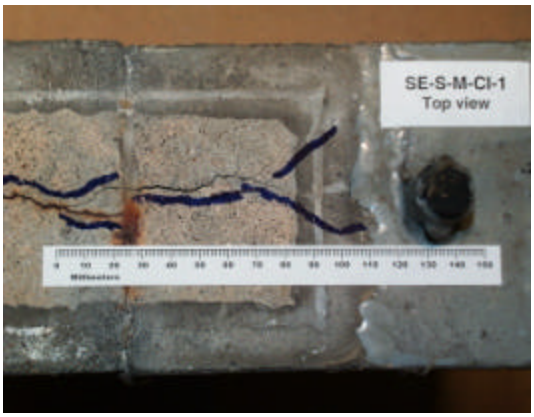

Specimen condition prior to autopsy (Top view)

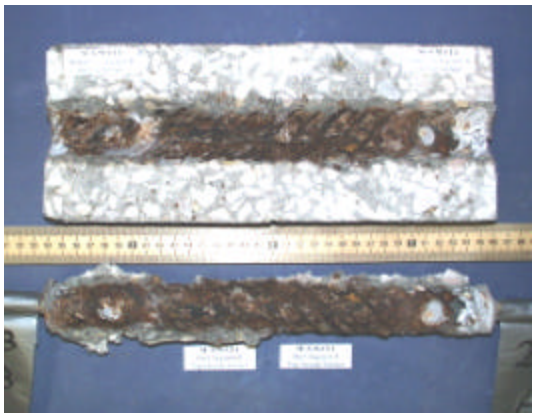

Duct

Strand

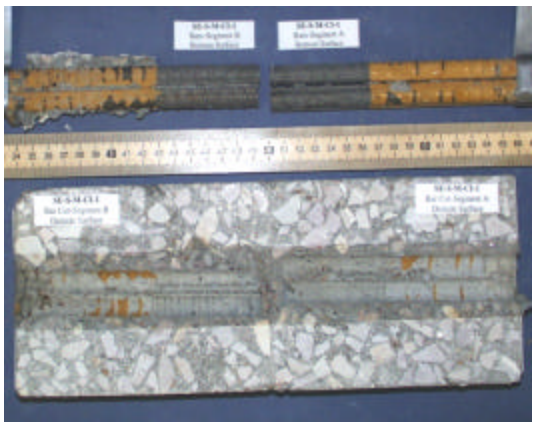

Mild Steel bars

Figure 4.23 Concrete, Duct, Strand and Bar Condition for Specimen SE-S-M-CI-1.

The strand showed very severe corrosion in the uncoated areas, especially on the bottom. Under the epoxy, the corrosion was severe and was worse in the top of the strand. The center wire had moderate to severe corrosion in its entirety.

The mild steel bars had only discoloration in the uncoated areas and light corrosion in the coated areas where the epoxy had peeled off.

The match-cast epoxy joint was incompletely filled in the top of the strand cut line, allowing water to penetrate to the duct. The joint had corrosion stains from the duct location up to the top of the specimen as shown in Figure 4.24.

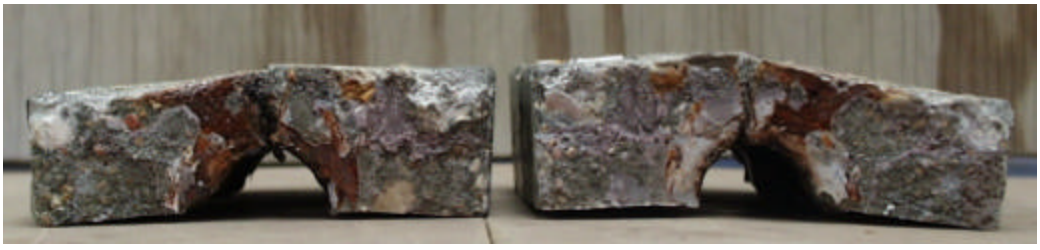

Figure 4.24 Incompletely Filled Epoxy Joint (SE-S-M-CI-1).

4.4.1.15 Specimen SE-S-H-CI-1 (Epoxy Joint, Steel Duct, High Precompression, Corrosion Inhibitor in grout)

The bottom of the specimen had one 0.010 in. maximum width crack extending two thirds of Segment B, from Face B, as shown in Figure 4.25. No cracks were found on the top and sides of the specimen.

Corrosion Rating:

Specimen	(2)	(1)
	4.4 yrs	8 yrs
Strand	3	78
Bars	1	132
Duct	10	44

After making the strand cut, the epoxy segmental joint came apart easily.

At the duct cut line, severe corrosion was found on the top of the duct in Segment A, centered at 1.75 in. from the joint section, as shown in Figure 4.25. Moderate corrosion and a heavy accumulation of white residue was found on the top of the duct, also centered at 1.75 in. from the epoxy segmental joint. No corrosion was found in the bottom of the duct.

Severe corrosion and pitting, and severe section loss, was found in the mild steel bars in Segment B, in the coated and uncoated areas. Light to moderate corrosion was found in the mild steel bars in the Segment A.

Strand corrosion was light in the outer wires with epoxy coat. In the uncoated areas, the wires showed only discoloration. The inner wire had light corrosion in its entirety.

Specimen condition prior to autopsy (Bottom view)

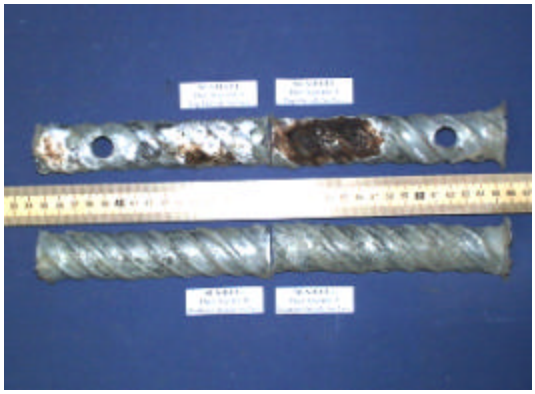

Duct

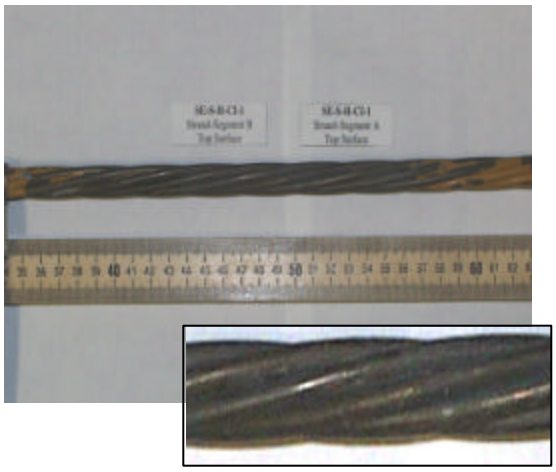

Strand

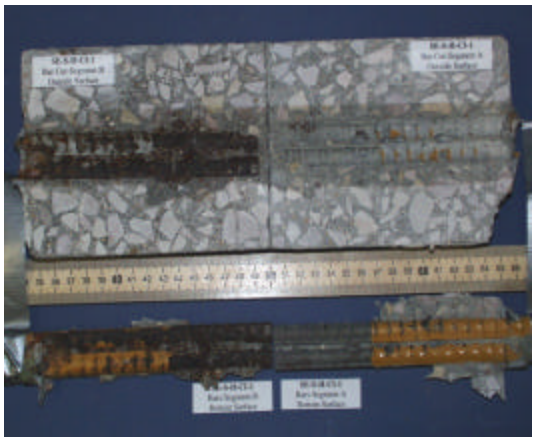

Mild Steel bars

Figure 4.25 Concrete, Duct, Strand and Bar Condition for Specimen SE-S-H-CI-1.

4.4.1.16 Specimen SE-S-L-SF-1 (Epoxy Joint, Steel Duct, Low Precompression, Silica Fume added to grout)

The concrete specimen had a crack in the top, with an approximately maximum width of 0.02 in. No cracks were visible in the sides or bottom of the specimen as shown in Figure 4.26.

The epoxy segmental joint separated easily after unloading the specimen, indicating lack of adequate bonding with the concrete surface. However, corrosion stains were found on the surface.

Corrosion Rating:

Specimen	(2)	(1)
	4.4 yrs	8 yrs
Strand	3	88
Bars	1	13
Duct	10	591

Specimen condition prior to autopsy (Top view)

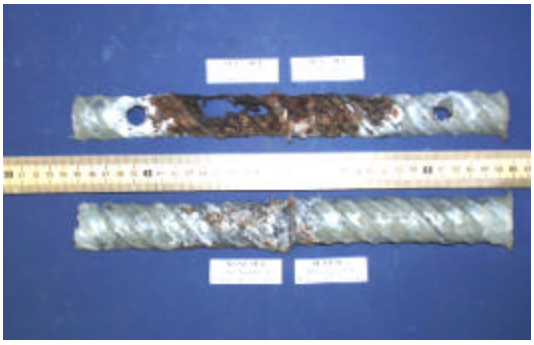

Duct

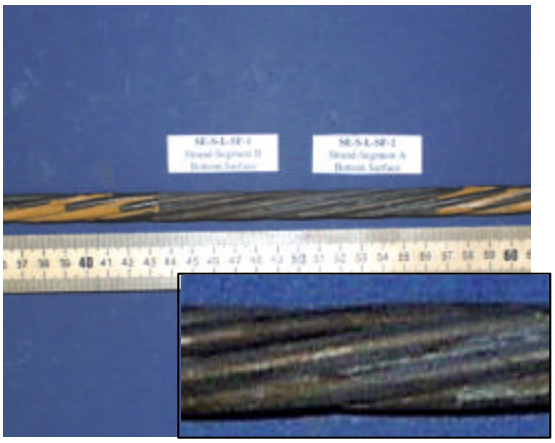

Strand

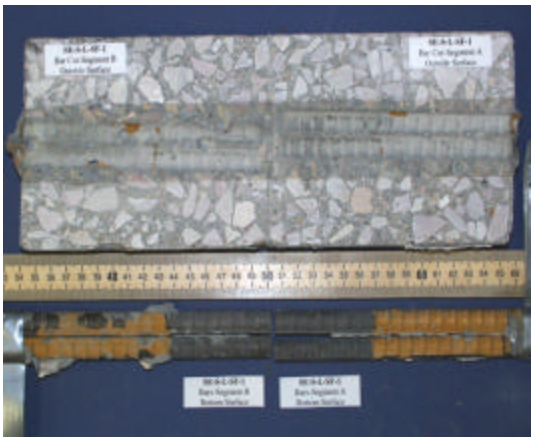

Mild Steel bars

Figure 4.26 Concrete, Duct, Strand and Bar Condition for Specimen SE-S-L-SF-1.

Severe corrosion was found in the top of the duct, between the locations of the grout vents. The most severe corrosion was centered at 1.75 in. from the epoxy joint towards Face B. Centered at this location, a large hole of approximately 0.62 in.^{2} was found. Another small hole of approximately 0.0023 in.^{2} was found in Segment A next to the joint section and another of similar size at 1.20 in. from the joint. Moderate to light corrosion, mixed with white residue, was found in the bottom of the duct, mainly in Segment B, and centered at 1.20 in. from the joint.

The concrete surface against the bottom of the galvanized metal duct had several small round shallow voids.

The grout had a very porous structure, with many micro voids.

The strand had discoloration in the uncoated areas and light corrosion in the outer epoxy coated wires. The inner wire had light corrosion with a small area of moderate corrosion.

No corrosion was found on the mild steel bars in the uncoated areas. Discoloration and light corrosion was found in few areas where the epoxy coating had peeled off.

4.4.1.17 Specimen EG-S-L-NG-1 (Epoxy Joint with Gasket, Steel Duct, Low Precompression, Normal Grout)

Corrosion in the galvanized metal duct produced a 0.020 in. maximum width longitudinal crack in the top of the specimen, 5.5 in. in length, and two additional hairline cracks of 1.2 in. and 2 in. respectively in the top of Segment B at the border of the ponded region and extending to the sides, as shown in Figure 4.27. No cracks were found in the sides or bottom of the specimen.

Corrosion Rating:

Specimen	(2)	(1)
	4.4 yrs	8 yrs
Strand	2	88
Bars	0	25
Duct	54	1096

The epoxy segmental joint was intact with no signs of moisture, salt or rust penetration. Examination of three sections through the joint showed it to be completely filled with epoxy and free from voids or cracks.

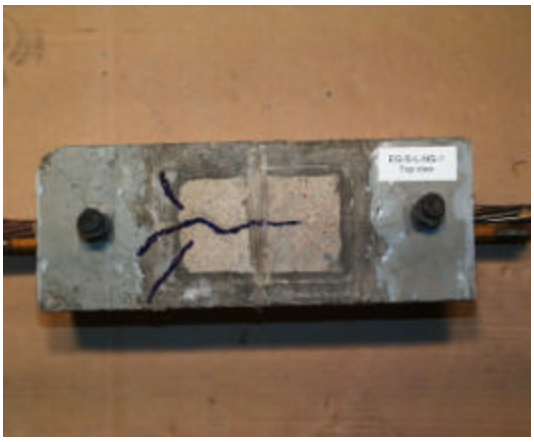

Specimen condition prior to autopsy (Top view)

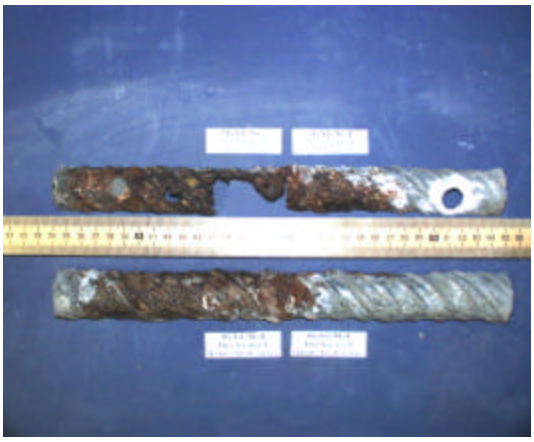

Duct

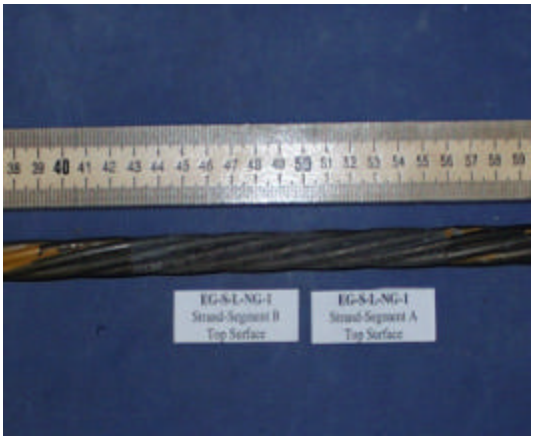

Strand

Mild Steel bars

Figure 4.27 Concrete, Duct, Strand and Bar Condition for Specimen EG-S-L-NG-1.

Severe corrosion was found in the top and bottom of the duct in segment B, and in half of the length in the top of the duct in Segment A, starting from the joint section. The heaviest corrosion was found at 1.75 in. from the joint in Segment B and at 1.40 in. from the joint in Segment A, corresponding to the holes found on each side of 1.33 in^2 and 0.030 $in.^2$, respectively. The corrosion products included black spots with moisture.

No voids were found on the grout.

The outer wires of the strand had discoloration in the uncoated areas and light corrosion in those areas where the epoxy coating had peeled off. The inner wire had light corrosion in its entirety. Inside the duct, the strand was positioned at the bottom on Segment B and on the side on Segment A.

Discoloration was found on the mild steel bars in the unpainted area, and discoloration and light corrosion were the epoxy had peeled off. There was a small area of approximately 0.12 $in.^2$ with moderate corrosion in the vicinity of Face B.

4.4.1.18 Specimen EG-S-M-NG-1 (Epoxy Joint with Gasket, Steel Duct, Medium Precompression, Normal Grout)

A 0.010 in. maximum width crack was at the top of the concrete specimen, extending 3 in. from the epoxy segmental joint towards face A. No cracks or corrosion signs were found on the sides or bottom of the specimen.

Corrosion Rating:

Specimen	(2)	(1)
	4.4 yrs	8 yrs
Strand	23	90
Bars	0	31
Duct	237	198

The top portion of the specimen above the strand cut line separated at the joint during autopsy. The gasket appears to have prevented complete bonding of the segments. Around the gasket there were signs of moisture, salt and rust stains. The incomplete epoxy coverage is shown in Figure 4.28.

Severe corrosion was found on the top of the duct, mainly in Segment A, as shown in Figure 4.29. The corrosion products were black, dark green and typical dark orange, mixed with white residue. The most severe corrosion was centered at 1.6 in. from the joint towards Face A. Centered at this point there were three small holes of 0.040 $in.^2$ each in the duct. Corrosion products were in the form of flakes or very thin layers.

Discoloration was found on the outer wires of the strand, in the unpainted (uncoated) region. Light corrosion was found on the areas where the epoxy had peeled off. The inner wire had light corrosion.

Mild steel bars had minor discoloration under the ponded region (uncoated areas) and light corrosion in those areas where the epoxy coating had peeled off.

Figure 4.28 Incomplete Epoxy Coverage in Epoxy/Gasket Joint (EG-S-M-NG-1).

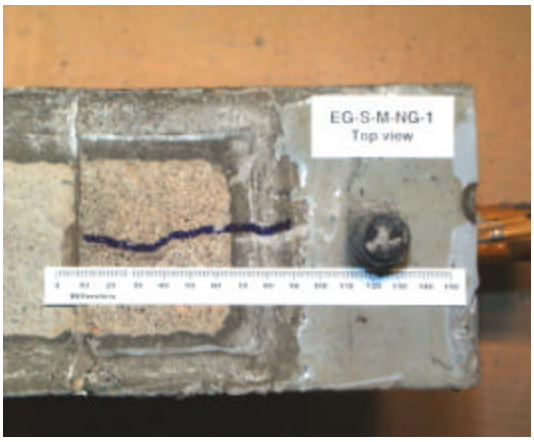

Specimen condition prior to autopsy (Top view)

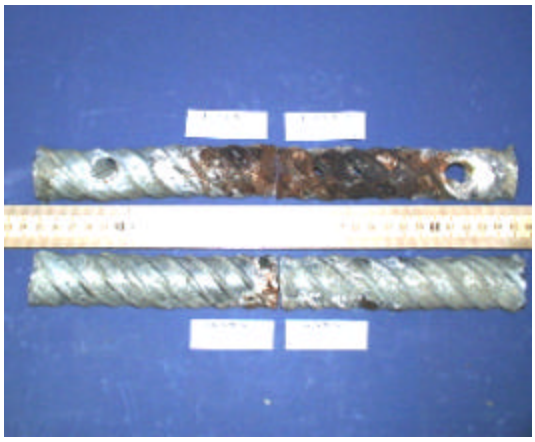

Duct

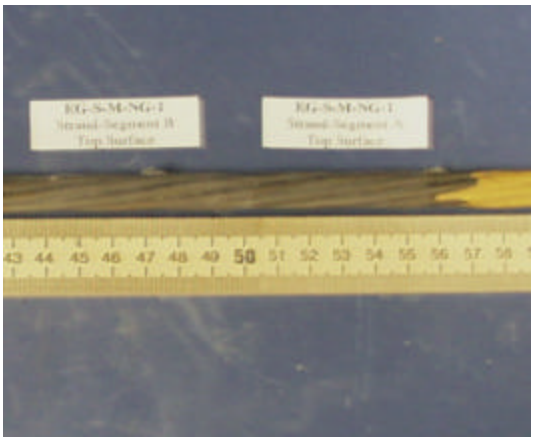

Strand

Mild Steel bars

Figure 4.29 Concrete, Duct, Strand and Bar Condition for Specimen EG-S-M-NG-1.

4.4.1.19 Specimen EG-S-H-NG-1 (Epoxy Joint with Gasket, Steel Duct, High Precompression, Normal Grout)

No cracks were found on the top, sides or bottom of the specimen.

Corrosion Rating:

Specimen	(2)	(1)
	4.4 yrs	8 yrs
Strand	16	84
Bars	1	34
Duct	78	131

Similar to specimen EG-S-M-NG-1, the side and bottom perimeter of the joint were intact and appeared to be filled with epoxy, but thin voids were visible at the joint on the top surface of the specimen. Sections through the joint at the mid-height and bar and strand cut lines showed it to be completely filled with epoxy and free from voids or cracks. However, the gasket again appears to have prevented complete bonding of the segments immediately above the duct opening. Salt penetration and rust stains were visible on the joint as shown in Figure 4.30. Similar results were obtained during autopsy performed at four and a half years of exposure, to the duplicate specimens EG-S-M-NG-2 and EG-S-H-NG-2[15].

The top of the duct had severe corrosion in Segments A and B, centered in each side at 1.60 in. from the epoxy joint with gasket, as shown in Figure 4.31. Holes in Segment A had 0.016 mm^2, same as the holes in Segment B. Corrosion products were very dark in color and there was one dark green spot close to the

hole in Segment B. The duct bottom had light to moderate corrosion extending a few millimeters from the joint section at each side, as seen in Figure 4.31. White residue was present around all the corroded areas.

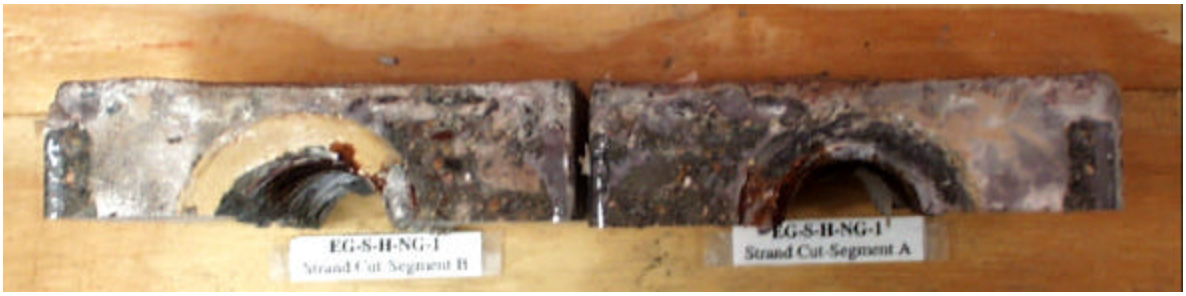

Figure 4.30 Incomplete Epoxy Coverage in Epoxy/Gasket Joint (EG-S-H-NG-1).

Specimen condition prior to autopsy (Top view)

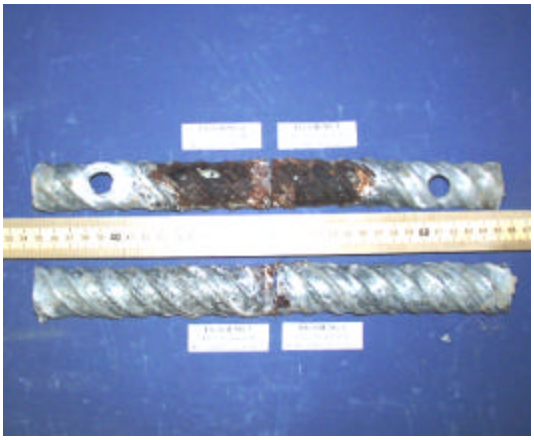

Duct

Strand

Mild Steel bars

Figure 4.31 Concrete, Duct, Strand and Bar Condition for Specimen EG-S-H-NG-1.

The strand had only discoloration in the unpainted section for the outer and inner wires, and light corrosion where the epoxy coating had peeled off.

Mild steel bars had discoloration and light corrosion in the unpainted areas and light corrosion where the epoxy coating had peeled off.

4.4.2 Corrosion Rating Summary

Strand, bar and duct corrosion ratings for all specimens are listed in Tables 4.5 and 4.6, and plotted in Figure 4.32 through Figure 4.34. Results from the autopsy performed at four and a half years of testing are included as a reference. Average, standard deviation and median values are listed at the bottom of the tables.

In order to put the corrosion ratings in perspective, a "Threshold of Concern" was assigned at the corrosion rating of 50 for the strands, bars and ducts. This threshold is used to indicate corrosion related deterioration deemed severe enough to warrant concern. In general, corrosion ratings greater than 50 corresponded to pitting corrosion for strands and bars, and holes in the galvanized steel duct caused by corrosion.

After four years and five months of exposure (Table 4.5), Specimen DJ-S-L-CI-1 had the most severe strand corrosion, with a strand corrosion rating of 114 compared to the average of 19.5 and median of 12. This was the only specimen with a strand corrosion rating greater than 50. Specimen DJ-S-H-NG-1 had the most severe mild steel reinforcement corrosion with a rating of 60 compared to the average of 9.1 and median of 1. This specimen was the only one with a bar corrosion rating greater than 50. Specimen DJ-S-L-NG-1 had the worst duct corrosion with a rating of 528 compared to the average of 122.9 and median of 79. In each case, the specimen with the largest corrosion rating was several times higher than the average and median values.

After eight years of aggressive exposure (Table 4.6), specimen DJ-S-M-NG-2 had the most severe strand corrosion with a corrosion rating of 780, followed by Specimen DJ-S-L-NG-2 with a corrosion rating of 612, both compared to the average of 164.8 and the median of 88. All specimens had strand corrosion ratings higher than the value of 50 that was chosen as the threshold of concern. Specimen SE-S-M-CI-1, in spite of being an epoxy jointed specimen, had high duct, strand and mild steel corrosion ratings of 305, 132 and 2445, respectively, when compared to the median values of 88, 29 and 268. Autopsy results for this specimen showed inadequate epoxy filling at the joint. Specimen DJ-S-H-NG-2 had the most severe mild steel corrosion, with a corrosion rating of 606, followed by specimen DJ-P-L-NG-2, with a corrosion rating of 201. The average value and median values for mild steel corrosion were 75.6 and 29, respectively. Fourteen specimens out of the nineteen specimens had negligible bar corrosion, below the value of 50. Specimen DJ-S-L-NG-2 had the worst duct corrosion, with a corrosion rating of 15779 compared to the average value of 1369.1 and the median of 268. This specimen was followed by specimens DJ-S-M-NG-2 and SE-S-M-CI-1, with duct corrosion ratings of 3054 and 2445 respectively. These values show that duct corrosion was extremely severe in a number of specimens, which is in agreement with the extremely large destruction of galvanized duct observed during the autopsy process and reported in Section 4.4.

Table 4.5 Corrosion Ratings for specimens autopsied after 4.4 years of exposure.[15]

Specimen Name	Strand	Corrosion Rating Bars	Duct
DJ-S-L-NG-1	26	12	528
DJ-S-M-NG-1	43	12	325
DJ-S-H-NG-1	38	60	64
DJ-P-L-NG-1	6	17	0
DJ-P-M-NG-1	9	24	0
DJ-S-L-CI-1	114	4	42
DJ-S-M-CI-1	24	20	151
SE-S-L-NG-2	13	6	22
SE-S-M-NG-2	2	16	61
SE-S-H-NG-2	3	0	8
SE-P-L-NG-2	5	0	0
SE-P-M-NG-2	6	0	0
SE-S-L-CI-2	24	0	85
SE-S-M-CI-2	2	0	114
SE-S-H-CI-2	3	1	10
SE-S-L-SF-2	12	0	12
EG-S-L-NG-2	2	0	54
EG-S-M-NG-2	23	0	237
EG-S-H-NG-2	16	1	78
Average	19.5	9.1	94.3
Std. Dev.	25.3	14.3	132.6
Median	12	1	54

Table 4.6 Corrosion Ratings for Specimens Autopsied after eight years of Exposure.

Specimen Name	Strand	Corrosion Rating Bars	Duct
DJ-S-L-NG-2	612	54	15,779
DJ-S-M-NG-2	780	44	3,054
DJ-S-H-NG-2	137	606	361
DJ-P-L-NG-2	116	201	0
DJ-P-M-NG-2	80	77	0
DJ-S-L-CI-2	86	22	674
DJ-S-M-CI-2	54	27	346
SE-S-L-NG-1	64	26	167
SE-S-M-NG-1	119	41	732
SE-S-H-NG-1	88	29	268
SE-P-L-NG-1	80	0	0
SE-P-M-NG-1	88	18	0
SE-S-L-CI-1	95	28	126
SE-S-M-CI-1	305	29	2,445
SE-S-H-CI-1	78	132	44
SE-S-L-SF-1	88	13	591
EG-S-L-NG-1	88	25	1,096
EG-S-M-NG-1	90	31	198
EG-S-H-NG-1	84	34	131
Average	164.8	75.6	1369.1
Std. Dev.	196.4	136.7	3587.3
Median	88	29	268

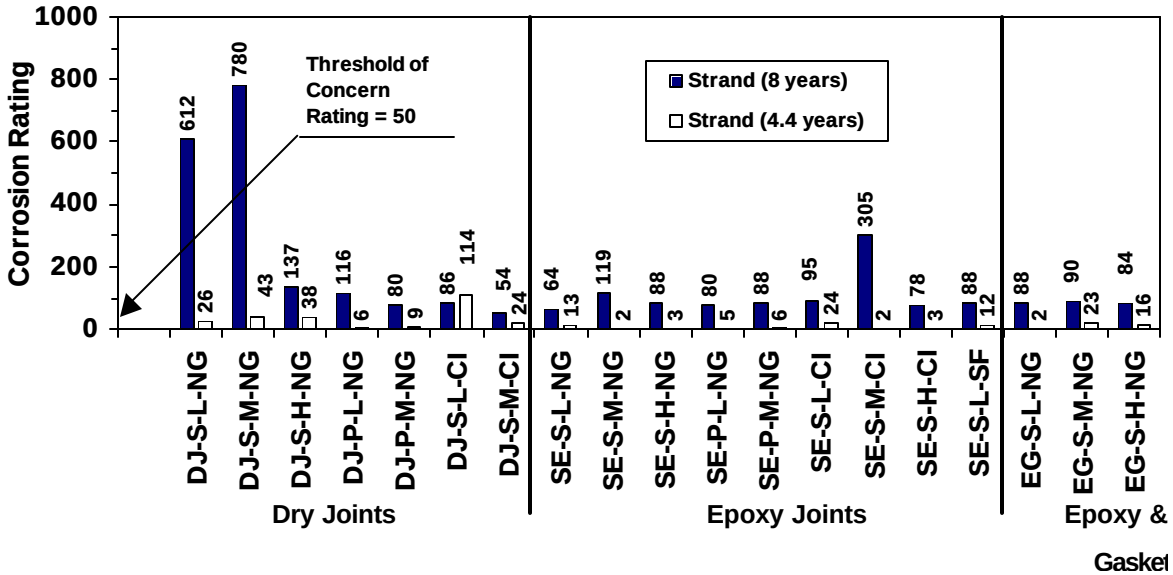

Figure 4.32 Strand Corrosion Ratings for All Specimens.

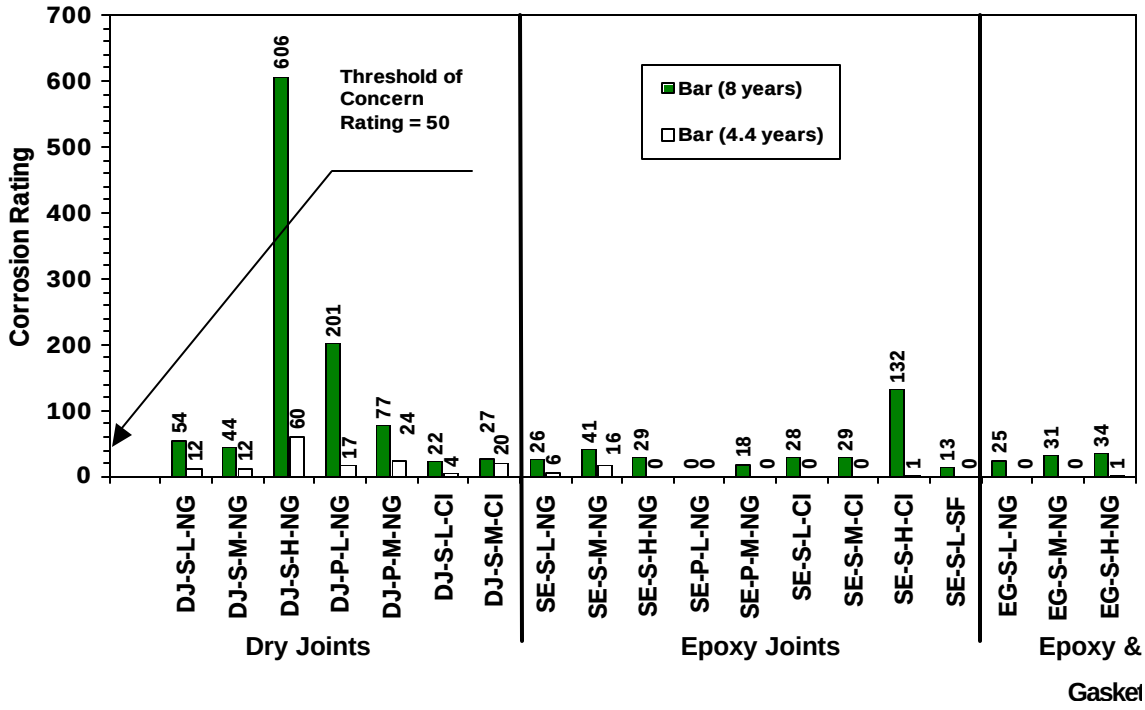

Figure 4.33 Mild Steel Bar Corrosion Ratings for All Specimens.

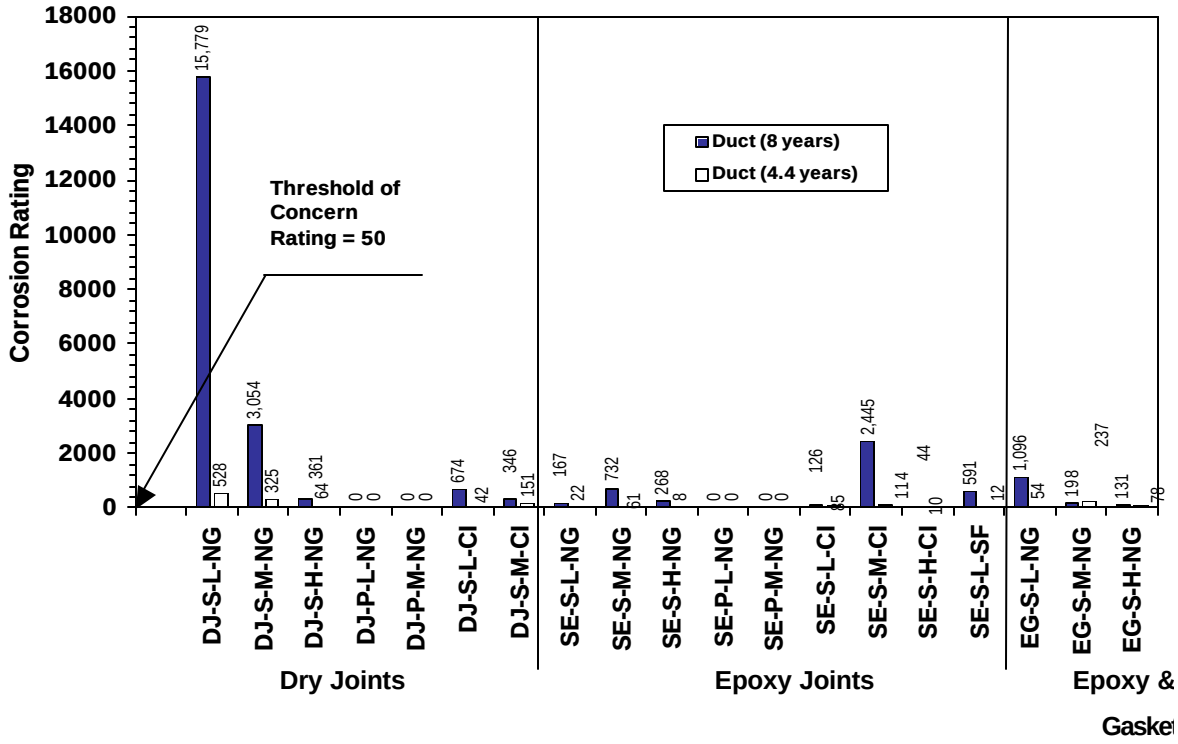

Figure 4.34 Duct Corrosion Ratings for All Specimens.

4.4.3 Chloride Analysis

Concrete powder samples were collected from six dry joint specimens and four epoxy joint specimens for chloride analysis, following the procedure described in Section 4.1.2. In addition, samples were collected from the grout in these specimens for chloride analysis. Concrete chloride ion profiles for these 10 specimens are shown in Figure 4.35 through Figure 4.44. Values plotted in the figures are acid soluble chloride levels, expressed as a percentage of concrete weight. The chloride threshold for corrosion is indicated in the figures at 0.033%. This value, intended as a guide only, is based on the widely accepted chloride threshold value of 0.2% of the weight of cement.[39] The same data has been rearranged in Figure 4.45 through Figure 4.48, to better compare the specimen chloride levels at the same depths. Data for Specimen DJ-S-L-NG-2, at 0.5 in. from the joint, is not shown in the above mentioned figures, since the advanced cracking in the specimen did not allow for the extraction of representative samples at various depths.

Chloride content analysis shows that in general under the area where the ponded region was located, there is a significant decrease in the level of chlorides with increasing depths, being more considerable in all four epoxy joint specimens analyzed, including the epoxy joint specimen with gasket.

Dry joint specimens showed significantly higher chloride contents adjacent to the joint in comparison to measurements away from the joint. This trend was also observed in the epoxy joint specimens but at a much lower scale, especially at higher depths.

Dry joint specimens in the proximity of the joint showed chloride contents well above the corrosion threshold, over the depth of the specimen. At 2 in. from the joint, also under the ponded region, these specimens showed very high chloride contents, except for Specimen DJ-S-L-CI-2 that showed low contents below the level of 3 in. At 4.25 in. from the joint, away from the ponded region, the dry joint Specimen DJ-S-L-NG-2 showed very high corrosion levels at all depths.

Epoxy joint specimens showed a different pattern with respect to dry joint specimens. Under the ponded region, these specimens showed very high chloride levels above the strand level, but below this depth, chloride levels were below the threshold value. Away from the joint, at 4.25 in., the chloride levels were negligible in Specimen SE-S-L-NG-1 at all four depths analyzed.

The epoxy joint specimen with gasket, EG-S-L-NG-1, showed a very similar pattern in the proximity of the joint, as those epoxy joint specimens without gasket. However, at 2 in. away from the joint this specimen still showed high chloride contents at a depth of 3 in., although below this depth the chloride content decreased considerably.

In general, no distinct trend was observed in all specimens with respect to different levels of precompression.

The chloride profile for Specimens DJ-S-H-NG-2, DJ-P-L-NG-2, DJ-S-M-CI-2, and SE-S-H-NG-1 exhibit a discontinuity in the measurements at 2 in. away from the joint, as shown in Figures 4.36 through 4.38, 4.40 and 4.43. Chloride measurements decrease at mid-height of the specimen, and increase at the level of the mild steel bars. This discontinuity is also observed in specimen DJ-S-L-CI-2 adjacent to the joint, as shown in Figure 4.39. After careful analysis of the possible reasons for this behavior, it was found that saltwater leakage from the ponded area ran down the exterior of the specimens to the bottom where it must have entered the concrete. For the epoxy joint specimen, the top surface and sides are sealed with epoxy according to ASTM G109[27] requirements, while the bottom is not. This mechanism is common in bridges, and the epoxy sealant on the top and sides would amplify the effect, leading to increased chloride levels near the bottom surface. In dry joint specimens, the saltwater also penetrates the joint and deposits in the bottom area.

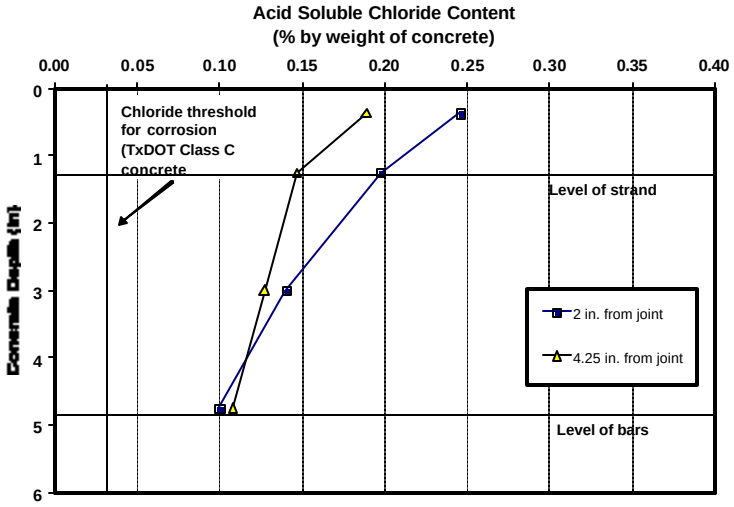

Figure 4.35 Concrete Chloride Ion Profiles for Specimen DJ-S-l-NG-2.

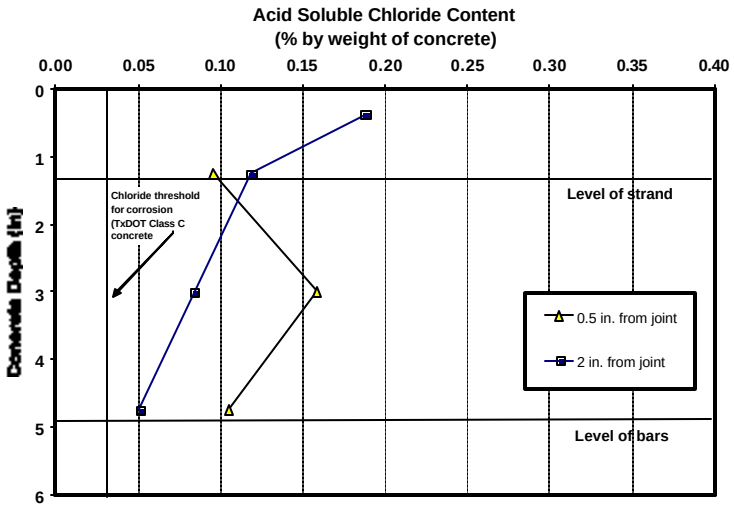

Figure 4.36 Concrete Chloride Ion Profiles for Specimen DJ-S-M-NG-2.

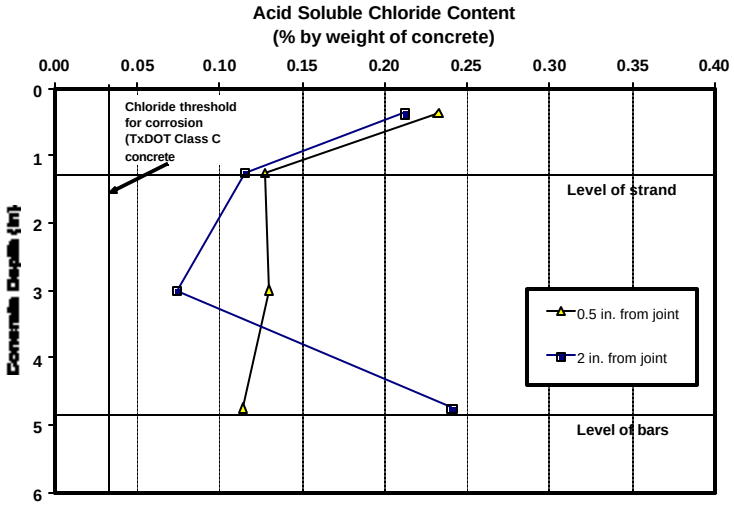

Figure 4.37 Concrete Chloride Ion Profiles for Specimen DJ-S-H-NG-2.

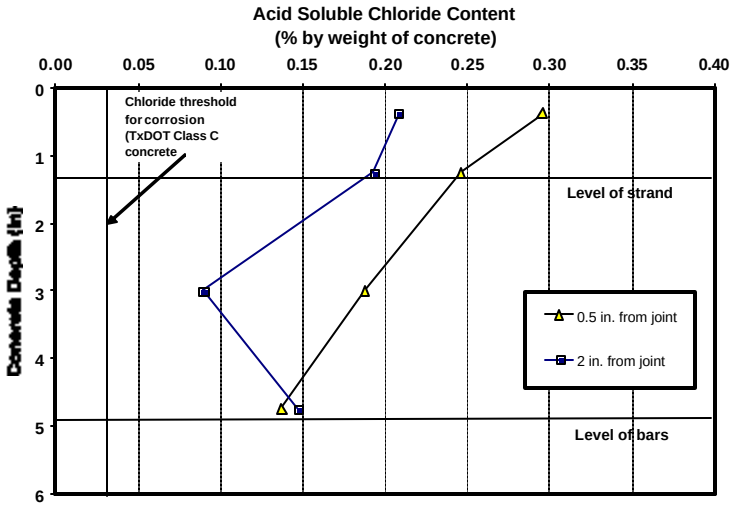

Figure 4.38 Concrete Chloride Ion Profiles for Specimen DJ-P-L-NG-2.

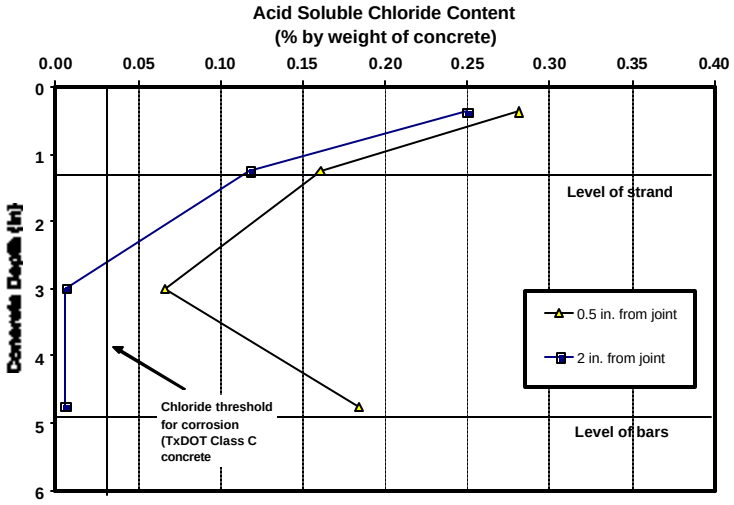

Figure 4.39 Concrete Chloride Ion Profiles for Specimen DJ-S-L-CI-2.

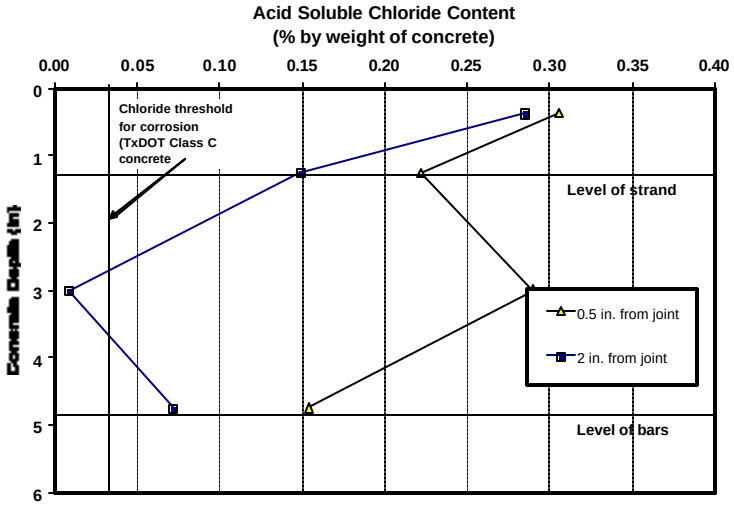

Figure 4.40 Concrete Chloride Ion Profiles for Specimen DJ-S-M-CI-2.

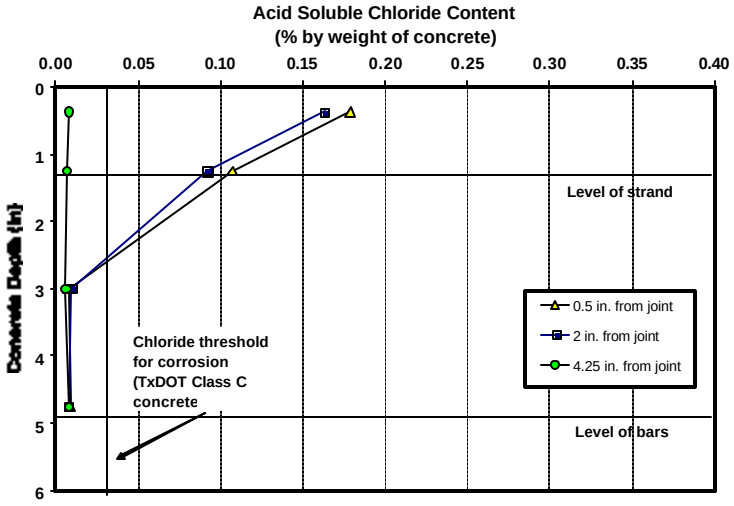

Figure 4.41 Concrete Chloride Ion Profiles for Specimen SE-S-L-NG-1.

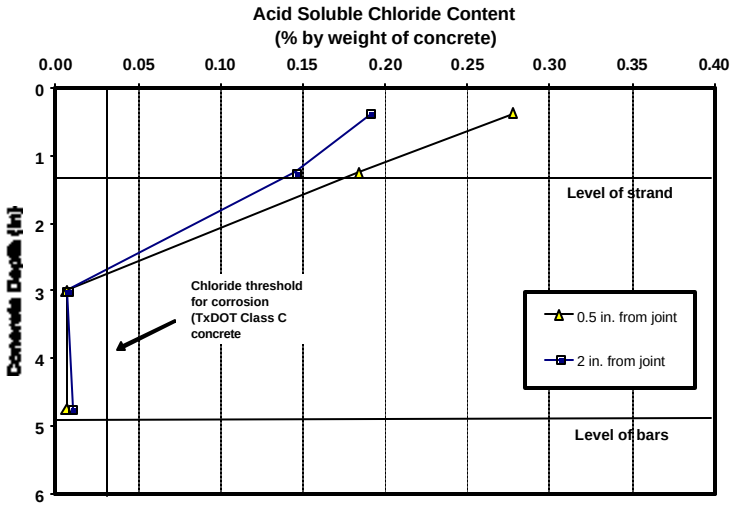

Figure 4.42 Concrete Chloride Ion Profiles for Specimen SE-S-M-NG-1.

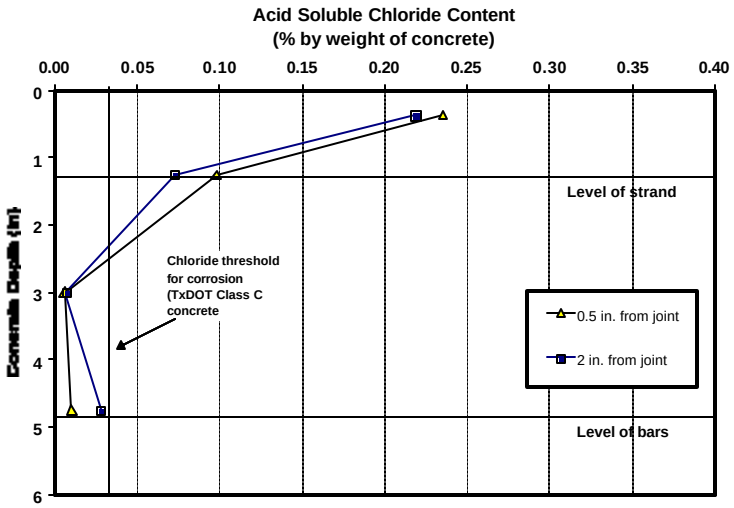

Figure 4.43 Concrete Chloride Ion Profiles for Specimen SE-S-H-NG-1.

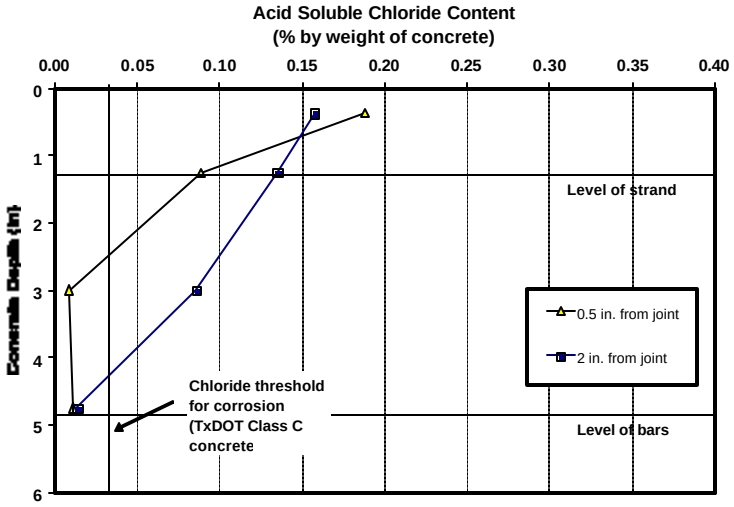

Figure 4.44 Concrete Chloride Ion Profiles for Specimen EG-S-L-NG-1.

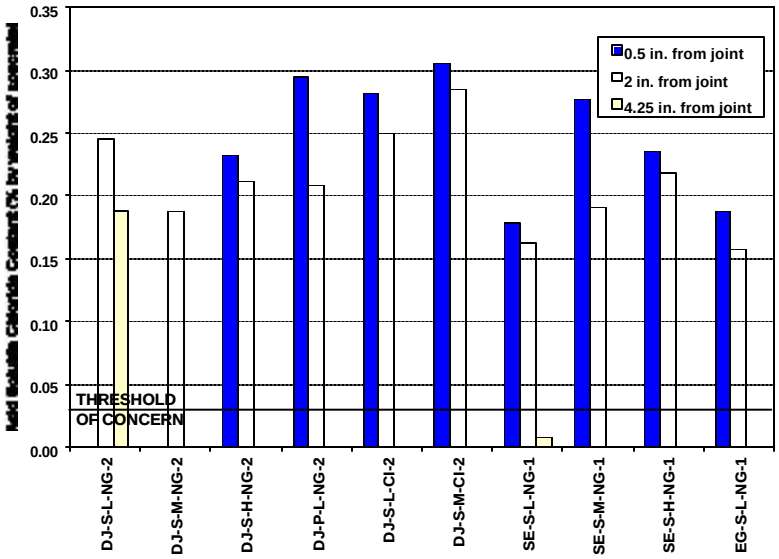

Figure 4.45 Acid Soluble Chloride Content at 0.5 in. Depth (Refer to Figure 4.2).

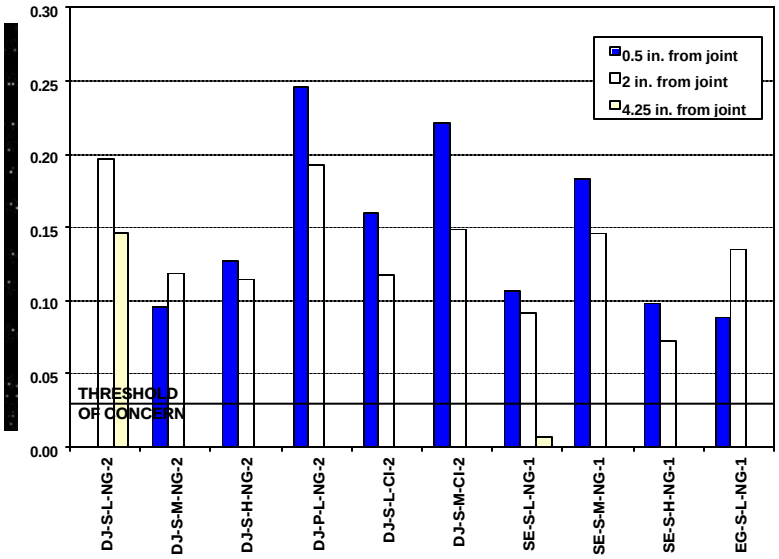

Figure 4.46 Acid Soluble Chloride Content at 1.25 in. Depth - Strand Level – (Refer to Figure 4.2).

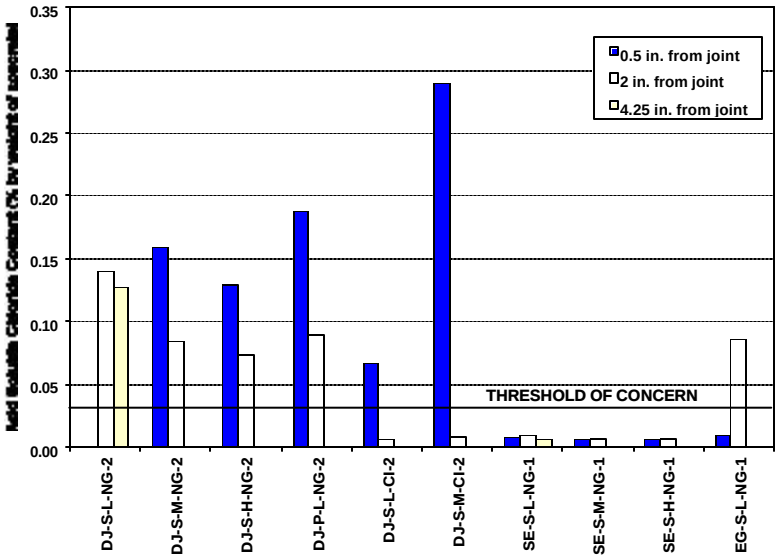

Figure 4.47 Acid Soluble Chloride Content at 3 in. Depth (Refer to Figure 4.2).

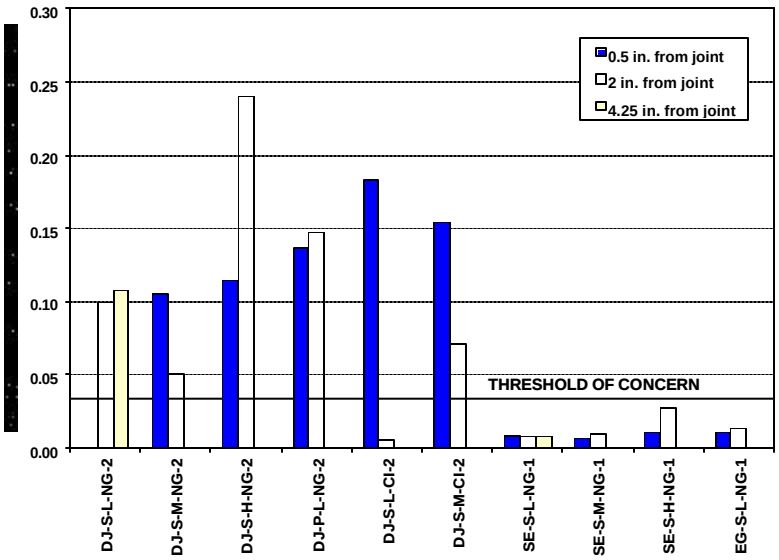

Figure 4.48 Acid Soluble Chloride Content at 4.75 in. Depth - Bar Level – (Refer to Figure 4.2)

The results of the chloride analysis on grout samples are shown in Figure 4.49. The values are plotted as acid soluble chlorides, as a percentage of the grout weight. The chloride threshold for corrosion in grout is taken as approximately 0.14%, assuming a chloride threshold of 0.2% by weight of cement and a water cement ratio of 0.44.

The results obtained from the analysis of the grout samples, are summarized as follows:

1. Dry joint specimens show higher chloride contents at the joint section than at a distance of 2 in. from the joint. Specimen DJ-P-L-NG-2 is the only exception. However, this specimen had a large and deep void at approximately 2 in. from the joint where there was a salt deposit, as described in Section 4.4.1.4. The sample for this specimen was taken from this location, which may explain the inconsistency.
2. Dry joint specimens with corrosion inhibitor show a dramatic decrease in the chloride content when comparing the sample taken at the joint with respect to the sample taken at 2 in.
3. Dry joint specimens show in general higher chloride contents (in the order of 1.5 to 10 times higher) than the corresponding Epoxy Joint specimens.
4. Specimen DJ-S-M-CI-2 shows a very large chloride content at the joint, in the order of two times that for Specimen DJ-S-M-NG-2. Since the chloride content was taken at the joint, no real influence of the grout type is expected. Since there are no other variables involved among these two specimens, the observed trend is unclear.
5. Epoxy joint specimens show higher chloride content at 2 in. from the joint, corresponding with the most severe corrosion areas and voids in the metal duct. The only exception occurs with Specimen SE-S-M-NG-1, where higher chloride content is shown at the joint. However, as it was reported in Section 4.4.1.9, the epoxy in this specimen did not cover the entire face of the joint, leaving small gaps, which may have allowed saltwater to penetrate the joint.
6. Dry joint specimens with steel duct, and normal grout, show a distinct trend with respect to the level of precompression, having less chloride content with higher levels of precompression. The same trend is observed with epoxy joint specimens with steel duct, normal grout and low and high levels of precompression. The only two exceptions are, Specimen DJ-S-M-CI-2, which has higher chloride content than Specimen DJ-S-L-CI-2; and, Specimen SE-S-M-NG-1, which has higher chloride content than the other epoxy joint specimens. The last case is explained following the same reasoning as in 5 above.

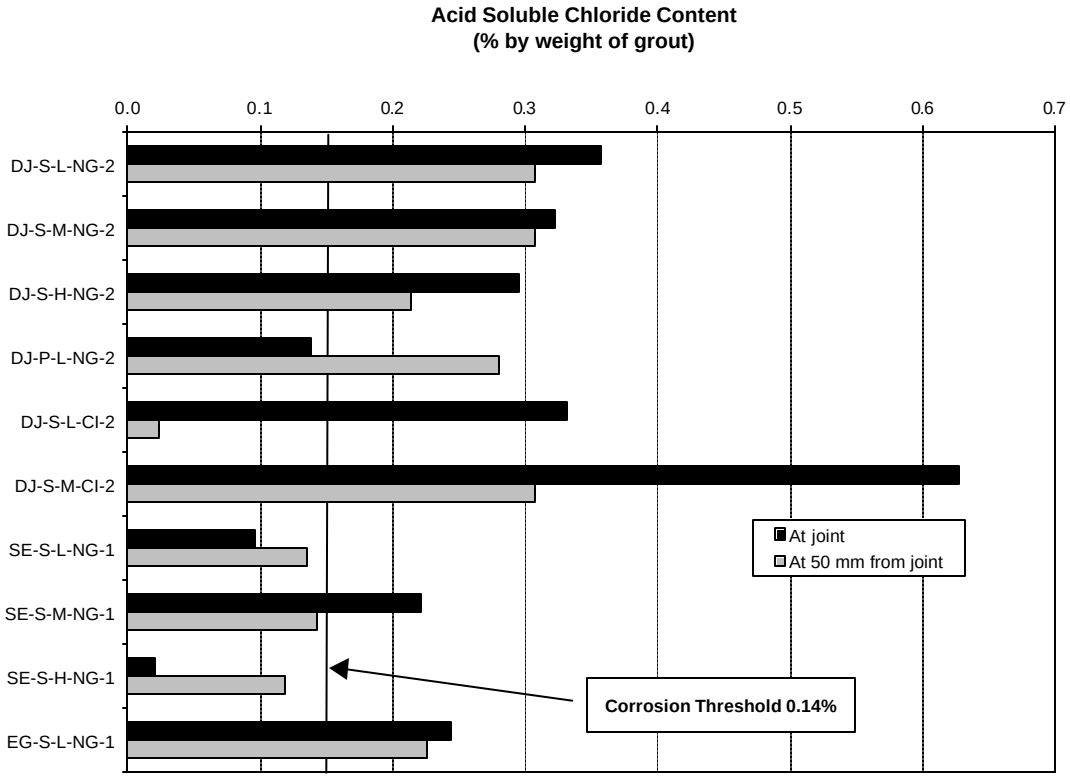

Figure 4.49 Measured Chloride Contents in Post-tensioning Grout after about Eight Years of Exposure.

CHAPTER 5:
ANALYSIS AND DISCUSSION OF RESULTS

After two forensic examinations, at four and a half years and at eight years of very aggressive exposure, the effect of all variables involved in this testing program can be analyzed and compared. Findings and conclusions after the autopsy at four and a half years were described in detail in Reference 15. This chapter includes the results after eight years of exposure, comparing them to results from the first forensic examination when appropriate.

5.1 OVERALL PERFORMANCE

The use of a specimen based on ASTM G109[27] in this testing program, modified to examine prestressing tendons in grouted ducts and to simulate segmental ducts, was found to be an excellent method for analyzing relative specimen performance and for evaluating the adequacy of corrosion protection variables. After eight years of aggressive exposure all specimens have shown a certain degree of strand and mild steel corrosion. The galvanized steel ducts have shown very large destruction.

The relative performance of the specimens in this testing program was studied by looking at the corrosion ratings for the prestressing strands, ordered from lowest to highest. Figure 5.1 shows the results at four and a half years and at eight years of exposure. As can be observed, important changes have occurred between the two autopsy dates. Major of these is the dramatic increase in strand corrosion between the two dates.

While at four and a half years Specimen DJ-S-L-CI-1 had the highest strand corrosion rating, suggesting a very poor performance of the corrosion inhibitor added to the grout, the duplicated Specimen DJ-S-L-CI-2 autopsied after eight years of exposure had a relatively good performance. Specimen SE-S-M-CI-1 was the only corrosion inhibitor specimen showing a very high strand corrosion rating after eight years. However, this specimen also had a faulty epoxy filling at the joint as illustrated in Figure 5.2. These results suggest that the corrosion inhibitor had a positive effect in limiting the corrosion rate after the onset of corrosion had started.

At the end of eight years of exposure, all prestressing strands had experienced a corrosion rating above the value of 50, chosen as the threshold of concern. At four and a half years, only one specimen had exceeded that value.

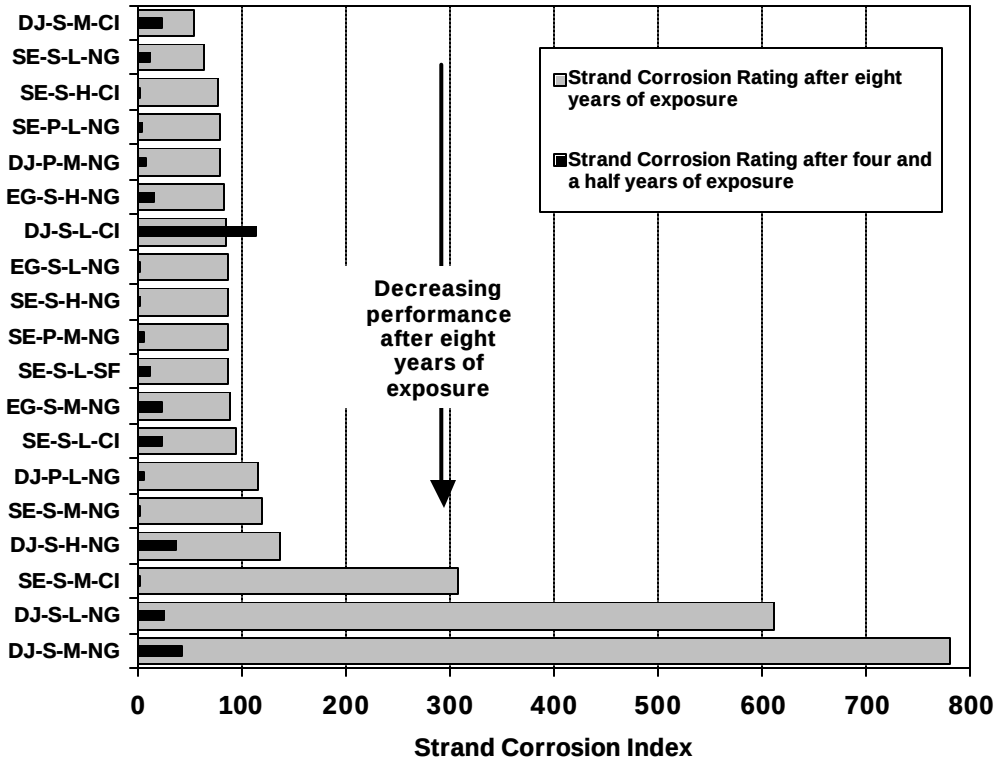

Figure 5.1 Comparison of Corrosion Ratings for Prestressing Strand (After Four Years and Five Months, and Eight Years of Exposure Testing).

Figure 5.2 Top View of the Effect of a Faulty Epoxy Joint (SE-S-M-CI-1) Compared to a Sound Epoxy Joint (SE-S-L-CI-1).

The overall performance of the specimens is better compared by considering the total corrosion rating, obtained by summing the ratings for the strand, bars and duct, as shown in Figure 5.3 and Figure 5.4. Comparison between these two figures showed overall corrosion increased dramatically for most specimens between four and a half years and eight years of exposure. After eight years, the best performance was shown in the plastic duct specimens, while the dry joint specimens with steel ducts and normal grout showed the worst performance. The poor performance observed for specimen SE-S-M-CI-1 clearly shows the detrimental effect of faulty epoxy filling at the joint.

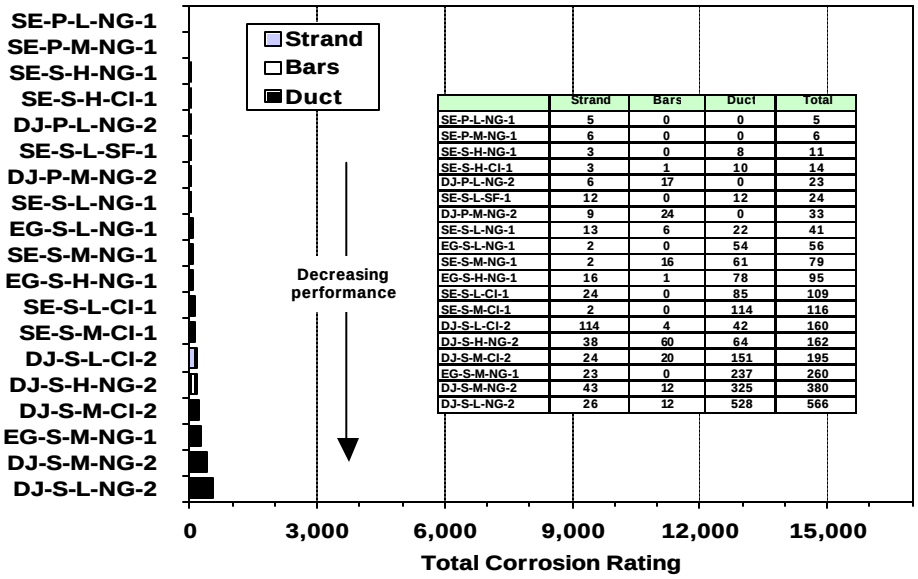

	Strand	Bars	Duct	Total
SE-P-L-NG-1	5	0	0	5
SE-P-M-NG-1	6	0	0	6
SE-S-H-NG-1	3	0	8	11
SE-S-H-CI-1	3	1	10	14
DJ-P-L-NG-2	6	17	0	23
SE-S-L-SF-1	12	0	12	24
DJ-P-M-NG-2	9	24	0	33
SE-S-L-NG-1	13	6	22	41
EG-S-L-NG-1	2	0	54	56
SE-S-M-NG-1	2	16	61	79
EG-S-H-NG-1	16	1	78	95
SE-S-L-CI-1	24	0	85	109
SE-S-M-CI-1	2	0	114	116
DJ-S-L-CI-2	114	4	42	160
DJ-S-H-NG-2	38	60	64	162
DJ-S-M-CI-2	24	20	151	195
EG-S-M-NG-1	23	0	237	260
DJ-S-M-NG-2	43	12	325	380
DJ-S-L-NG-2	26	12	528	566

Figure 5.3 Total Corrosion Rating Ordered According to Performance (After Four Years and Five Months of Exposure).

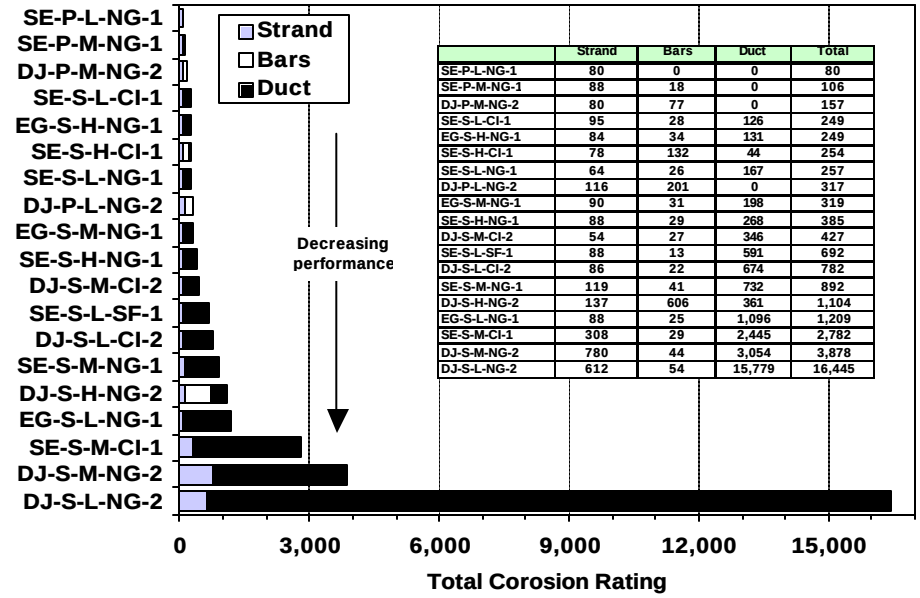

	Strand	Bars	Duct	Total
SE-P-L-NG-1	80	0	0	80
SE-P-M-NG-1	88	18	0	106
DJ-P-M-NG-2	80	77	0	157
SE-S-L-CI-1	95	28	126	249
EG-S-H-NG-1	84	34	131	249
SE-S-H-CI-1	78	132	44	254
SE-S-L-NG-1	64	26	167	257
DJ-P-L-NG-2	116	201	0	317
EG-S-M-NG-1	90	31	198	319
SE-S-H-NG-1	88	29	268	385
DJ-S-M-CI-2	54	27	346	427
SE-S-L-SF-1	88	13	591	692
DJ-S-L-CI-2	86	22	674	782
SE-S-M-NG-1	119	41	732	892
DJ-S-H-NG-2	137	606	361	1,104
EG-S-L-NG-1	88	25	1,096	1,209
SE-S-M-CI-1	308	29	2,445	2,782
DJ-S-M-NG-2	780	44	3,054	3,878
DJ-S-L-NG-2	612	54	15,779	16,445

Figure 5.4 Total Corrosion Rating Ordered According to Performance (After Eight Years of Exposure).

5.2 EFFECT OF JOINT TYPE

After the eight-year forensic examination, it was determined that the joint type is the variable with the most significant effect on specimen performance. Significantly higher corrosion ratings for the strands, mild steel and galvanized ducts were obtained from dry joint specimens with steel ducts and normal grout. The only epoxy joint specimen showing high strand and duct ratings was the poor epoxy joint

Specimen SE-S-M-CI-1. The effect of joint type on the measured and observed results is described below.

5.2.1 Galvanized Steel Duct Corrosion

Duct corrosion was highly influenced by joint type. Figure 5.5 shows typical corrosion found in galvanized steel ducts in each of four joint types. The specimens have been cut open at the level of the duct, and the photos show the top view of each duct and the corresponding corrosion stains and corrosion products attached to the concrete. Duct corrosion in dry joint specimens was extremely severe, with a high percentage of metal loss and concrete cracking at the top of the specimen. Duct corrosion in sound epoxy joint specimens was moderate to severe, with localized section loss extending approximately 2 in. at each side of the joint, below the ponded region. Cracking was also evident in some epoxy joint specimens when the corrosion had been extensive. Figure 5.5 also shows the damaging effect of the faulty epoxy joint on duct corrosion, corresponding to Specimen SE-S-M-CI-1. Epoxy joints with gaskets performed similar to those without gasket, when the epoxy was able to fill the entire joint area during construction. However, as was emphasized, in some cases gaskets prevented the epoxy from adequately filling the joint area, allowing for moisture and chlorides to penetrate the joint.

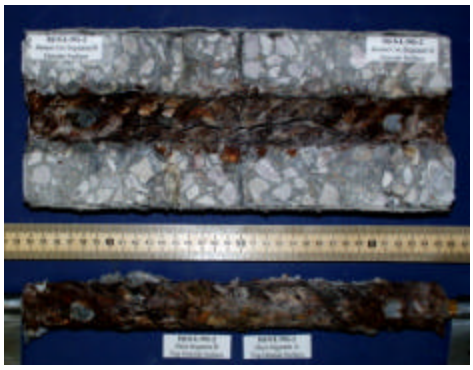

Dry Joint

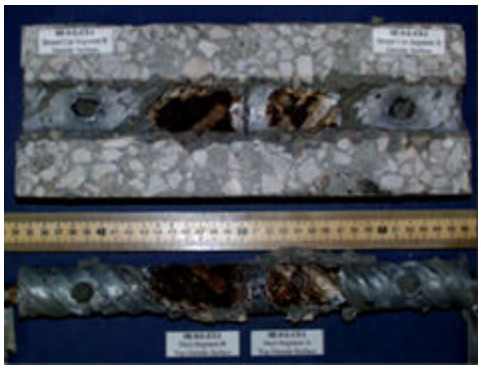

Sound Epoxy joint

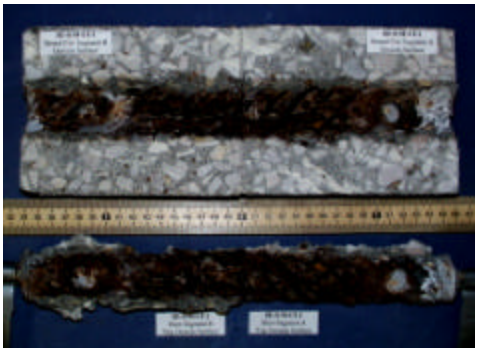

Faulty Epoxy joint

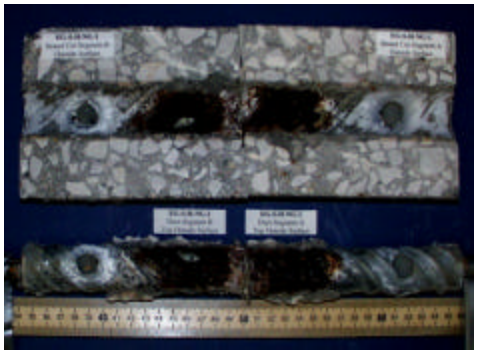

Epoxy/Gasket Joint

Figure 5.5 Galvanized Steel Duct Corrosion: Effect of Joint Type.

The better performance of epoxy joint specimens with respect to dry joint specimens was clearly shown in Figure 4.32. In that figure, the following comparisons can be made: Specimen DJ-S-L-NG-2 versus Specimen SE-S-L-NG-1, Specimen DJ-S-M-NG-2 versus Specimen SE-S-M-NG-1, Specimen DJ-S-H-NG-2 versus Specimen SE-S-H-NG-1; and, Specimen DJ-S-L-CI-2 versus Specimen SE-S-L-CI-1.

5.2.2 Prestressing Strand Corrosion

After eight years of exposure, corrosion above the corrosion rating of 50 chosen as the threshold of concern had occurred in all specimens. This means that most strands showed some degree of pitting and section loss. With respect to joint type there is a distinct difference in the strand corrosion. The highest strand corrosion ratings, and therefore the largest deterioration, were found on dry joint specimens with normal grout and low to medium precompression. These specimens show very severe strand section loss. The corresponding epoxy joint specimens, with the same duct, precompression force and grout type, showed strand corrosion ratings on the order of eight to ten times smaller. Other dry joint specimens, either with plastic ducts or with corrosion inhibitor added to the grout, showed similar results to the corresponding epoxy joint specimens. The only difference was observed in the faulty epoxy joint Specimen SE-S-M-CI-1, which showed a much higher strand corrosion rating than the corresponding dry joint specimen. In this case, the faulty epoxy joint produced misleading results.

5.2.3 Mild Steel Reinforcement Corrosion

Four dry joint specimens (DJ-S-L-NG-2, DJ-S-H-NG-2, DJ-P-L-NG-2 and DJ-P-M-NG-2) and one epoxy joint specimen (SE-S-H-CI-1) showed mild steel corrosion ratings above the threshold value of 50, where there was pitting corrosion and section loss. The largest mild steel bar deterioration was observed in specimen DJ-S-H-NG-2, whose bar corrosion rating was more than 20 times higher than the corresponding epoxy joint specimen, with the same variables. In general, dry joint specimens showed larger bar deterioration than epoxy joint specimens, except for specimens with corrosion inhibitors in the grout, where the results were practically the same in most cases. Epoxy joint specimens with gaskets showed very similar results to those without gaskets in all three cases studied.

5.2.4 Chloride Penetration

Measured acid soluble chloride contents in the concrete adjacent to and at two inches from the joint were always higher for all dry joint specimens. They were in all cases above the threshold value of 0.033% of concrete weight. These dry joint specimens showed very high chloride contents across the entire face of the concrete adjacent to the joint, but lower chloride contents 2 in. inside. Salt deposits were observed on the interior of the ducts in the dry joint specimens, clearly indicating that moisture and chlorides had penetrated through the joint.

Epoxy joint specimens had a very similar low chloride content at 0.5 in. and at 2 in. from the joint, suggesting a good performance of the joint. Below the depth of 3 in. (mid-height between the strand and mild steel bars) all epoxy joint specimens without gaskets showed negligible chloride contents. However, the faulty epoxy joint specimen SE-S-M-CI-1 had much higher chloride values for the reasons described previously.

Epoxy joint specimen with gasket EG-S-L-NG-1, showed a very similar pattern in the proximity of the joint as the epoxy joint specimens without gasket. However, at 2 in. away from the joint, this specimen showed high chloride contents at a depth of 3 in.

5.2.5 Grouting

Grout leaked into the joint region in two of the seven dry joint specimens autopsied at eight years of exposure. During the autopsy at four and a half years, five out of seven dry joint specimens were found with grout leakage through the joint. The extent of the leaks in both autopsies ranged from very minor around the duct opening to almost 80% of the joint face covered with grout. No leakage was found in the standard epoxy joint and epoxy/gasket joint specimens.

5.3 EFFECT OF DUCT TYPE

5.3.1 Duct Corrosion

Galvanized steel duct corrosion was severe in all seven dry joint specimens, producing longitudinal cracks in the top of the concrete specimen ranging from 0.010 in. to 0.12 in. in width. Dry joint specimens with normal grout and low to medium precompression showed very high steel duct consumption by corrosion, up to 50% of the total duct area. The six epoxy joint specimens with steel ducts showed cracks in the top of the concrete specimens in all cases, but smaller than those in dry joint specimens, ranging from hairline cracks up to 0.020 in. cracks. The only exception was Specimen SE-S-L-CI-1 with no concrete cracking. Specimen SE-S-M-CI-1 showed very severe duct corrosion, similar to Specimen DJ-S-M-NG-1, due to the incomplete filling of the match-cast epoxy joint as explained in Section 4.4.1.14 and shown in Figure 5.2. In addition, two out of three epoxy joint specimens with gaskets and steel ducts showed top cracks of 0.010 in. and 0.020 in. in width.

Plastic ducts performed extremely well in all four specimens tested. The two dry joint specimens with plastic ducts showed bottom cracks, below the mild steel, of 0.020 in. and 0.040 in. in width, while the two epoxy joint specimens with plastic ducts did not show any concrete cracking.

As was explained in Reference 15, the concrete cover in these specimens was substantially thinner than would be allowed by specifications. This condition contributed to the severe galvanized duct corrosion in such a short period of time. However, the test results indicate the potential corrosion problems when using galvanized ducts in aggressive exposures. The relative performance of the galvanized and plastic ducts should not be affected by the thin cover. Plastic ducts performed extremely well in spite of the thin cover.

5.3.2 Prestressing Strand Corrosion

Strand corrosion ratings for dry joint specimens with steel ducts, normal grout and low to medium precompression showed much higher values, in the order of six to nine times, with respect to strand corrosion ratings in specimens with plastic ducts. This trend was not clearly shown in epoxy joint specimens, where strand ratings were much lower overall and were all in the same range.

Strand corrosion with plastic ducts ranged from no corrosion to light corrosion. In galvanized steel ducts, strand corrosion ranged from no corrosion to very severe uniform corrosion and pitting.

5.3.3 Reversed Macrocell

Dry joint specimens with plastic ducts (DJ-P-L-NG-2 and DJ-P-M-NG-2) showed reversed macrocell behavior, while the corresponding specimens with steel duct (DJ-S-L-NG-2 and DJ-S-M-NG-2) showed strand corrosion activity, as it was indicated in Table 3.1. These results were confirmed after forensic examination where was found that the mild steel bars in these plastic duct specimens were corroding as the primary corrosion area.

Corrosion currents did not indicate corrosion activity for epoxy joint specimens with either plastic ducts or steel ducts, except for Specimens SE-S-M-CI-1 and SE-S-H-CI-1.

The results of dry joint specimens clearly show the superiority of plastic ducts in improving strand corrosion protection.

5.4 EFFECT OF JOINT PRECOMPRESSION

5.4.1 Strand and Mild Steel Corrosion

The results with regard to strand and mild steel corrosion did not show any distinct trend with respect to the three levels of joint precompression used in the testing program. The isolated result for dry joint

Specimen DJ-S-H-NG-2 with respect to Specimens DJ-S-L-NG-2 and DJ-S-M-NG-2 in Figure 4.32 and Figure 4.33, indicates that at very high levels of precompression there is an increased level of protection of the strand and mild steel bars. This result is not clearly shown for epoxy joint specimens with and without gaskets.

5.4.2 Duct Corrosion

Galvanized steel duct corrosion in dry joint specimens shows a clear trend with respect to the level of precompression. Figure 4.34 compares similar specimens where joint precompression is the only variable (DJ-S-L-NG-2, DJ-S-M-NG-2 and DJ-S-H-NG-2). For these specimens, a higher level of precompression (or prestress) results in significant corrosion rating reduction, and therefore, it improves significantly the duct corrosion protection. The same trend was observed during the autopsy performed at four and a half years of exposure, with the duplicate specimens.[15]

The improved duct corrosion protection with higher levels of precompression is also observed when comparing dry joint specimens with corrosion inhibitor added to the grout and when comparing epoxy joint specimens with gaskets.

Duct corrosion levels in epoxy joint specimens do not show any distinct trend with respect to the level of precompression.

Similar results are obtained from the use of a crack rating, defined as the length of the crack in the top of the concrete specimen multiplied by the maximum crack width. This seems a valid comparison since the concrete and clear cover are the same for all specimens. Crack ratings for all autopsied specimens with steel ducts have been plotted along with duct corrosion ratings in Figure 5.6. From these results, it can be seen that crack ratings are generally proportional to duct corrosion ratings.

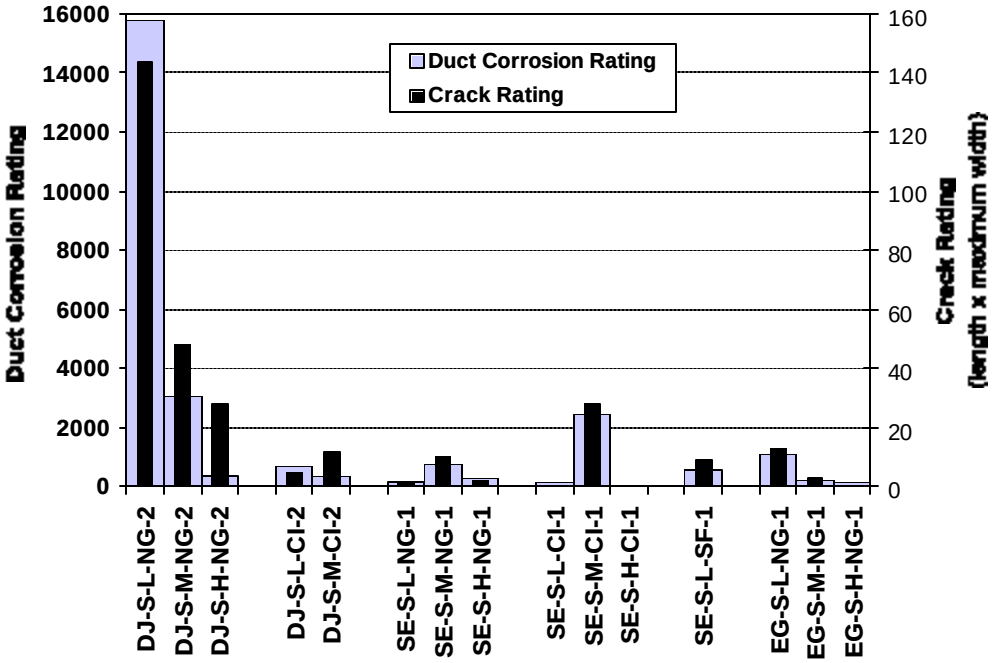

Figure 5.6 Effect of Joint Precompression on Duct Corrosion (After Eight Years of Exposure Testing).

Proportionality between crack ratings and duct corrosion ratings shown in Figure 5.6 after eight years of exposure, was more evident than after four and a half years of exposure as shown in Figure 5.7.

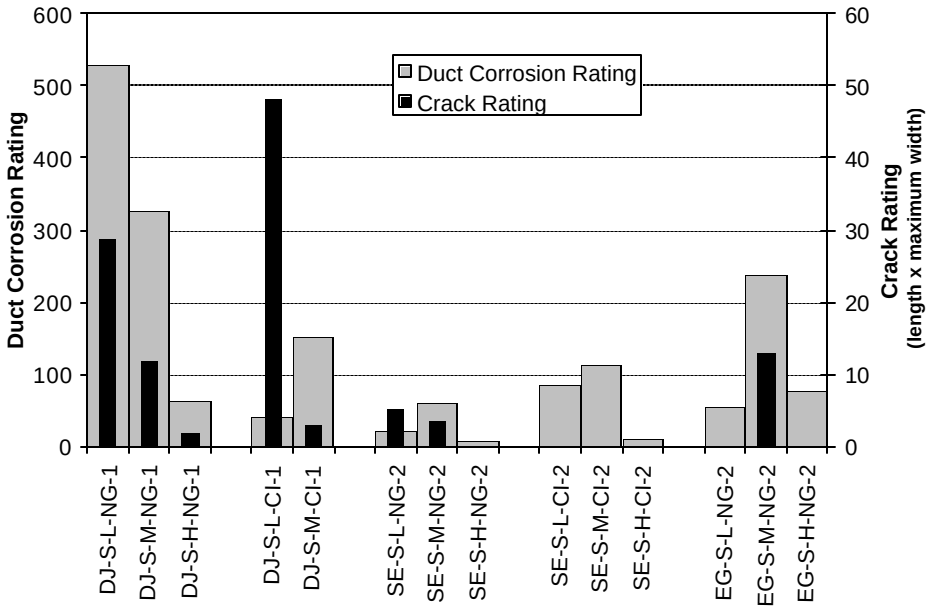

Figure 5.7 Effect of Joint Precompression on Duct Corrosion (After Four Years of Exposure Testing)[15]

5.5 EFFECT OF GROUT TYPE

To examine the effect of grout type on strand corrosion severity, similar specimens with grout type as the only variable were grouped as shown in Table 5.1 and Figure 5.8. From these, a clear trend is observed from dry joint specimens with and without corrosion inhibitor. Specimens with corrosion inhibitor (Calcium Nitrate) added to the grout showed very low strand corrosion ratings when compared to those with normal grout. This trend was also observed from the results based on macrocell currents and half-cell potentials, as included in Table 3.5 and Table 3.6, respectively.

Standard epoxy joint specimens had much lower corrosion values so that they did not show a distinct trend with the use of normal grout, corrosion inhibitor, silica fume, and low precompression. For these specimens light to moderate corrosion was found, without pitting. Similar results were obtained for standard epoxy joint specimens with high precompression. In this case there was light to negligible corrosion and discoloration. The only exception was found with Specimen SE-S-M-CI-1 due to the faulty epoxy joint.

The above results suggest that calcium nitrite corrosion inhibitor was not detrimental with respect to the rate of corrosion. It may even be concluded that it was somewhat effective in counteracting the negative effects of chlorides in strand corrosion. These results contradict the earlier conclusions reached after four and a half years of exposure testing. However, as reported[15] these conclusions were based on very limited data available. They also contradict results obtained by Koester[40] who reported research performing anodic polarization tests on grouted prestressing strands to investigate the corrosion protection provided by various cement grouts. Koester concluded that calcium nitrite significantly reduced the time to corrosion in comparison to plain grout, and had no effect on corrosion rate after the initiation of corrosion. The calcium nitrite dosage used in that series was adjusted to account for the higher cement content in the grout, a factor that was not adjusted in the series reported herein.

Table 5.1 Effect of Grout Type – Strand Corrosion Ratings.

Specimen	Strand Corrosion Rating	Comments
DJ-S-L-NG-2	612	Uniform corrosion extending complete length of strand and pitting.
DJ-S-L-CI-2	86	Light to moderate corrosion.
DJ-S-M-NG-2	780	Severe corrosion and pitting
DJ-S-M-CI-2	54	Light to negligible corrosion. Strand discoloration.
SE-S-L-NG-1	64	Light to moderate corrosion
SE-S-L-CI-1	95	Light to moderate corrosion
SE-S-L-SF-1	88	Light to moderate corrosion
SE-S-M-NG-1	119	Moderate to severe corrosion.
SE-S-M-CI-1	305	Moderate to severe corrosion.
SE-S-H-NG-1	88	Light to negligible corrosion. Strand discoloration.
SE-S-H-CI-1	78	Light to negligible corrosion. Strand discoloration.

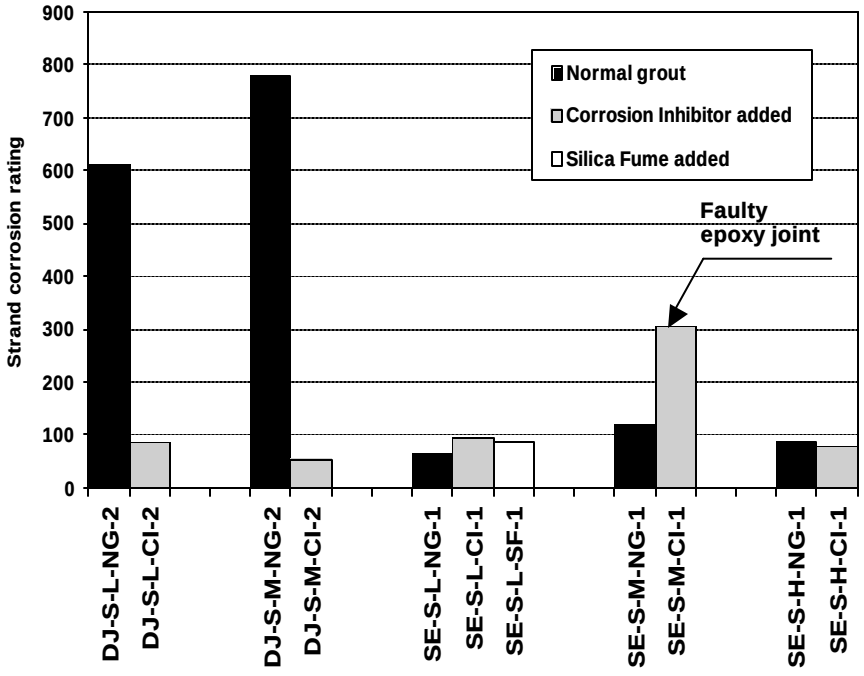

Figure 5.8 Effect of Grout Type – Strand Corrosion Rating.

5.6 GROUT VOIDS

Grout voids were found in seventeen out of the nineteen specimens autopsied at eight years of exposure. In nine specimens the shape of the voids suggests that they resulted from lack of grout fluidity. In the remaining specimens the voids may be attributed to entrapped air, bleed water or incomplete filling. Typical voids are shown in Figure 5.9.

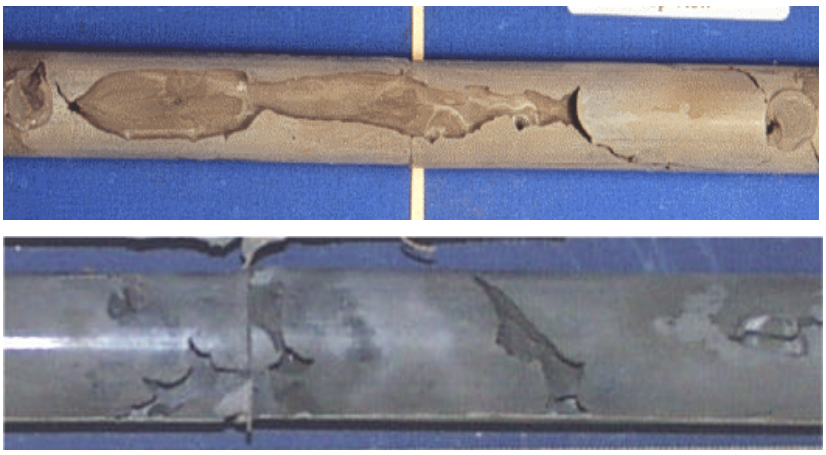

Void caused by entrapped air, bleed water or incomplete filling (from reference 15)

Voids caused by lack of grout fluidity

Figure 5.9 Typical Grout Voids.

In eleven cases the duct was corroded at the top of a grout void in different degrees as shown in Figure 5.10 for Specimen DJ-S-M-NG-2. Similar findings were obtained in two specimens during the first autopsy at four an a half years, as shown in Figure 5.11. The new findings reinforced the conclusion that the presence of a void in the grout may lead to more severe corrosion of the galvanized steel duct and define the area for a premature onset of corrosion.

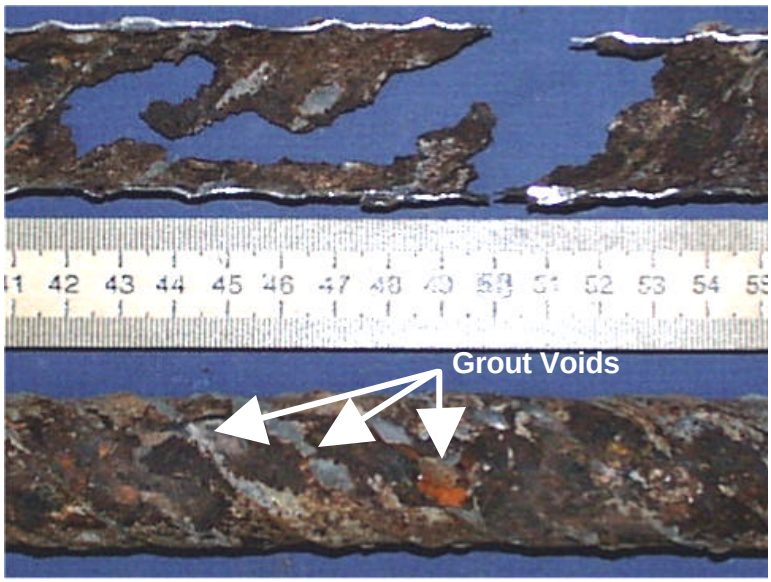

Figure 5.10 Hole in Duct Corresponding to Grout Void (Specimen DJ-S-M-NG-2) (From Autopsy at Eight Years of Exposure Testing).

Figure 5.11 Hole in Duct Corresponding to Grout Void (Specimen DJ-S-M-NG-1) (From Autopsy at Four and a Half Years of Exposure Testing).[15]

5.7 REVERSED CORROSION MACROCELL

As shown in Table 3.1, six of the nineteen specimens were found to have reverse macrocell corrosion. This means that the mild steel bars were corroding (anodic reaction), instead of the prestressing strand. Four of these specimens were dry joint specimens, while the other two were specimens SE-S-M-CI-1 and EG-S-L-NG-1, both with epoxy joints. Specimen SE-S-M-CI-1 as discussed previously, had a very poor epoxy filling of the joint, which allowed water and chlorides to penetrate the joint. Specimen EG-S-L-NG-1 was found to have a sound epoxy joint.

As mentioned previously in reference 15, the development of a reversed macrocell in typical macrocell specimens is unlikely and is not addressed by ASTM G109.[27] The development of the reversed corrosion macrocell in this testing program was considered to be attributed to the transverse segmental joint. The use of a dry joint is particularly severe, as indicated by the experimental data. A possible mechanism is shown in Figure 5.12. The dry joint allows easy penetration of chlorides to the bottom layer of steel. The small end cover for the bottom bars, 0.25 in., provides little protection from lateral migration of the chlorides. The steel becomes quickly depassivated while the prestressing steel benefits from the additional protection provided by the grout and duct. It is assumed that the added protection is primarily due to the extra thickness of the grout over the strand in comparison to the end cover of the bars. Although the duct is discontinuous at the joint, it may also contribute to corrosion protection. These conditions are conducive to the formation of a reversed corrosion macrocell.

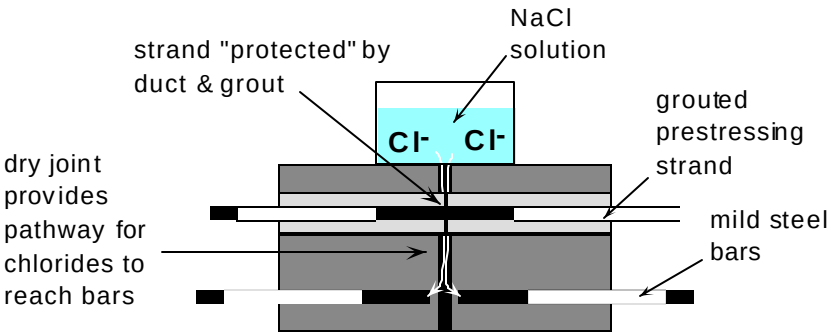

Figure 5.12 Mechanism for Development of Reversed Macrocell in Dry Joint Specimens or in Poor Epoxy Joint Specimens.

The occurrence of a reversed macrocell was not clearly confirmed by forensic examination. Only Specimens DJ-S-H-NG-2 and DJ-P-L-NG-2 show a distinct behavior with very high mild steel corrosion and low prestressing strand corrosion. However, Specimens DJ-P-M-NG-2 and SE-S-H-CI-1 showed high mild steel and strand corrosion ratings at the same time. Specimens DJ-S-M-CI-2 and EG-S-L-NG-1 showed low corrosion in both mild steel and strand. Chloride profiles (where available) indicated chloride levels in excess of the corrosion threshold in all specimens, except in Specimen EG-S-L-NG-1.

5.8 TEST MEASUREMENTS

5.8.1 Comparison Between Half-Cell Potentials and Macrocell Corrosion Current

Similar results were obtained using Half – Cell Potentials and Macrocell Corrosion Currents when assessing strand corrosion in all macrocell specimens, as reported in Section 3.1 and Section 3.2. Table 3.3 showed that most specimens had a good correlation between times to corrosion initiation, and Table 3.5 and Table 3.6 showed that conclusions with respect to the four main variables in the testing program were basically the same. However, these methods were not able to detect corrosion in seven specimens in the case of Half-Cell Potentials, and nine specimens in the case of Corrosion Currents, all of which were found to have some degree of strand corrosion during forensic examination.

Figure 5.13 shows the comparison between corrosion currents and half-cell potentials for Specimen DJ-S-M-NG-2 and Specimen SE-S-M-CI-1. As can be observed, half-cell potentials (above 90% probability of corrosion as per ASTM C876[29]) showed very good correlation with corrosion currents, with regard to the onset of corrosion and corrosion activity.

Based on the above, half-cell potentials can readily be taken in in-service concrete structures to detect the onset of corrosion, where the corrosion current cannot be measured directly. However, as it has to be noted the particular conditions of in-service structures may differ considerably from those in the experimental specimens, which may affect the reliability of the readings. The prestressing strand in this testing program was not in contact with the metal duct. Thus, in typical situations half –cell potentials taken on the prestressing tendon may in fact reflect the very negative potential of the zinc on the galvanized steel duct, leading to erroneous conclusions. In the experimental specimens, it is possible that the discontinuity in the duct at the segmental joint facilitated ion flow through the grout, allowing half-cell potential readings from the prestressing strands to be taken.

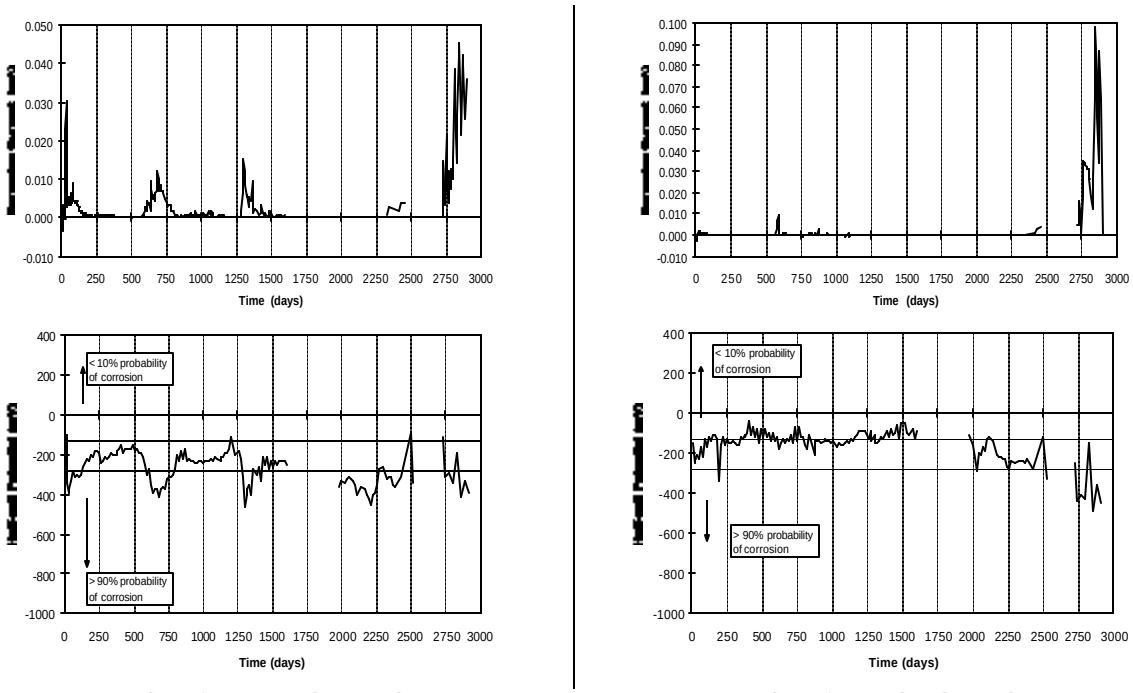

Specimen DJ-S-M-NG-2 *Specimen SE-S-M-CI-1*

Figure 5.13 Comparison Between Corrosion Current and Half-Cell Potential Readings.

5.8.2 Comparison Between Macrocell Corrosion Current and Forensic Examination

Metal loss values calculated in Section 3.3.3.3 and summarized in Table 3.8 were compared against the strand corrosion ratings presented in Section 4.4.2 and summarized in Table 4.6. Figures 5.14 and 5.15 show the results. As can be observed in these figures, there are many discrepancies. Computed metal loss calculations based on current measurements did not show major strand corrosion activity in many of the specimens, contrary to what was found during forensic examination. In addition, specimens with maximum values of calculated metal loss do not correspond to specimens with the maximum corrosion ratings observed.

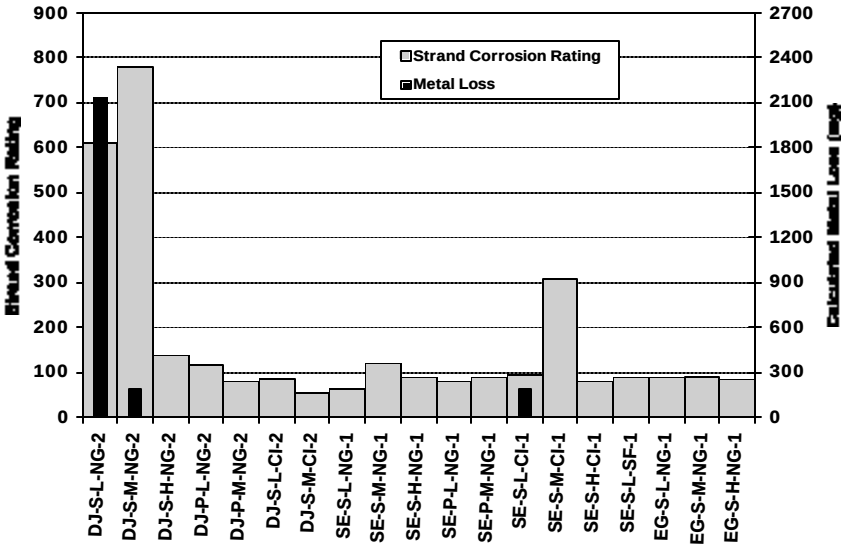

Figure 5.14 Comparison of Corrosion Rating and Metal Loss for Prestressing Strand.

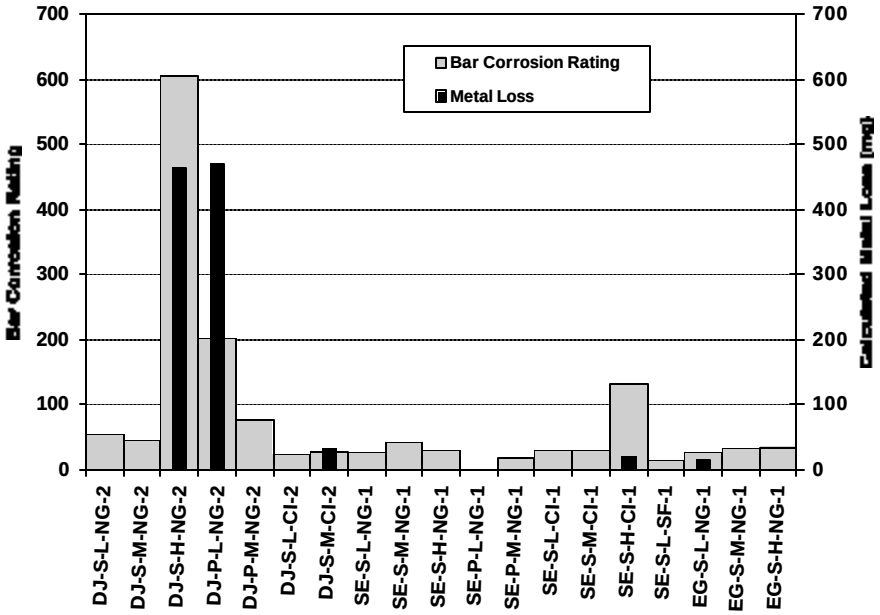

Figure 5.15 Comparison of Corrosion Rating and Metal Loss for Mild Steel Bars.

The above results comparing computed metal loss based on macrocell corrosion currents with the actual corrosion rating noted from the forensic examination results are similar to those obtained at four and a half years of exposure, and the same conclusions apply:

1. Some strand corrosion may be due to microcell corrosion activity or low corrosion currents that were not detected during exposure testing measurements.
2. The calculated metal loss procedure misses the fact that both layers of steel are corroding at the same time. Macrocell corrosion current would correctly indicate if either the mild steel bars or the prestressing strands were experiencing the more severe corrosion activity, but the other would be overlooked. The charge flux calculated from macrocell corrosion current would underestimate the actual corrosion severity or metal loss.
3. Since the driving force for macrocell corrosion is the potential difference between the two layers of steel (resulting from variations in chloride and moisture concentrations), this may disappear during a long-term test. The advanced moisture and chloride penetration may occur before corrosion can be initiated on the steel. This phenomenon may indicate an important limitation of the use of the metal loss calculation procedure in analyzing dry joint segmental construction with macrocell specimens.

CHAPTER 6:
SUMMARY AND CONCLUSIONS

Thirty eight macrocell specimens were used to investigate the corrosion protection of internal tendons at segmental joints. Half of the specimens were autopsied after around four and a half years of highly aggressive exposure and preliminary conclusions were reported.[15] The variables analyzed during the testing program included: joint type (dry or epoxy), duct type (galvanized steel or plastic), grout type (3 grouts with differing additives) and level of joint compression (3 different levels). After the second half of the specimens had been autopsied with over eight years of very aggressive exposure, several conclusions can be drawn.

6.1 OVERALL PERFORMANCE

- Thin epoxy joints provided substantially improved corrosion protection when compared to dry joints. Incompletely filled epoxy joint performance was very similar to that of a dry joint.
- Superiority of plastic ducts was evident. Specimens with plastic duct had the best overall performance (quantified in terms of strand, mild steel and duct corrosion).
- All steel duct specimens showed some degree of duct corrosion: twelve had duct destruction and pitting, two had severe uniform corrosion and one had moderate uniform corrosion.
- Post-tensioning strands were corroded in all specimens: Three had pitting corrosion, one had severe corrosion, one had moderate corrosion, thirteen had light corrosion and one had light to negligible corrosion.
- Mild steel bars were corroded in seventeen out of the nineteen specimens: three had pitting corrosion, two had severe corrosion, three had moderate corrosion, and eight had light corrosion. Mild steel in the other specimens had only minor discoloration.
- In many instances, the epoxy coverage, provided on the strand and mild steel bars to limit the exposed length of the anode and cathode, failed to provide complete corrosion protection to these areas. Epoxy paint peeled off in many instances allowing for moisture and chloride ingress. Corrosion under the epoxy paint was in many cases comparable to the corrosion condition in the exposed lengths. Among others, this affected the current density calculations.
- Metal loss calculations failed to indicate the amount of corrosion in the specimens.

6.2 ASSESING CORROSION ACTIVITY USING HALF-CELL POTENTIAL MEASUREMENTS

Half-Cell Potentials were taken at two-week intervals at the start of the wet period and at the start of the dry period. All measurements were performed according to ASTM C876[29] using a saturated calomel electrode (SCE). In all cases the prestressing tendon was not in contact with the galvanized duct, and it was considered that the segmental joint allowed for ion movement. However, while HC-Potentials in dry joint specimens had a good correlation with forensic examination results, they failed to detect corrosion activity in six out of nine epoxy joint specimens, and in one epoxy joint specimen with gasket.

With respect to testing variables, the following conclusions are drawn based on half-cell potential data:

- Epoxy joint specimens showed less probability of strand corrosion than dry joint specimens.
- Macrocell specimens with plastic ducts (discontinuous) at the joint showed less probability of strand corrosion than similar specimens with steel ducts.

- Dry joint specimen data indicated less probability of strand corrosion with increasing levels of joint precompression. This trend was not clearly shown in epoxy joint specimens.
- Dry Joint specimens with Corrosion Inhibitor (Calcium Nitrate) showed less probability of strand corrosion with respect to specimens with Normal Grout.

6.3 SEGMENTAL JOINTS

To address typical North American practice, dry joints and epoxy joints, with and without gaskets, were selected for investigation in this testing program. All joint types were match-cast. The AASHTO Guide Specifications for Segmental Bridges[28] do not permit the use of dry joints with internal tendons. However, dry joints were included as a worst case scenario for comparison purposes. The thin epoxy-jointed specimens were assembled according to the standard practice. In the epoxy/gasket joint, a foam gasket was glued to the face of one segment around the duct opening prior to application of the epoxy. Forensic examination after eight years of exposure included: seven specimens with dry joints, nine specimens with epoxy joints and three specimens with epoxy joints with gasket. The conclusions are as follows:

- All galvanized steel ducts and prestressing strands in the nineteen specimens showed some degree of corrosion. The higher corrosion ratings were obtained from dry joint specimens with steel ducts and normal grout. Ducts in these specimens were extremely corroded, with corrosion centered at the joint, and with concrete cracking in the top of the specimen. In general, dry joint specimens showed increased chloride penetration and increased corrosion of galvanized steel duct, prestressing strand and mild steel reinforcement. These results show that dry joints do not provide adequate corrosion protection for internal tendons in aggressive environments.
- Sound epoxy joint specimens with galvanized steel ducts showed moderate to very severe duct corrosion away from the joint. Clear cover for specimens was small, (five eights to three quarters of an inch) significantly lower than would be allowed by specifications. However, the test results indicate the potential corrosion problems when using galvanized ducts in aggressive environments.
- Thin epoxy joints provided substantially improved corrosion protection when compared to dry joints. However, test results showed that poor epoxy filling at the joint is extremely detrimental to the performance of the duct, the prestressing strand and the mild steel reinforcement. Incomplete filled epoxy joint performance was very similar to that of a dry joint.
- Corrosion of mild steel in some epoxy joint specimens was found to be the result of an external source of moisture and chlorides rather than from penetration at the epoxy joint or through the concrete. This conclusion was reinforced with chloride levels measured at the joint and away from the joint. These findings reinforce the need to provide adequate clear cover over the ends of longitudinal bars in the segments, even if external post-tensioning is used.
- In some cases, the use of gaskets in epoxy jointed specimens prevented a good epoxy coverage of the joint. This condition could worsen under field conditions.

6.4 DUCTS FOR INTERNAL POST-TENTIONING

Two duct types were investigated; standard galvanized steel duct and plastic duct. Due to size limitations, PVC pipe was used for the plastic duct. Test results indicated:

- Galvanized steel duct was corroded in all specimens. Severe corrosion and large duct destruction was observed in dry joint specimens. Such corrosion was often centered on the dry joint. Epoxy joint specimens showed moderate to severe duct corrosion. The corrosion was often centered away from the joint.

- Superiority of plastic ducts was evident. Strand corrosion encased in plastic ducts showed only light corrosion and discoloration. Specimens with plastic duct had the best overall performance (quantified in terms of strand, mild steel and duct corrosion).
- Concrete cover in specimens was lower than allowed by specifications; however, test results indicate the potential corrosion problems when using galvanized steel ducts in aggressive exposures. Plastic ducts performed well in spite of the small cover.

6.5 JOINT PRECOMPRESSION

Due to the small specimen size, the strand could not be post-tensioned effectively. To simulate precompression across the joint due to post-tensioning, the pairs of match –cast segments were stressed together using external loading frames. Three levels of precompression were selected; 5 psi, 50 psi and $3\sqrt{f'c}$ psi. The lowest level of 5 psi could represent the level of precompression encountered in a precast segmental column under self weight. The precompression of 50 psi is based on AASHTO Guide Specifications.[28] The highest precompression value corresponded to 190 psi for this testing program. Eight out of the nineteen specimens (at eight years of exposure) had low precompression, seven medium precompression and four high precompression. Conclusions are as follows:

- Test results did not show a clear trend with respect to joint precompression when analyzing time to corrosion initiation and rate of corrosion in prestressing strands and mild steel bars. An isolated result for dry joint specimens with steel ducts and normal grout showed that at very high levels of precompression, there is an increased level of strand and mild steel protection. This result is not clearly shown for epoxy joint specimens with and without gasket.
- Galvanized steel duct corrosion in dry joint specimens also showed better performance with a higher level of precompression. However again, this result is not clearly shown in epoxy joint specimens. Precompression level is much important in dry joint specimens.

6.6 GROUTS FOR BONDED POST-TENSIONING

Three cement grout types were selected for evaluation; normal grout (plain cement grout, no admixtures, w/c = 0.40), grout with silica fume (13% cement replacement by weight, w/c = 0.32, superplasticizer added) and grout with a commercial calcium nitrite corrosion inhibitor (w/c = 0.40). The dosage of corrosion inhibitor used in this testing program was the same dosage normally used for concrete (aprox. 20 liters/m^3 concrete). The Calcium Nitrate dosage was not adjusted to account for the higher cement content in grout. The testing program for the nineteen remaining specimens at eight years of exposure included thirteen specimens with normal grout, five with corrosion inhibitor and one with silica fume. Conclusions are as follows:

- Dry joint specimens with corrosion inhibitor (calcium nitrate) added to the grout showed a lower strand corrosion rating (less strand corrosion severity) at eight years of exposure, than specimens with normal grout (in the order of seven times smaller). This trend was not clearly shown in epoxy joint specimens. This result contradicts those obtained at four and a half years of exposure where the most severe corrosion of the prestressing tendon was found where calcium nitrite corrosion inhibitor was used.
- Epoxy joint specimens with silica fume, corrosion inhibitor and normal grout had very similar performances. No clear distinction was evident.
- Grout voids, due to entrapped air, bleed water, incomplete grout filling or lack of grout fluidity showed to be detrimental not only to the prestressing strand, but also to the galvanized steel duct.

CHAPTER 7:
IMPLEMENTATION OF RESULTS

After final autopsy of all macrocell specimens, research results generated the following findings for immediate implementation to improve corrosion protection for bonded internal tendons in precast segmental construction.

Joint Type

Dry joints should not be used with internal prestressing tendons.

Dry joints should be avoided with external tendons in aggressive exposures, to protect segment mild steel reinforcement.

Epoxy joints should be used in aggressive exposures, when corrosion is a concern due to coastal salt water or deicing chemicals, when internal prestressing tendons are used.

Stringent inspection and construction practices must be exercised to guarantee good epoxy filling at the joints.

Gaskets in epoxy joints should be avoided since there is a potential for incomplete epoxy coverage of the joint. Preferred practice with epoxy joints is to utilize a thorough swabbing of tendon ducts immediately after initial segment placement and stressing to seal the duct edges at the joint.

Duct type

Plastic ducts for post-tensioning should be used in all situations where aggressive exposure may occur.

Grout type

Calcium nitrate corrosion inhibitor added to the grout had little effect on the onset of corrosion but did seem to provide enhanced long-term strand corrosion protection.

REFERENCES

(1) **Matt, P. et al. (2000)**, "Durability of Prestressed Concrete Bridges in Switzerland", 16th Congress of IABSE, September 2000, Congress Report.

(2) **Woodward, R. (2001),** "Durability of Post-tensioned tendons on road bridges in the UK."Durability of Post-tensioning tendons. *fib-IABSE Technical Report, Bulletin 15*. Workshop 15-16 November 2001, Ghent (Belgium). pp.1-10.

(3) **Godart, B. (2001),** "Status of durability of post-tensioned tendons in France." Durability of Post-tensioning tendons. *fib-IABSE Technical Report, Bulletin 15*. Workshop 15-16 November 2001, Ghent (Belgium). pp.25-42

(4) **Mutsuyoshi, H (2001),** "Present Situation of Durability of Post-Tensioned PC Bridges in Japan." Durability of Post-tensioning tendons. *fib-IABSE Technical Report, Bulletin 15*. Workshop 15-16 November 2001, Ghent (Belgium). Pp.75-88

(5) **Bertgagnoli, G. , et al (2001),** "Repair and strengthening of damaged prestressed structures." Durability of Post-tensioning tendons. *fib-IABSE Technical Report, Bulletin 15*. Workshop 15-16 November 2001, Ghent (Belgium). Pp.139-153

(6) **Freyermuth, C.L. (2001),** "Status of the durability of post-tensioning tendons in the United States." Durability of Post-tensioning tendons. *fib-IABSE Technical Report, Bulletin 15*. Workshop 15-16 November 2001, Ghent (Belgium). pp. 43-50.

(7) **Jungwirth, D. (2001),** "Problems, Solutions and Developments at Pot-Tensioning Tendons from the German Point of View," Durability of Post-tensioning tendons. *fib-IABSE Technical Report, Bulletin 15*. Workshop 15-16 November 2001, Ghent (Belgium). Pp.11-24

(8) **Eibl, J. (2001),** "External prestressing of German bridges and its further development." Durability of Post-tensioning tendons. *fib-IABSE Technical Report, Bulletin 15*. Workshop 15-16 November 2001, Ghent (Belgium). Pp.227-234

(9) ***fib* Bulletin No. 15 (2001),** "Durability of Post-Tentensioning Tendons." Proceedings of Workshop, Ghent, Belgium, November 2001

(10) **Poston, R.W.,West, J.S. (2001),** "North American Strategies for Improving Bonded Post-tensioned Concrete Construction." Durability of Post-tensioning tendons. *fib-IABSE Technical Report, Bulletin 15*. Workshop 15-16 November 2001, Ghent (Belgium). Pp.245-255

(11) **Chandra, V. (2002),** "A Review of Post-Tensioning Tendons in the Boston Central Artery/Tunnel Project", 1st Annual Concrete Bridge Conference, FHWA, NCBC, PCI. Nashville, TN, Octobre 9, 2002.

(12) **Potter, J.L. (2002)**,"National Status of Post-Tensioning Condition Evaluations and Enhancements." 1st Annual Concrete Bridge Conference, FHWA, NCBC, PCI. Nashville, TN, October 9, 2002.

(13) **DeHaven, T.A. (2002),** "Overview of Recent Developments in Grouting of Post-Tensioning Tendons" 1st Annual Concrete Bridge Conference, FHWA, NCBC, PCI. Nashville, TN, October 9, 2002.

(14) **Vignos, R.P. (1994)**, "Test Method for Evaluating the Corrosion Protection of Internal Tendons Across Segmental Bridge Joints." Master of Science Thesis, The University of Texas at Austin, May 1994.

(15) **West, J.S., Vignos, R.P., Breen, J.E., and Kreger, M.E. (1999),** "Corrosion Protection for Bonded Internal Tendons in Precast Segmental Construction," Research Report 1405-4,Center for Transportation Research, The University of Texas at Austin, Austin, Texas, October 1999.

(16) **Schokker, A.J., Koester, B.D., Breen, J.E., and Kreger, M.E. (1999), "** High Performance Grouts for Bonded Post-Tensioning", Research Report 1405-2, Center for Transportation Research, The University of Texas at Austin, October 1999.

(17) **Schokker, A.J., West, J.S., Breen, J.E., and Kreger, M.E. (1999),** "Interim Conclusions, Recommendations, and Design Guidelines for Durability of Post-Tensioned Bridge Substructructures," Research Report 1405-5, Center for Transportation Research, The University of Texas at Austin, October 1999.

(18) **Post-Tensioning Institute, PTI, Guide Specification (2001)**, "Grouting of Post-Tensioned Structures", February 2001.

(19) **Barnes, R.W. (1996),** "Development of a High Performance Substructure System for Prestressed Concrete Girder Highway Bridges," Master of Science Thesis, The University of Texas at Austin, 1996.

(20) **Armstrong, S.D., Salas, R.M., Wood, B.A., Breen, J.E. and Kreger, M.E. (1997),** "Behavior and Design of Large Structural Bridge Pier Overhangs," Research Report 1364-1, Center for Transportation Research, The University of Texas at Austin, 1997, 272 pp.

(21) **Koester, B.D. (1995),** "Evaluation of Cement Grouts for Strand Protection Using Accelerated Corrosion Tests," Master of Science Thesis, The University of Texas at Austin, December 1995.

(22) **Kotys, A.L.** "Durability Examination of Bonded Tendons in Concrete Beams under Aggressive Corrosive Environment" Unpublished Master of Science Thesis, The University of Texas at Austin. (under preparation)

(23) **Larosche, C.J. (1999),** "Test Method for Evaluating Corrosion Mechanisms in Standard Bridge Columns," Master of Science Thesis, The University of Texas at Austin, August 1999.

(24) **Salas, R.M.** "Accelerated Corrosion Testing, Evaluation and Durability Design of Bonded Post-Tensioned Concrete Tendons." Unpublished Doctor of Philosophy Dissertation, The University of Texas at Austin. (under preparation)

(25) **Schokker, Andrea J. (1999),** "Improving Corrosion Resistance of Post-Tensioned Substructures Emphasizing High Performance Grouts," Doctor of Philosophy Dissertation, The University of Texas at Austin, August 1999.

(26) **West, J.S. (1999)**, "Durability Design of Post-Tensioned Bridge Substructures," Doctor of Philosophy Dissertation, The University of Texas at Austin, May 1999.

(27) **ASTM (1992)**, "Standard Test Method for Determining the Effects of Chemical Admixtures on the Corrosion of Embedded Steel Reinforcement in Concrete Exposed to Chloride Environments," ASTM G109-92, American Society for Testing and Materials, Philadelphia, PA, 1992.

(28) **AASHTO (1999)**, *Guide Specifications for Design and Construction of Segmental Concrete Bridges*, American Association of State Highway and Transportation Officials, Washington, D.C., 1999. 2nd Edition.

(29) **ASTM (1991)**, "Standard Test Method for Half-Cell Potentials of Uncoated Reinforcing Steel in Concrete," ASTM C876-91, American Society for Testing and Materials, Philadelphia, Pa., 1991.

(30) **Broomfield, J.P., Rodriguez, J., Ortega, L.M., and Garcia, A.M. (1993)**, "Corrosion Rate Measurement and Life Prediction for Reinforced Concrete Structures," Proceedings of the 5th International Conference on Structural Faults and Repair held on June 29, 1993, Vol. 2, Venue, University of Edinburgh, pp 155-163.

(31) **Al-Qadi, I.L., Peterson, J.E., and Weyers, R.E. (1993)**, "A Time to Cracking Model for Critically Contaminated Reinforced Concrete Structures," Proceedings of the 5th International Conference on Structural Faults and Repair held on June 29, 1993, Vol. 3, Venue, University of Edinburgh, pp 91-99.

(32) **Concrete Reinforcing Steel Institute (1992)**, "CRSI Performance Research: Epoxy-Coated Reinforcing Steel," Interim Report, CRSI, Schaumburg, Ill, January 1992.

(33) **Virmani, Y.P., Clear, K.C., and Pasko, T.J. (1983)**, "Time-to-Corrosion of Reinforcing Steel in Concrete Slabs, Vol. 5,: Calcium Nitrite Admixture or Epoxy-Coated Reinforcing Bars as Corrosion Protection Systems," Report No. FHWA/RD-83/012, Federal Highway Administration, Washington, D.C., September 1983, 71p.

(34) **AASHTO (1994),** "Sampling and Testing for Chloride Ion in Concrete and Concrete Raw Materials," AASHTO T 260-94, American Association of State Highway and Transportation Officials, Washington, D.C., 1994.

(35) **Poston, R.W. (1984),** "Improving Durability of Bridge Decks by Transverse Prestressing," Doctor of Philosophy Dissertation, The University of Texas at Austin, 1984.

(36) **Hamilton, H.R. (1995),** "Investigation of Corrosion Protection Systems for Bridge Stay Cables," Doctor of Philosophy Dissertation, The University of Texas at Austin, 1995.

(37) **Sason, A.S. (1992),** "Evaluation of Degree of Rusting on Prestressed Concrete Strand," *PCI Journal*, Vol. 37, No. 3, May-June 1992, pp. 25-30.

(38) **Wouters, J.P. (1998),** Personal Communication, Whitlock Dalrymple Poston and Associates, Inc., Manassas, Virginia, July 1998.

(39) **ACI Committee 222, (1996), "**Corrosion of Metals in Concrete," ACI 222R-96, American Concrete Institute, Detroit, Michigan, 1996.

(40) **Koester, B.D. (1995)**, "Evaluation of Cement Grouts for Strand Protection Using Accelerated Corrosion Tests," Master of Science Thesis, the University of Texas at Austin, December 1995.